UNIVERSITÀ DI PARMA

UNIVERSITÀ DEGLI STUDI DI PARMA

Dipartimento di Scienze Chimiche, della Vita e della Sostenibilità Ambientale
Dipartimento di Eccellenza (MIUR 2018-2022)

DOTTORATO DI RICERCA IN
"Biotecnologie e Bioscienze"

CICLO XXXIV

in CO-TUTELA con
Ludwig-Maximilians-Universität München

"Contribution of applied biology to mitigation of urban air pollution and prevention of its effects on health and environment"

Coordinatore:
Chiar.mo Prof. Marco Ventura

Tutore:
Chiar.mo Prof. Elena Maestri
Chiar.mo Prof. Nelson Marmiroli
Chiar.mo Prof. Annette Peters
Gent.ma Dr.ssa Regina Pickford

Dottorando: Megi Vogli

Anni Accademici 2018/2019 – 2020/2021

Aus dem Institut für Medizinische Informationsverarbeitung Biometrie und Epidemiologie
Institut der Ludwig-Maximilians-Universität München
und Università degli studi di Parma

"Contribution of applied biology to mitigation of urban air pollution and prevention of its effects on health and environment"

Dissertation
zum Erwerb des Doktorgrades der Humanbiologie
an der Medizinischen Fakultät der
Ludwig-Maximilians-Universität München
im Rahmen eines Cotutelle-Vertrages mit der
Università degli studi di Parma

vorgelegt von
Megi Vogli

aus
Tirana (Albanien)

Jahr
2022

Mit Genehmigung der Medizinischen Fakultät der
Ludwig-Maximilians-Universität zu München

Erster Gutachter : Prof. Dr. Annette Peters

Zweiter Gutachter :

Dritter Gutachter :

ggf. weitere Gutachter

Mitbetreuung durch den
promovierten Mitarbeiter : Dr. Regina Pickford, Prof. Dr. Elena Maestri

Dekan: Prof. Dr. med. Thomas Gudermann

Tag der mündlichen Prüfung:

Contents

List of Figures

List of Tables

Summary

Traditionally, atmospheric air pollution particles are classified by size, such as PM_{10}, $PM_{2.5}$ (particles with less than 10 μm and 2.5 μm in aerodynamic diameter, respectively) and ultrafine particles (UFPs), which have a diameter below 100 nm. Because of their fine and small size, both $PM_{2.5}$ and UFPs, can penetrate deep into the lungs and settle in the alveolar region where they can translocate into the bloodstream through the capillary barrier and reach other organs. We want to better understand how UFPs can affect human health and to obtain an overview of the inducing biological mechanisms. To do so, we tackled the matter with two different approaches: a molecular one, using "omic" technologies, and an epidemiological one, focusing on the investigation of specific blood biomarkers.

The molecular approach consists of working with engineered nanoparticles (ENPs) as a manageable tool to study UFPs toxicity mechanisms on human cells, given their similarities in size, metal contents, biological effects induced and exposure routes. We investigated the toxicity of Cadmium Sulfide Quantum Dots (CdS QDs) on two different cell lines, which are HepG2 (liver hepatocellular carcinoma) and THP-1 (peripheral blood monocyte), in order to represent different routes of exposure. Both cell lines were treated with sub-toxic dose of CdS QDs and Cd^{2+}, respectively. RNA was then isolated and RNA sequencing and miRNome profiling were performed. The transcriptomic data and miRNAs-mRNAs interactions analyses reveal for HepG2, exposed to CdS QDs, the activation of RAS and the calcium signaling pathways, which could induce an increase in intracellular calcium and lead to apoptosis as final step. On the other hand, THP-1 exposed to CdS QDs points at Janus kinase/signal transducers and activators of transcrip-

tion (JAK/STAT) signaling and inflammatory pathways, which are directly related with autophagy. In both cell lines the response to Cd^{2+} is different compared to the ones for CdS QDs treatments. The apoptotic pathway seems to be imminent after a 24h exposure. In conclusion, in our study, we highlight potential risks associated with exposure to engineered nanoparticles at the molecular level.

In the second section an epidemiological approach was used. We conducted a long-term analysis at population scale to assess the link between air pollutants (including UFPs) and inflammation and coagulation blood biomarkers reflecting cardiovascular health. This cross-sectional study is based on the German KORA S4 study, the exposure data were provided by the ULTRA III project. The air pollutants considered were: $PM_{(10;\ 2.5;\ coarse)}$, $NO_{(x;\ 2)}$, O_3 and UFPs measured as particle number concentration (PNC). The ULTRA III measurements took place in Augsburg, the study area of KORA. Long-term exposure (annual average) to air pollutants was predicted by using Land-use regression modeling (LUR) at the home address of each participant of the study. Multiple linear regression models were used for these analyses. Models were adjusted for different confounders. The results show an association between biomarkers of inflammation and coagulation with almost all the pollutants, in particular with UFPs.

In summary, we observed adverse effects of nanoparticles on two different human cell lines at molecular level after short-term exposure, as well as at population-scale in association with long-term exposure. Moreover, this study highlights the association of inflammatory and coagulation blood-biomarkers with PM and gaseous pollutants, linking it directly with an increased risk of cardiovascular disease.

Zusammenfassung

Traditionell werden Luftschadstoffpartikel nach ihrer Größe klassifiziert, und als PM_{10}, $PM_{2.5}$ (Partikel mit einem aerodynamischen Durchmesser von weniger als 10 μm bzw. 2.5 μm) und ultrafeine Partikel (UFP), die einen Durchmesser von weniger als 100 nm haben. Aufgrund ihrer Große können $PM_{2.5}$ und UFP tiefe in die Lunge eindringen und sich in der Alveolarregion absetzen, wo sie über die Kapillarschranke in den Blutkreislauf gelangen und andere Organe erreichen können. Um besser zu verstehen, wie sich die UFP auf die menschliche Gesundheit auswirken können, und uns einen Überblick über auslösende biologische Mechanismen verschaffen, haben wir zwei verschiedene Ansätze gewählt: einen molekularen, bei dem "omic"-Technologien zum Einsatz kommen, und einen epidemiologischen, der sich auf die Untersuchung spezifischer Biomarker konzentriert.

Für meine Forschungsstudie über die Toxizitätsmechanismen von UFP besteht der molekulare Ansatz darin, mit technisch hergestellten Nanopartikeln (engineered nano particles, ENPs) als praktischem Werkzeug zu arbeiten, da sie UFP in Bezug auf Größe, Metallgehalt, ausgelöste biologische Effekte und Expositionswege ähneln.
Wir untersuchten die Toxizität von Cadmiumsulfid Quantenpunkten (CdS QDs) an zwei verschiedenen menschlichen Zelllinien, nämlich HepG2 (hepatozelluläres Leberkarzinom) und THP-1 (periphere Blutmonozyten), um verschiedene Expositionswege zu repräsentieren. Beide Zelllinien wurden jeweils subtoxischen Dosen von CdS QDs und Cd^{2+} ausgesetzt. Anschließend wurde die RNA isoliert und eine RNA-Sequenzierung sowie ein miRNome-Profiling durchgeführt. Die transkriptomischen Daten und miRNAs-mRNAs Interaktionsanalysen zeigen für die mit CdS QDs behandelte HepG2 Zel-

llinie, eine Aktivierung von RAS und der Kalzium Signalwege, die einen Anstieg des intrazellulären Kalziums induzieren und schließlich zur Apoptose führen könnten. In mit CdS QDs behandelte THP-1 hingegen, finden wir Hinweise auf Janus kinase/signal transducers and activators of transcription (JAK/STAT) Signalwege und Entzündungswege, die direkt mit der Autophagie verbunden sind. In beiden Zelllinien ist die Reaktion auf Cd^{2+} anders als bei der Behandlung mit CdS QDs. Apoptose scheint unmittelbar nach 24 Stunden Exposition zu erfolgen. Zusammenfassend lässt sich sagen, dass wir in unserer Studie das mögliche Risiko hervorheben, das mit einer Exposition gegenüber technisch hergestellten Nanopartikeln auf molekularer Ebene zusammenhängt.

Im zweiten Teil wurde ein epidemiologischer Ansatz gewählt. In einer Langzeitstudie auf Bevölkerungsebene untersuchen wir den Zusammenhang zwischen Luftschadstoffen (einschließlich UFP) und Entzündungs- und Gerinnungs Blutbiomarkern, die kardiovaskuläre Gesundheit widerspiegeln. Diese Querschnittsstudie basiert auf der KORA S4 Kohorte. Die Expositionsdaten stammen aus dem ULTRA III-Projekt. Die für diese Arbeit berücksichtigten Luftschadstoffe waren: $PM_{(10;\,2.5;\,grob)}$, $NO_{(x;\,2)}$, O_3 und UFP gemessen als Partikelanzahlkonzentration. Die ULTRA III-Messungen fanden in Augsburg statt, dem Untersuchungsgebiet von KORA. Die langfristige Belastung (Jahresmittelwert) gegenüber Luftschadstoffen wurde mit Hilfe der Landnutzungsregressionsmodellierung (LUR) an der Wohnadresse jedes Studienteilnehmers geschätzt. Für die Analysen wurden multiple lineare Regressions modelle verwendet, die für verschiedene Störfaktoren adjustiert wurden. Die Ergebnisse zeigen einen Zusammenhang zwischen Biomarkern für Entzündung und Gerinnung mit fast allen Schadstoffen, insbesondere mit UFP. Wir haben in zwei verschiedenen menschlichen Zelllinien nachteilige Auswirkungen einer kurzfristigen Exposition gegenüber Nanopartikeln auf molekularer Ebene sowie einer langfristigen Exposition auf Bevölkerungsebene beobachtet. Darüberhinaus hebt diese Studie den Zusammenhang zwischen Entzündungs- und Gerinnungs Blutbiomarkern und Feinstaub sowie gasförmigen Schadstoffen hervor, und weist damit auf einen direkten physiologischen Link für ein erhöhtes Risiko von Herz-Kreislauf- Erkrankungen.

Chapter 1

Introduction

The main objective of my PhD project is to study the link between air pollutants and human health, which is a persistent worldwide problem. According to World Health Organization (WHO), each year 7 million of people in the world die prematurely because of indoor and outdoor air pollutants. Air pollution is a complex mixture of gaseous and particulate components [1], the main ones are: Nitrogen oxides (NO_2 and NO_x), Sulfur dioxide (SO_2), Ozone (O_3), Carbon monoxide (CO), Volatile Organic Compounds (VOCs) and Particulate Matter (PM) in different size fractions. The processes that contribute to air pollutants generation are both anthropogenic and natural. The main ones in relation to human activities are: vehicle emissions, industrial and agricultural emissions, residential heating, the production, distribution and use of chemical products [2]. Some natural agents are sea salt, suspended soils, natural wildfires, volcanoes and organic compounds from plants. Air pollutants are grouped into main classes which are primary and secondary pollutants. Primary pollutants are those that are released into the environment directly as a result of the process that generated them. Secondary pollutants, on the other hand, are those substances that are generated as a result of chemical and physical interactions among primary pollutants, or between primary pollutants and the atmosphere. These interactions can be activated by solar energy and often involve atmospheric oxygen.
Considering the fact that human contribution to air pollutants is very rel-

evant, it is important to have strong and effective policies that limit their emissions both for our health and for the environment. It is a big challenge for us as a society to try and achieve this goal, but it is necessary in order to prevent disease, improve our quality of life and that of future generations.

Currently, the EU has set limit values for $PM_{10,2.5}$, O_3, SO_2, NO_2, Polycyclic Aromatic Hydrocarbons (expressed as concentration of Benzo(a)pyrene), lead and other pollutants that may adversely affect human health or ecosystems. These are included in the 2008 Directive on Air Quality and Cleaner Air for Europe (2008/50/EC) and the 1996 Framework Directive on Air Quality Assessment and Management (96/62/EC) [3, 4]. After the introduction of such limits a decrease in air pollutants levels have been recorded, as can be seen in Figure 1.1 [5]. The European Commission wants to further reduce those limits to minimize by 55% the number of deaths caused by air pollution in 2030 [6].

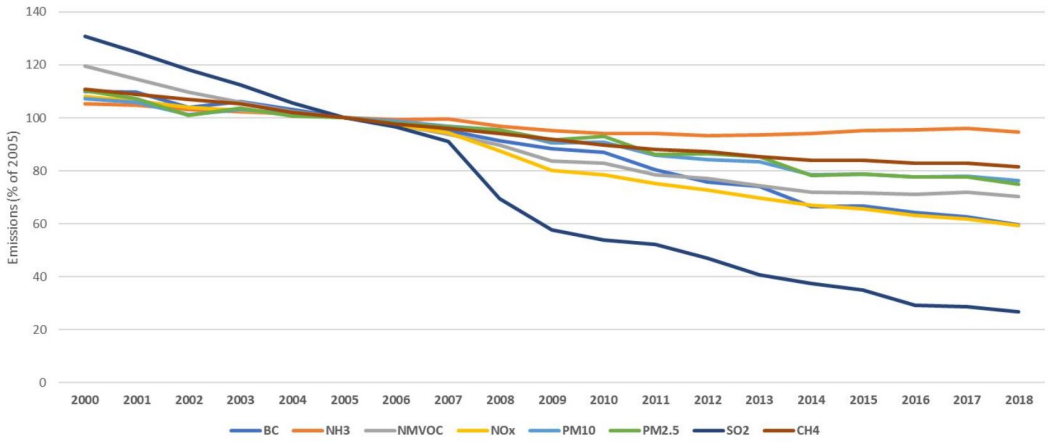

Figure 1.1: Decrease in emissions of most air pollutants in the EU from 2000-2018. From EEA 'Air quality in Europe - 2020 report' published in November 2020 [5].

Moreover, in September 2021, the WHO updated its "Air Quality Guidelines" [7] recommendations, decreasing the annual and daily emission limits for key pollutants, PM_{10}, $PM_{2.5}$ and NO_2 as shown in Table 1.1 [8]. The European Commission's objective is to move in parallel with these new WHO's guidelines.

Table 1.1: Limit values: global WHO Air quality guidelines 2005 and 2021; Air Quality Directives (2008/50/EC, 2004/107EC) [8]

Pollutant	Averaging Period	WHO 2005 Air Quality Guidelines	WHO 2021 Air Quality Guidelines	EU Air Quality Directives
$PM_{2.5}$	Annual	10 µg/m^3	5 µg/m^3	25 µg/m^3
$PM_{2.5}$	Daily 24h	25 µg/m^3	15 µg/m^3	-
PM_{10}	Annual	20 µg/m^3	15 µg/m^3	40 µg/m^3
PM_{10}	Daily 24h	50 µg/m^3	45 µg/m^3	50 µg/m^3
NO_2	Annula	40 µg/m^3	10 µg/m^3	40 µg/m^3
NO_2	Daily 24h	-	25 µg/m^3	50 µg/m^3

This action is indicative of the increased interest that the problem is receiving, and it exemplifies the urge to act in a coordinated fashion at the international level. In recent years, special attention was given to fine and ultrafine fraction of particulate matter, these are $PM_{2.5}$ and $PM_{0.1}$ respectively. Their relevance is due to their potential effects on human health.
The following section is an overview about what airborne particles are, and why the decreasing size of such particles have a strong impact on health.

1.1 Airborne particulate matter

Airborne particulate matter (PM) is defined as a mixture of solid particles and liquid droplets suspended in air [9]. PM can be both: directly emitted from different sources, indicated as primary; or formed within the atmosphere from the condensation of trace gases, referred to as secondary particulate matter [10]. Traditionally, atmospheric particles are classified by size, in term of aerodynamic diameter. By definition it refers to the equivalent diameter of a unit density spherical particle with the same terminal settling velocity as the particles being measured [11]. PM_{10} and $PM_{2.5}$ are defined as particles with less than 10 µm and 2.5 µm in aerodynamic diameter, respectively. Ultrafine particles (UFPs) are also called $PM_{0.1}$ or "nanoparticles", they include all the ones with diameter below 100 nm [12].

Going into more detail, two metrics are mostly used to describe PM, which are number concentration, meaning the number of particles within a given volume (particles/cm^3), and the mass concentration, defined as the mass of particles within a given volume (µg/cm^3) [13,14]. Particles that are measured by mass passing through a sampler inlet with a 50% efficiency cut-off at 10 µm and 2.5 µm are referred to as PM_{10} and $PM_{2.5}$ respectively. On the other hand, UFPs are quantified as particle number concentration since their mass is negligible. Unlike the main air pollutants, particulate matter is not a specific chemical entity, but, being a mixture of particles from different sources, it can have a highly variable composition, depending on the sampling season and size. In general, particulate matter consists of: sulphates, nitrates, ammonium ion, sodium chloride, carbonaceous particles, metals, mineral dust, biologic materials (such as pollen, spores, bacteria, endotoxins) and water. Carbonaceous particles are generally defined by measurement techniques and thermal and optical properties.
I report here the following definitions:

- Total carbon (TC) mass: describe the mass of all carbonaceous matter in airborne particles [15].
- Elemental Carbon (EC): defined as a "substance containing only carbon, not bound to other elements, but which may be present in one or more of multiple allotropic forms" [16], it is quantified using thermal and optical methods [17].
- Organic carbon (OC): comprises a large set of compounds in which carbon is chemically bonded with other carbon atoms, hydrogen and other elements such as oxygen, sulphur, nitrogen, phosphorus, chlorine, etc.. Polycyclic aromatic hydrocarbons are (PAHs) are included in this category.
- Black carbon (BC): the term "black" implies that this component is responsible for the absorption of visible light. BC is a useful qualitative description when referring to light-absorbing carbonaceous substances in atmospheric aerosol. It is quantified using optical methods [15, 17].

- Black soot (BS): referring to carbonaceous particles formed from incomplete combustion. It is itself a harmful air pollutant and is a climate forcing agent contributing to climate change.

As reported in Figure 1.2 (b), depending on their size, the particles can settle in different regions of our respiratory system. Specifically, decreased particles size increases the penetration into the lungs: the coarse fraction tends to deposit in the upper tract of the respiratory system, from the nose to the tracheobronchial region, whereas the fine and ultrafine fractions go deeper to deposit in the alveoli region, where some of them can also enter into the bloodstream. This characteristic mainly concerns UFPs, which deserve their own section as they are one of the topic of my analysis.

The interaction of the airborne particles with human cells results in oxidation stress and inflammation as a first response [19–21]. The mechanisms with which these particles act are represented in Figure 1.3 (b). The first defense cellular response to increasing level of reactive oxygen species (ROS) is the activation of Nuclear factor (erythroid-derived 2)–like 2 (Nrf2) [22, 23] which induces the expression and activation of antioxidant, antiapoptotic and detoxification proteins. When this mechanism fails, ROS accumulation induce the activation of inflammatory pathways, as NF-kβ and consequently release of cytokines [24]. The imbalance between ROS and anti-oxidative compounds, with the prevalence of the former may in the long-term culminate in a plethora of cardiovascular risks [24, 25].

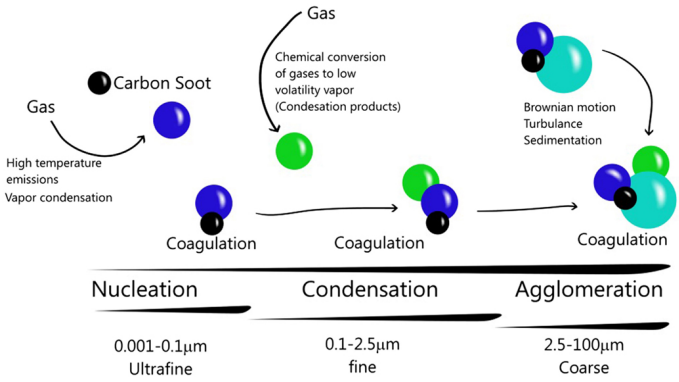

(a) Particulate matter formation.

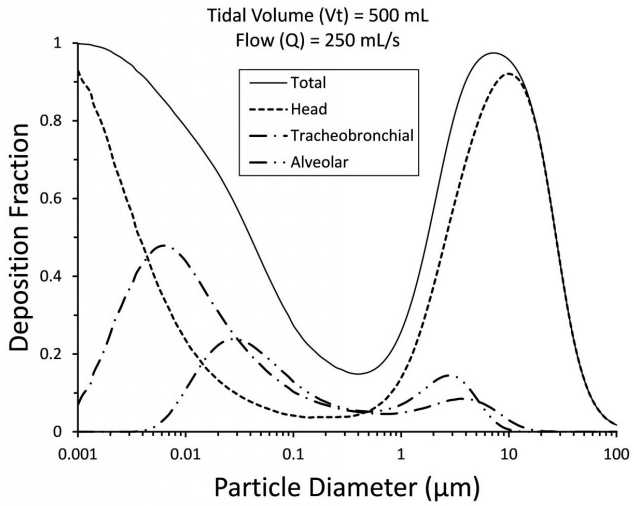

(b) Deposition based on particles diameter.

Figure 1.2: Figure (a): secondary aerosols formation consisting of three major steps, nucleation-condensation-agglomeration, in which particles can be modified or increase their size. From [26].
Figure (b): Deposition fraction based on particle diameter at a respiration rate of 15 breaths per minute (bpm) for a tidal volume (Vt) of 500 mL and a flow rate (Q) of 250 mL/sec. From [3]

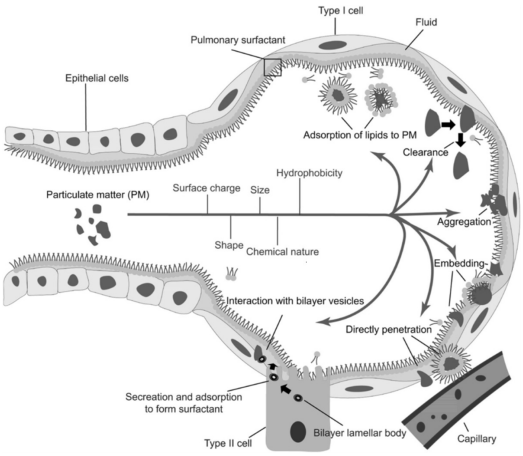

(a) Particulate matter into alveoli.

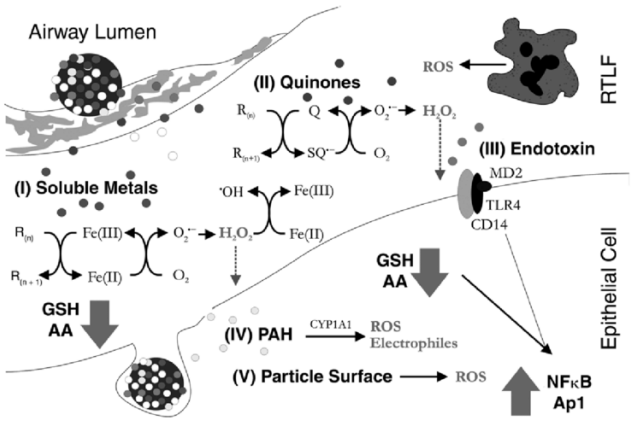

(b) Mechanisms of induction oxidative stress by the particles.

Figure 1.3: Figure (a): Inhalation of particulate matter and their interaction with pulmonary surfactant. PM can penetrate lung surfactant to invade capillaries barrier and enter into the bloodstream. Re-adapted from [27].
Figure (b): in [19] they reported the following principal mechanisms of oxidative stress induction by air particles inhaled by the respiratory system. As a first step particles diffuse in the respiratory tract lining fluid (RTLF) where they can induce oxidative stress to the alveolar macrophages and to epithelial cells. The main mechanisms are: 1) introduction of metals, that might be adsorbed on the surface of the particles that can react with O_2 and H_2O_2 and promoting further radical generation, including the highly reactive hydroxyl radical (OH^-); 2) Polycyclic aromatic hydrocarbons (PAHs) and Quinones on the PM surface can undergo in redox cycling to form the semi-quinone radical that also result in O_2 and H_2O_2. Specifically to PAHs, they are converted in Quinones by cytochrome P450 1A1 (CYP1A1) and and epoxide hydrolase. 3) The bacterial components on particles surfaces can also trigger inflammation.

1.1.1 Ultrafine particles

UFPs are nanoparticles with unique properties. They are dispersed in the environment all around us and can be generated by both anthropogenic and natural processes. The ones which come from human activities are part of anthropogenic incidental nanomaterials category, defined in [28] as "nanomaterial unintentionally produced as a result of any form of direct or indirect human influence or anthropogenic process". UFPs have a short life span in the atmosphere: by Brownian diffusion they are rapidly deposited, they otherwise accumulate and coagulate with each other into larger particles (1.2a). They show in fact a decreasing gradient dependent upon time and distance from the generating source [29,30]. However, the level of concentration in urban environments remains persistent due to the effects of the internal vortex of traffic flow and/or the temperature gradient within the city [31]. Vehicle emissions are the main anthropogenic source of UFPs within urban environments, as indicated in "Industrial emissions of nano- and ultrafine particles" report [32] of the European Commission. They estimate, in 2008, that 34% of UFP is emitted from road transport and 22% from other transport and machinery, 12% industrial combustion, agriculture 8%, industrial processes 5% and 4% of power generation [32]. It can be deduced therefore that those most exposed to such negative impacts are individuals living closer to highly trafficked roads and those driving across the urban grid on a daily basis [33–35]. It is also important to consider indoor environments, ranging from one's own living space to workplaces, where inadequate ventilation can lead to high concentrations of nanoparticles. The question that arises is why these particles are so dangerous to our health. Certainly, the first reason is their size. After the inhalation of UFPs, they enter into the lungs where they can persist longer because they can escape phagocytosis by alveolar macrophages, thus they deposit in the alveolar cavities. Here, as already mentioned above, a part of them can translocate into the bloodstream through the capillary barrier, as shown in Figure 1.2 (a) [27,33] and reach the other organs. UFPs have high oxidative potential due to their large surface area, and can therefore adsorb hazardous metal and organic compounds that are deleterious to

our health increasing their toxicity [20,23,36,37]. This can lead to cell injury and tissue damage, which in return enhance inflammation. Another concern of UFPs is that, unlike other PM fractions, they have not been directly targeted by standard regulation yet. This obviously makes it more difficult to try and tackle the problem. The most effective general measure to diminish their air concentration today is to limit the magnitude of traffic flows by particles-emitting vehicles.

1.2 Overview of the work

My PhD project is part of a co-tutorship agreement between Università degli Studi di Parma, Ludwig-Maximilians-University of Munich and in association with Helmholtz Zentrum München, where I had the chance to spend part of the time dedicated to my research. The project begun as part of AWAIR (Environmental integrated, multilevel knowledge and approaches to counteract critical air pollution events, improving vulnerable citizens quality of life in Central Europe functional urban areas), a program with the goal of defining new air quality indicators at European level to achieve greater health protection for EU citizens. The project was financed by Interreg Europe and was coordinated by ARPAE - Emilia Romagna, and has as Italian partners the Municipality of Parma and Consorzio CINSA (National Inter university Consortium for Environmental Sciences). The European partners involved in the project are the municipalities of Budapest (Hungary), Katowice (Poland), and the Institute of Epidemiology at Helmholtz Munich (Germany).

My role as a researcher has been to evaluate the effects that air pollution can have on human health, investigating this broad topic from different points of view and considering its complexity at microscopic and macroscopic level.

The first phase of my research, conducted at the University of Parma, consisted of a toxicological study assessing how UFPs impact our health at molecular level, by studying molecules' interactions and consequent pathways activation. To tackle this question we used specific Engineered Nanomaterials (ENMs) as a proxy for environmental UFPs to facilitate the study of their

toxicity.

The second phase, conducted at Helmholtz Munich, aimed at exploring the association of cardiovascular health with long-term exposure to air pollutants. This association was studied in detail comparing cross-sectional data on pollutants concentration and specific inflammation- and coagulation-reflecting biomarkers.

This dissertation is divided in two parts, reflecting the two paths of my PhD project. Both parts are developed with a similar structure, and comprehend specific conclusions at the end of each part. A conclusive chapter can be found at the end of the thesis, with remarks and observations regarding the broader topic of my entire project.

Part I

Engineered nanoparticles: an opportunity to study toxicological effects of Ultrafine particles

Chapter 2

Background I

The general research question of my work has been: what is the effect of UFPs exposure on human cells?

Performing *in vitro* toxicological studies with UFPs poses some challenges in regard to the sampling procedure. For instance, the amount of UFPs mass required is very large, and there is a risk of inducing physico-chemical changes during sample preparation [31, 38]. Furthermore, the classical "sampling-extraction-exposure" procedure, which has always been used in toxicological PM *in vitro* studies, would not reliably reproduce real exposure to UFPs given the strong dependency of their physico-chemical characteristics on the emission [39] source. Since size is the key feature of UFPs related to their impact on human health, we chose to use Engineered nanoparticles (ENPs) as surrogate particles to investigate this impact at the cellular and molecular level. This makes it possible to extrapolate useful information on the size-dependent effect of nanoparticles, and it also consistently simplifies the sampling procedure. Nanotoxicology has taught us a lot about the molecular mechanism induced by nanoscale particles. This part of the work wants to progress in this direction, and contributes to expanding our knowledge on the topic.

2.1 The Nano world

Before starting with the definitions, I think it is important to point out that the "definition of nanomaterials (NMs)" is still an active scientific and political debate because of their use in regulatory assessment.
Today, NMs in REACH (Registration, Evaluation, Authorisation and Restriction of Chemicals), are treated as any other chemicals [40]. I will give here the main and accepted definition. NMs are defined as materials that have structural components smaller than 1 µm in at least one dimension; generally speaking any organic, inorganic, or mixed (organometallic) material that presents distinct chemical, physical, and/or electrical properties owing to their nano sized [28,41]. According to [42] NMs can be classified by their dimensionality. One-dimensional (1D) structured materials have two nano dimensions [43] and one no-nanometer size [44]. Examples in 1D NMs include nanotube, nanofiber, nanowire and nanorod, and nanofilaments. 1D nanomaterials are widely used in electronics, as they can be highly conductive and sensitive. Those with two-dimensional (2D) materials in the nanoscale include ultra-thin films on a surface and multi-layer material, disc and platelets. They have been explored for various applications in electronics, optoelectronics, sensors, catalysis, etc. [45]. The third type nanomaterials (3D) are also known as bulk nanomaterials. The 3D materials contain dispersions of nanoparticles, bundles, nanowires, and nanotubes. Zero-dimensional (0D) materials are sized at nanoscale level in all three dimensions [43, 46], simply nanoparticles. Nanoparticles (NPs) are the subject of my study so we will focus mainly on these. NPs are produced from both natural and anthropogenic processes (Figure 2.1).
The former are mainly produced by biogeochemical process, such as sea spray, dust storms, forest fires, volcanic eruptions [28, 47, 48].

On the other hand, the latter can indirect and direct produce NPs, and are divisible in: incidental nanopoarticles which are an unintentionally result of any anthropogenic process such as from vehicle emission (UFPs), incomplete combustion in heating and cooking and in industry emission etc.; while intentional nanoparticles are designed to have specific chemical and physical

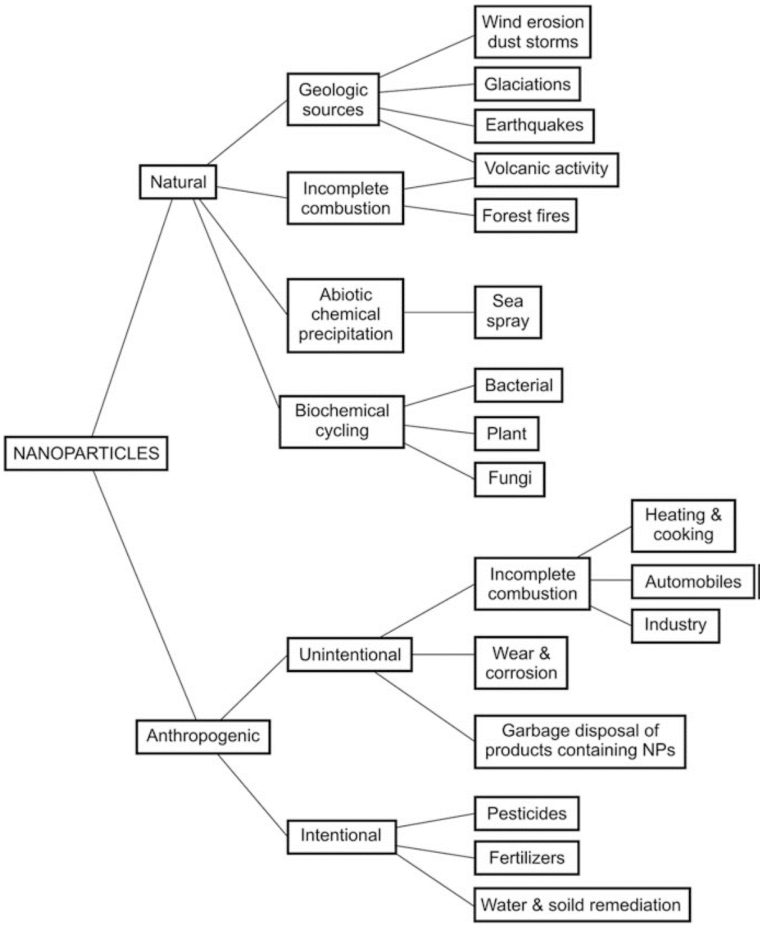

Figure 2.1: Natural and anthropocentric sources of nanoparticles. From Cristina Buzea and Ivan Pacheco [47]. Nanoparticles (referring to zero-dimensional (0D) nanoscale materials in all three dimensions [42])can be divided into: natural NPs, mainly produced by biogeochemical processes, and into anthropogenic NPs, which include unintentional (UFP) and intentional (engineered NPs).

properties, which are ENPs [28]. Considering the definitions above, NPs are not only present as a component of outdoor air pollution, certain working-environments have been demonstrated to provide conditions of nanoparticles' concentration even higher than the outdoor environment [35, 49]. Specifically, these conditions have been found in relation to the use and production of ENPs [33, 35, 50], which today represent an interesting technology with a growing number of applications in a wide range of sectors. In Figure 2.2, the graph shows a representation of ENPs applications in different fields [51].

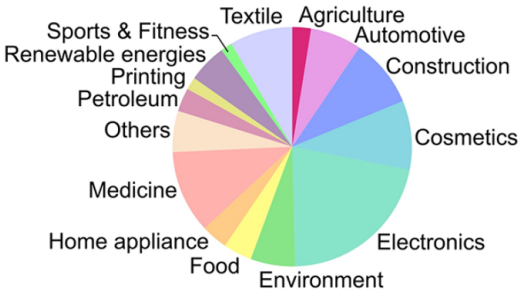

Figure 2.2: "Global nanoproducts stats by the end of 2018", distribution across industries. From [51]

Some of these fields are: electronics, biomedical science for diagnosis, imaging and drug delivery, agriculture, food industry, cosmetics and other purposes [52]. The increasing frequency for occasions of exposure to ENPs necessarily leads to the need of information on their possible health impact. To this purpose, already in 2004, K. Donaldson and colleagues [53] founded a subcategory of toxicology, namely Nanotoxicology.

The effects of ENPs are closely linked to their physico-chemical properties, which may be very different from UFPs. Nevertheless, ENPs present various characteristics that make them a suitable and easily accessible proxy for the study of the interactions between UFPs and human health [23, 54]. Some of these characteristics are presented in the following Table 2.1, re-adapted from [55].

The main common feature is the size, and focusing on inhalation as a

Table 2.1: Comparison table between UFPs and ENPs. Re-adapted from [55].

Nano-sized particles		
	Unincidental	**Incidental**
Features	**ENPs**	**UFPs**
Sources	Manufacturing processes	Incomplete combustion(vehicles, industry, etc..)
Morphology	Regular (sphere, as 0D-NMs)	Irregular
Homogeneity	Yes	No
Organic chemical content	Low	High
Metal impurities	Varies	High
Ros generation	Varies	Yes
Exposure routes	Inhalation, skin, ingestion, injection	Inhalation
Adverse health effects	Varies	Yes

route of exposure, they share the same entrance into our system where both can induce oxidative stress and systemic inflammation.

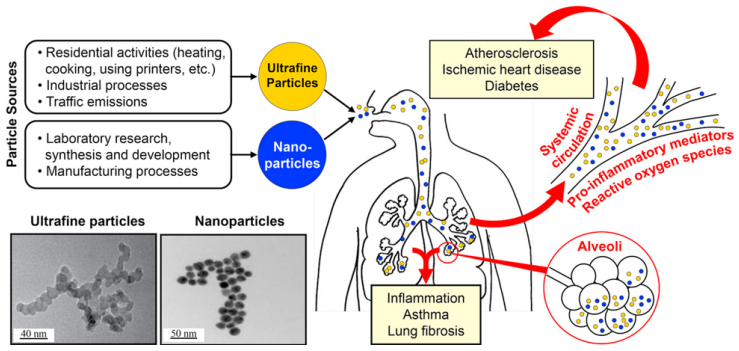

Figure 2.3: Inhalation of different types of nanoparticles and entry into our bodies. From [23].

I reproduced here the following Figure 2.3 taken from [23], because I think it sums up well what has been said so far. We used a specific kind of ENPs for our research in order to study the effects of nanometer-sized particles at

the cellular level. These are Cadmium Sulfide Quantum Dots (CdS QDs). In the following section I will cover some of their most meaningful characteristics.

Quantum Dots (CdS QDs)

Quantum dots (QDs), engineered nanomaterials, are zero-dimensional semiconductors in the size range of 1-10 nm in which electrons are strongly and completely confined. Because of this, size and shape, they have unique optical properties: sharp and symmetrical emission spectra and high fluorescence and photostability [56]. Larger QDs of 5-6 nm in diameter emit longer wavelengths, producing colours such as orange or red. Smaller QDs (2-3 nm) emit shorter wavelengths, producing colours such as blue and green. However, the specific colours vary depending on the exact composition of the QDs. The core-shell design implies that the nanocrystals consist of a semiconductor core material with quantum dots, surrounded by a semiconductor shell and surface capping ligands to reduce the vulnerability of the core. They have found applications in various fields, but particularly in nanomedicine as they are, for example, a useful tool as biological labels: by surface modifications (ligands) they can be adapted to bioconjugate with biological molecules such as proteins, oligonucleotides, antibodies [57]. Other examples in nanomedicine of QDs applications are in bio-imaging, in diagnostic agents for tumor detection, and in molecular probes for drug delivery to monitor therapeutic efficacy. Given these exciting results, it is important to study their toxic effects at the molecular level. In my PhD project I used Cadmium Sulfide QDs (CdS QDs), which have attracted much interest in biomedical applications because of their high surface area and good conductivity [58],

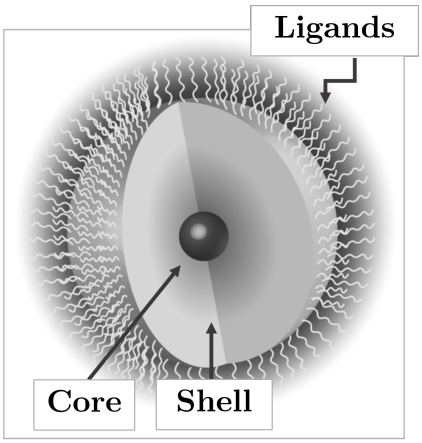

Figure 2.4: Core-shell QDs structure.

which makes them excel in terms of optical and electrical properties [58, 59]. On the other hand, the concern about their cytotoxicity is still a topic of discussion today, especially regarding their interaction with biological molecules. They could aggregate and agglomerate within the cells, and, moreover, the possible release of cadmium is not fully understood.

2.2 Overview of the impact on human health

We are constantly exposed to NPs, being them natural or anthropogenic, in indoor or outdoor environments.

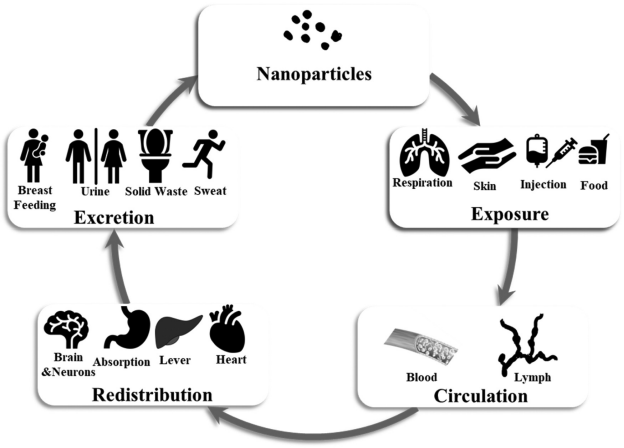

Figure 2.5: Complete cycle from inhalation of NPs to final excretion from the human body. From [50].

With nanotoxicology we want to know how these particles affect us. The main route of exposure to NPs is through inhalation followed by ingestion, skin absorption, and injection [50]. Malakar [50] and colleagues have clearly represented graphically the exposure pathway and the complete cycle of NPs in our body, Figure 2.5. As already mentioned above, the biological impact of NPs depends on their physical and chemical properties, which are: size, agglomeration or aggregation, surface morphology and charge, solubility in different media [60]. These parameters can modify internalization by cells, binding to proteins, translocation within the organism and the possibility of cause tissue damage [61]. Their small size allow them to reach every part of

our body and this can be both, an opportunity and a threat. In relation to the inhalation of nanoparticles, the first organ target are the lungs where they can cause pulmonary inflammation, bronchitis, asthma and in the worst case lung cancer. From the lungs, a small fraction of them enter the bloodstream through the capillary barrier and travel to other parts of the body that larger particles cannot reach. In addition, several studies [60,62–64] evidenced that the spherical shape of NPs facilitates uptake by cells since more time is needed to envelop elongated particles [65], consequently affecting the toxicity level. Surface charge is the major determinant of cellular internalization, positively charged particles were generally better taken up than the negative ones [66]. Conversely, neutral charged particles do not interact much with biological materials [65]. The chemical composition is a key parameter to consider; the chemicals adsorbed on the surface of the core can influence their effects both negatively and positively. The negative effects are often attributable to metals compounds on both natural and anthropogenic particles, which increase the toxicity. On the other hand, specific modification on the surface of ENPs can also result in a diminishing of cytotoxicity. Moreover, due to the high surface energy, when NPs are close to each other tend to agglomerate and aggregate. The former is characterized by weak forces and tend to form larger particles resulting in a reduction of surface free energy; instead, the latter consist of strong chemical forces between the particles [67]. Just to mention that NPs also interacts with proteins resulting in the formation of a dynamic nanoparticle-protein corona. This interaction may affect the uptake by the cells of NPs with changes in the cellular response [68–70].

2.2.1 Mode of action of NPs

The primary mechanism of NPs' toxicity appears to be the increase in reactive oxygen species (ROS) and the consequent imbalance in the antioxidant level. In general, NPs generate ROS production via chemical interactions or via direct contact with membrane and organelles. Rising ROS levels can induce a variety of signaling pathways. They can influence the homeostasis of intracellular calcium level, the increase of which can lead to the activation of

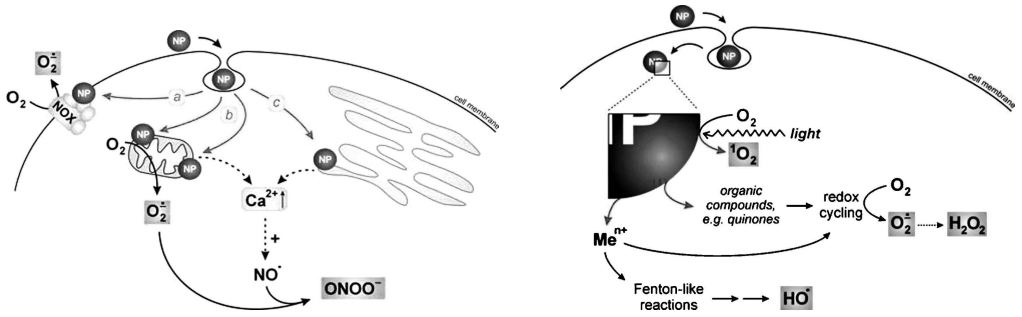

(a) Direct contact of NPs with cellular comparts.

(b) Chemical reactivity of NPs.

Figure 2.6: ROS production via chemical and physical interactions.
Figure (a) shows the interactions of NPs with NADPH oxidase (NOX) complexes, mitochondria and the endoplasmic reticulum. These interactions cause membrane damage and induce an unbalanced level of ROS. As a result, Ca^{2+} is released from the damaged organelles.
Figure (b):represent the generations of ROS through chemical reactivity. The details have already been explained in the introduction, Figure 1.3 (b).

other different signaling pathways, such as c-Jun N-terminal kinase (JNK), Nuclear factor kappa B (NF-kβ), as well as extracellular signal-regulated kinases/ mitogen-activated protein kinases (Erk/MAPK) [71]. Two important cellular defense mechanisms are apoptosis and autophagy, which will be briefly discussed in the following section.

Apoptosis

Apoptosis is programmed cell death that occurs in response to a variety of stimuli. It is a normal process that is already used during early development, for example to select cells during embryogenesis and to eliminate the unwanted ones [72]. Apoptosis, in contrast to necrosis, is a process of controlled cell death that does not induce inflammation of the surrounding tissue. Stimuli, like DNA damage (which cannot be repaired), abnormal folding of proteins, infection can induce apoptosis and its absence can lead to cancer. There are two main mechanisms that induce apoptosis: extrinsic and intrinsic pathway. The extrinsic one occurs when the cell is stimulated by an external event through ligand binding to the death receptors, which

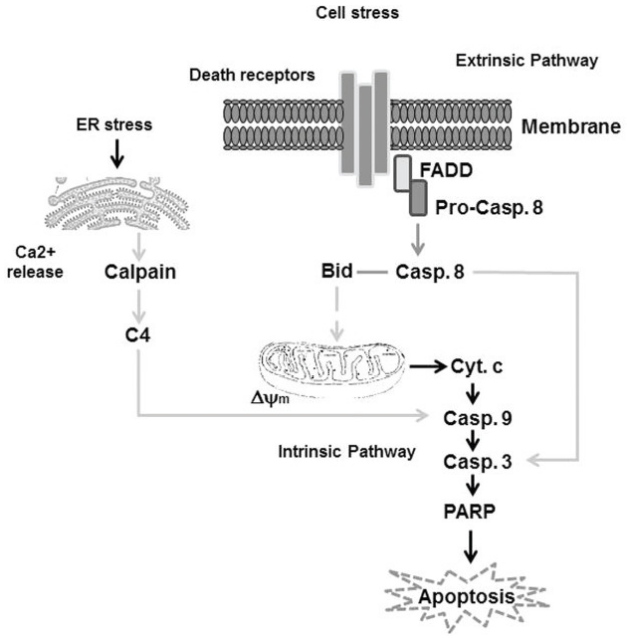

Figure 2.7: Schematic representation of the extrinsic and intrinsic apoptosis pathway, from [73]. Generally, extrinsic apoptosis is induced through activation of the Fas-associated death domain (FADD) as a result of cellular stress, which activates recruitment of caspases. Intrinsic apoptosis is induced as a consequence of damage to mitochondria as a loss of membrane potential, as well as being mediated by increased levels of ROS and consequently by dysregulation of intracellular Ca^{2+} [73].

are: Fas receptors, tumor necrosis factor (TNF) receptors, and TNF-related apoptosis-inducing ligand (TRAIL) receptors. When receptors are bound to their ligand they induce the activation of FADD and TRADD, adaptor proteins, which activate intracellular pro-caspases 8 and 10 and the effector phase begins.

On the other hand, the intrinsic apoptosis is trigger by different cellular stresses, such as DNA damage. It is called also mitochondrial apoptosis because it is mediated by these organelles, the control of apoptosis is ensured by the balance of anti- and pro-apoptotic signals by proteins called BCLs: the main anti-apoptotic factor is BCL2, while the most important pro-apoptotic BCLs are BAX and BAK [74]. If the action of BCL2 prevails over the others, the cell does not undergo apoptosis, but if proteins known as BH3, which are only sensors of cellular stress, intervene, the BAX and BAK channels open

and allow the pro-apoptotic enzymes that activate caspases (e.g. cytochrome c) to leave the mitochondrion. The caspase activated in the intrinsic pathway is caspase 9. Both mechanisms lead to the execution pathway that starts with caspase 3; the results of apoptotic process are the following: in characteristic cytomorphological features including cell shrinkage, chromatin condensation, formation of cytoplasmic blebs and apoptotic bodies and finally phagocytosis of the apoptotic bodies by macrophages [75, 76]. Nanoparticles can induce apoptosis through both mechanisms described above. Increased expression of caspase-8, Fas, FasL, FADD was observed in cells treated with NP (nanoparticles) in both *in vitro* and *in vivo* experiments [77]. It has been observed that NPs can induce the activation of death receptors through activation of the NF-kβ pathway which is the main signaling pathway of the inflammatory response [78]. NPs are more frequently associated with intrinsic apoptosis because the most recognized targets of NP-induced cytotoxicity are mitochondria. The increased level of ROS production due to mitochondrial damage, in addition to DNA damage and other organelles, can increase the inflammatory response that can lead to apoptosis. As already mentioned, dysregulation of the normal apoptotic process may lead to cancer due to uncontrolled cell division and permit to survive genetically unstable cells [79].

Autophagy

Sevaral studies have reported the link between NPs and the autphagic process [80–82]. Autophagy is a natural biological pathway that occurs when the cell needs to be "cleaned" of unnecessary or dysfunctional cellular components or to eliminate harmful material, it is a kind of recycling process also called "self-eating" [83]. Autophagy consist of three major steps which are initiation, nucleation and elongation in autophagosome formation. Its induction is originated from various condition of stress e.g. oxidative stress, hypoxia and starvation. Mammalian target of rapamycin (mTOR) kinase is a mediator of autophagy in the initiation phase: its activation leads to inhibition of the autophagic process through the phosphorylation of multiple proteins included in ULK- unc-51 like autophagy

activating kinase complex involved in the nucleation of phagophore. Conversely, non-activation of mTOR leads to induction of autophagy by the activation of ULK complex which phosphorilate III PI3KC complex components to trigger the nucleation of the phagosome. The components of III PI3KC activate PI3P (phosphatidylinositol-3-phosphate), which enriches the membrane of the omegasome, the precursor of the autophagosome. Subsequently, the complex ATG5-ATG12-ATG16 is recruited for the elongation and conjugation with LC3 proteins. In this reaction LC3-I is converted to LC3II and it is involved in closing the membrane of the phagophore and also in the cargo sequestration. The vesicle resulting from the closure of the phagophore membrane is the autophagosome, which fuses with the lysosome to form the autolysosome to degrade the sequestered cargo [80–82, 85]. This is the key mechanism of macroautophagy [86]. NPs enter cells via endocytosis [87] and they are recognized as foreign, hence the first reaction is to eliminate them via the endolysosome pathway and/or through sequestration by autophagosomes, following the macroautophagy mechanism.

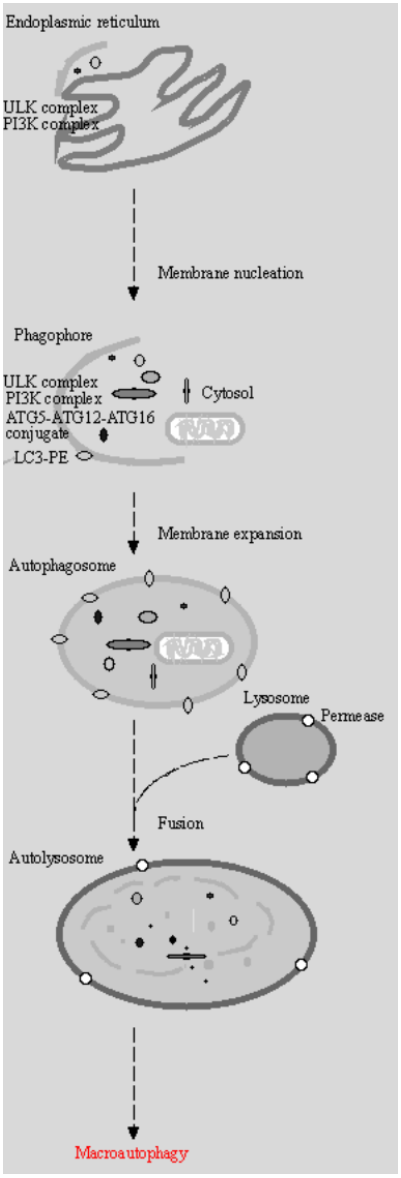

Figure 2.8: Graphical representation of autophagy steps. From KEGG maps website [84]

The problem occurs when there is a malfunction of the lysosomes due to interaction with NPs that can lead to blockage of autophagic flow and, in the worst-case scenario, in pyroptosis. Excessive production of ROS causes damage to mitochondria resulting in a selective autophagic

process called mitophagy [88–91], which is a cellular response pathway linked to NPs exposure. Mitophagy and apoptosis are correlated; if the damage is not resolved the cell goes into apoptosis.

2.3 Studing the nanotoxicity

In vitro studies are an efficient, rapid and cost-effective tool to investigate the effects of nanoparticles. The advantages and disadvantages of an *in vitro* study compared to an *in vivo* study also depend on the final purpose of the work. In our case, the main advantage is the identification of primary mechanisms of toxicity at molecular level in a particular tissue in the absence of secondary effects and compensatory factors. We conducted an *in vitro* study in order to investigate the cellular responses of two different cell lines, which are: 1) HepG2 derived from human hepatocellular carcinoma, and 2) THP-1 monocytes from an acute monocytic leukemia patient. We chose these two cell lines because they represent two important routes of exposure: macrophages are the first to respond to external agent, therefore represent our first response to NPs inhalation; Hepatocytes, on the other hand, are involved in the detoxification process in the liver, where Cd (II) and also NPs can accumulate [92, 93].

2.3.1 Interactome analysis: miRNA-mRNA

What happens inside the cell is difficult to predict, a dynamic and complex network of interacting molecules based on the Central dogma of molecular biology [94]. Starting with DNA, cells read and express genetic instructions by transcription and pass them on to proteins by translation. Epigenetic modifications play an important role in the control of gene expression in response to specific stimoli. MicroRNAs (miRNAs), as epigenetic modulators at the post-transcriptional level, can inhibit the expression of target genes. In this work we tried to analyze the interaction between miRNAs-mRNAs. MiRNAs are small noncoding RNA molecules longer $\sim$ 22 nucleotides. MiRNAs are known to inhibit their target genes, however several studies have reported

that miRNAs can also induce up-regulation of a gene target [95, 96]. These interactions are reflected in various biological processes and thus, in pathologies. Indeed, miRNAs are considered to be promising biomarkers [97] since they result to be organ-, tissue- or cell-specific [98]. Canonical miRNA biogenesis begins in the nucleus with transcription of the relevant gene by RNA polymerase II to generate the primary miRNA (pri-miRNA).

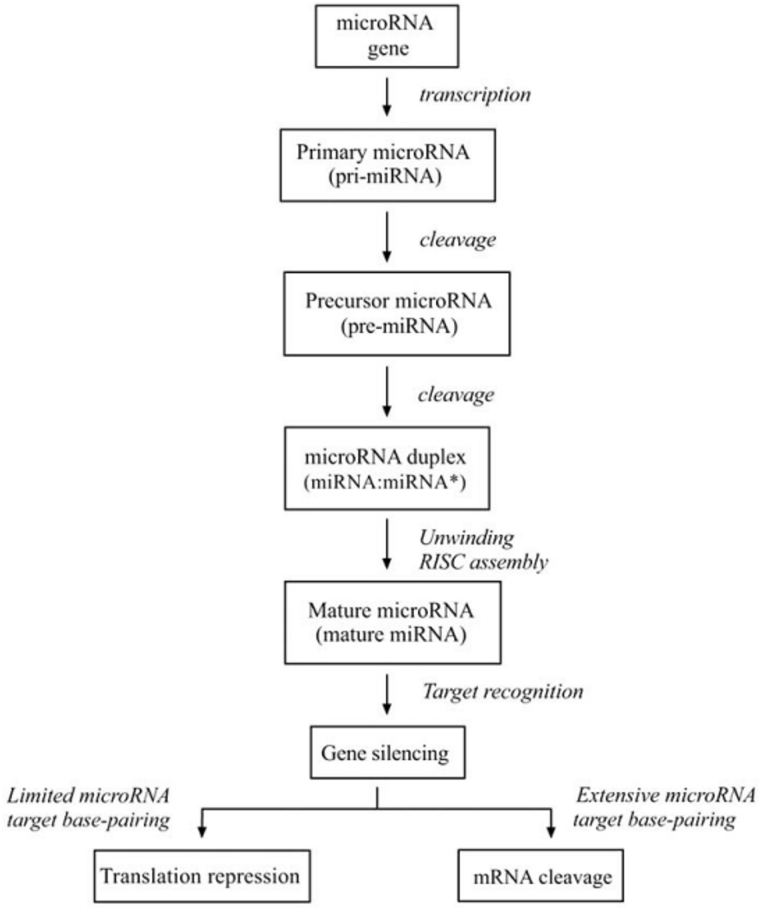

Figure 2.9: Diagram of miRNA biogenesis and how they interact with mRNAs, from [99]. Generally, transcription of the miRNA gene produces the miRNA precursor (pre-miRNA). This is subjected to cleavage to generate the microRNA duplex, which then results in mature miRNA that can induces gene silencing [99].

The pri-miRNA molecule is cleaved by the microprocessor complexes,

Drosha and DGCR8, into pre-miRNA with hairpin shape. Exportin-5 transports the pre-miRNA into the cytoplasm where it is processed by the RNase III Dicer endonuclease resulting in a mature miRNA duplex [100]. From the mature miRNA, one strand, 5' ends with lower stability, bind with AGO protein to form RNA-induced silencing complex (RISC) [101]; instead the other strand of the duplex is degraded [102]. The miRNAs 5' seed region bind with mRNAs target usually at the 3' untranslated region (3'UTR) and based on their base pair complementarity, the mRNA is either directly cleaved and degraded or its translation is repressed [95, 99, 100, 102]. A single mRNA can be regulated by several miRNAs; conversely, a single miRNA could affects hundreds of mRNAs targets. The result is a large network of interactions that may help to better understand the molecular mechanisms behind exposure to toxic substances. In addition, analysis at the protein level can help to get an overall picture. In our previous work [90], we deeply analyzed the response of miRNome profiles of HepG2 and THP-1 exposed to CdS QDs, and Cd^{2+}. Here, using RNA sequencing we studied the transcriptomic responses of both cell lines through the Differentially Expressed Genes (DEGs) and pathway analysis. Then, we integrated the resulting transcriptomic data with miRNome profiles to obtain a comprehensive picture of miRNA-target interactions and induced biological processes.

Chapter 3

Materials and Methods I

3.1 Preparation of CdS Quantum Dots

Quantum dots used for this work were manufactured at IMEM-CNR (Parma, Italy), the synthesis process is described in [103]. In general CdS QDs were synthesized by thermolysis of a cadmium bis-thiolate precursor in octadecene (ODE) at boiling temperature 315 °C. The synthesis was carried out by a simple one-pot process. They were characterized in deionized water by transmission electron microscopy (Hitachi HT7700, Hitachi High Technologies America, Pleasanton, CA). Other specific information about synthesis and characterization are in [103]. The resulting CdS QDs have crystalline structure with a mean static diameter of 5 nm with approximately 78% in Cd. Measurements in deionised water reported the zeta potential to be +15.0 mV and the average particle size (dh) of the aggregates to be 178.8 nm (Zetasizer Nano Series ZS90, Malvern Instruments, Malvern, UK) [104]. CdS QDs were suspended in Milli-Q water at a concentration of 100 µg mL^{-1}, then sonicated with a pulsed probe to minimize aggregation. For cell treatment, the stock particle suspension was vortexed and sonicated for 30 min, and then diluted as appropriate into complete culture medium [90].

3.2 Cell culture and treatments

Cell culture method is reported in [90]. HepG2 were cultured in Dulbecco's Modified Eagle's Medium (DMEM) containing 10% fetal bovine serum (FBS), 100 µg mL^{-1} streptomycin, 100 U mL^{-1} penicillin, 4 mmol L^{-1} glutamine. THP-1 cells were cultured in RPMI-1640 medium containing 10% fetal bovine serum (FBS), the glutamine concentration was reduced and it contained an high concentrations of vitamins. Cells were cultured in 10-cm Petri dishes under a humidified atmosphere at 37°C in the presence of 5% CO_2. Prior to treatment, THP-1 cells were differentiated into macrophages through an incubation with 0.1 µM of phorbol 12-myristate 13-acetate (PMA) for 3 days. The medium was replaced after 24 h with a fresh one containing either CdS QDs or Cd(II) (as $CdSO_4$ 8/3 -hydrate). Each treatment was carried out in triplicate (biological replicates) and each replicate was measured three times (technical replicates). The cells were treated with a subtoxic dose of CdS QDs and with the equivalent dose of Cd(II). Specifically, HepG2 cells were exposed to 3 µg mL^{-1} of CdS QDs and to 5.2 µg mL^{-1} of Cd(II); THP-1 cells were exposed to 50 µg mL^{-1} of CdS QDs and 11.4 µg mL^{-1} of Cd(II). The latter does not correspond to the equivalent dose of 50 CdS QDs µg mL^{-1} because this would be too high for the cells, but corresponds to 6.4 µg mL^{-1} of CdS QDs.

3.3 Mitochondrial membrane potential assay

We performed the JC-1 kit (Abcam Ltd, Cambridge, UK) assay to assess the mitochondrial health. The JC-1 dye is a cationic carbocyanine marker of mitochondrial membrane potential ($\Delta\Psi m$) that accumulates in mitochondria: when the $\Delta\Psi m$ is low the dye is present as a monomer and produces a green fluorescence ∼529 nm; conversely, when the $\Delta\Psi m$ is high JC-1 tends to aggregate and accumulates within the mitochondria and emit red/orange fluorescence ∼590 nm. Active mitochondria reveal a red fluorescence signal as opposed to the green fluorescence that is a signal of depolarization of the mitochondrial membrane. Both cell lines, HepG2 and THP-1 were

examined with JC-1 and as a positive control we used Carbonyl cyanide-p-trifluoromethoxyphenylhydrazone (FCCP), proton ionophore which interferes with the proton gradient. The preparation of cell lines is described in [90]. Both of them were seeded into 96-well plates at a density of 7.5×10^4 cells per well and were incubated for 24h. Subsequently, were exposed to CdS QDs and to the equivalent dose of Cd^{2+}. We performed several washes of the cells in phosphate buffered saline (PBS) in order to remove adherent particles or aggregates of QDs. Then, we incubated them with JC-1 dye for 30 minutes at 37 ℃ without light. After that, the cells were washed with PBS and the fluorescence was assessed by a multimode plate reader (Perkin Elmer Enspire and expressed as Relative fluorescence unites -RFU-. Each experiment was conducted in triplicate.

3.3.1 Confocal microscopy

Cells were seeded on four-chamber slides at a density of 5×10^4 cells mL^{-1} and treated with CdS QDs and with the equivalent dose of Cd^{2+}. Then, cells were transferred to a medium containing 5 µmol L^{-1} of JC-1 for 30 min. HepG2 and THP-1 cells were rinsed in complete culture medium and maintained in culture medium, at 37 °C and 5% CO_2, thus using an inverted Zeiss LSM 510 Meta laser scanning microscope, we were able to observe them. JC-1 dye conditions was detected by excitation at 480 nm and the emission was passed through a filter of 535-595 nm. In selected experiments 5 µmol L^{-1} of DRAQ5™ (Alexis Biochemicals, CA, USA) fluorescent probe was added together with JC-1; for visualization, excitation was set at 633 nm and emission through a long-pass filter at 670 nm. Furthermore, to visualize the cytoplasm of THP-1 cells exposed to 50 µg mL^{-1}, 1 µmol L^{-1} of Calcein-AM (Millipore Merck, Burlington, MA, USA) was use for 2h. Subsequently, THP-1 cells were excited at 488 nm and the fluorescence were measured through a 515-540 nm band pass filter.

3.4 RNA Isolation and mRNA Expression Profiling

RNA was isolated from both cell lines after 24h exposure with CdS QDs and Cd (II) using *mir*VANA™ miRNA Isolation kit (Ambion, Life Technologies) following the manufacturer's instructions. Integrity of RNA samples was monitored by gel electrophoresis and quantified using spectrophotometer. The same RNA samples were used for miRNome profile quantification and RNA sequencing.

miRNAs quantification

TaqMan®Array Human MicroRNA A+B Card Set v3.0 (Applied Biosystems, Foster City, CA, USA), was used for miRNA quantification analysis, quantifying a total of 754 miRNAs, 384 per card. Megaplex™ RT Primers (Applied Biosystems), was used in order to reverse-transcribe 1 µg of RNA isolated. Subsequent, PCR array was run using a 7900 H T Fast Real Time PCR system (Applied Biosystems), following the MegaPlex™ Pool Protocol (PN 4399721 RevC). Raw data were analyzed using RQ Manager 1.2 software (Applied Biosystems) and relative abundances were calculated using the $2^{-\Delta\Delta Ct}$ with a threshold set at 2 for increased miRNAs and 0.5 for the decreased ones [105].

RNA sequencing

RNA sequencing was performed by IGA Technology Services (Udine, Italy). Treatment and control samples, for both cell lines, were sequenced following the manufacturer's instructions developed by the IGA laboratory. CASAVA version 1.8.2 of the Illumina pipeline was used to process the raw data for both format conversion and de-multiplexing. Cuffdiff tool was used to perform comparisons between gene expression levels and transcripts by calculating the FPKM (Fragments Per Kilobase Million) of each transcript. Differentially expressed genes were identified using a 2 threshold of FPKM data (in log 2) and selected for further analysis.

3.5 Western blotting: Autophagy detection

The cell lines lysate was prepared in a buffer containing 20 mmol L^{-1} of Tris–HCl, pH 7.5, 150 mmol L^{-1} NaCl, 1 mmol L^{-1} EDTA, 1 mmol L^{-1} EGTA, 1% Triton, 2.5 mmol L^{-1} sodium pyrophosphate, 1 mmol L^{-1} β-glycerophosphate, 1 mmol L^{-1} Na3VO4, 1 mmol L^{-1} NaF, 2 mmol L^{-1} imidazole and supplemented with a cocktail of protease inhibitors (Complete, Mini, EDTA-free, Roche, Monza, Italy). SDS-polyacrylamide gels at 15% was used too separate a equal amount of proteins from our samples, which were transferred to PVDF membranes (Immobilon-P, Millipore, Millipore Merck Corporation, MA, USA). In order to detect LC3II - microtubule–associated protein light chain 3- (Cell Signaling Technology, Danvers, MA, USA) and p62 - Ubiquitin-binding protein p62- (Abcam Ltd), the membranes were incubated in TBS with 10% of blocking solution (Western Blocking Reagent, Roche) for 1 h and exposed overnight at 4 °C to their primary antibodies. After that, the membranes were washed three time x10 minutes each in TBS-T (50 mmol L^{-1} Tris Base, 150 mmol L^{-1} NaCl, pH 7.5); then, they were exposed to HRP-conjugated secondary anti-rabbit or anti-mouse IgG antibodies for 1 h at room temperature (HRP, Cell Signaling Technology). As a control Tubulin (Sigma-Aldrich) was used. The visualization of the protein bands was performed using Immobilon Western Chemiluminescent HRP Substrate (Millipore, Merck).

3.6 Statistical and Bioinformatic analysis

The statistical analysis was conducted with the software package SPSS Statistics v.21 (IBM, Armonk, NY, USA) to compare control and treatment effects. Levene, Shapiro-Wilk and Kolmogorov-Smirnov tests were applied to ascertain data normality and variance homogeneity. One-way analysis of variance, followed by the Tukey test was used to identify and order means differing significantly from one another. The significance threshold probability was set at 0.05. Details on the statistical and bioinformatic analysis of miRNome expression profile are given in [90]. The RNAseq results were visualized us-

ing the CummeRbund package available from the Bioconductor website in the statistics environment R [106]. In order to obtain biological information on differentially expressed genes (DEGs) and to investigate the biological process and pathway in which they were involved, we used DAVID Bioinformatics Resources 6.8 [107, 108]. Preliminary analysis of target genes for the miRNA expression profiles was performed using the DIANATarbase v.7 database [109]. In addition, to get a complete picture of miRNA-target interactions we used multiMiR from Bioconducter [110], a R package with a collection of microRNAs-targets from external resources. The external database are divided in three category: validated miRNA–target databases, predicted miRNA–target databases and disease-/drug-related miRNA databases. We worked on the first two databases which include different sources. "Validated" database incorporate: miRecords [111], miRTarBase [112] and TarBase [113]. Predicted miRNAs–target databases include: DIANA-microT [114], ElMMo [114], MicroCosm [115], miRanda [116], miRDB [117], PicTar [118], PITA [119] and TargetScan [120]. We searched for targets of miRNAs regulated by real-time PCR using the $2^{-\Delta\Delta Ct}$ method and selected only those already validated by previous experiments, thus in 'validated' category.

Chapter 4

Results and discussion I

The experiments were conducted to study the response of two different cell lines exposed to subtoxic doses of engineered nanoparticles, which in our case are CdS QDs. In addition, we also treated both cell lines with the equivalent dose of cadmium to see if the cellular responses differed. The miRNome expression profiles have been published in [90] and led us to investigate two specific pathways, which are apoptosis and autophagy. Consequently, now, in my part of the work we want to verify the validity of these hypotheses by looking at the interactions between miRNA-mRNA target and the resulting biological process induced.

4.1 RNA sequencing data

The analysis of the Differentially Expressed Genes (DEGs) have shown different responses of HepG2 to the two treatments. RNAseq experiment in HepG2 exposed to CdS QDs identified 1947 significantly regulated genes, of which 1037 up-regulated and 910 down-regulated (Table 4.1 and Figure 4.1 (a)). On the other hand, exposure to Cd(II) shows an increase in the number of regulated genes: 1359 up-regulated and 3227 down-regulated (Table and Figure 4.1 (a)). A total amount of 2566 DEGs were identified in RNAseq experiment for THP-1 exposed to CdS QDs, 838 are up-regulated and 1728 are down-regulated (Table 4.1 and Figure 4.1 (b)). Cadmium expo-

sure results for THP-1, reveals 1945 significantly regulated genes, including 935 up-regulated and 1010 down-regulated (Table 4.1 and Figure 4.1 (b)). We assessed significantly regulated genes, common to the two cell lines, in response to the two types of treatment using Venn diagrams (Figure 4.1). 98 genes are commonly up-regulated in both cell lines exposed to subtoxic doses of CdS QDs, while 159 genes are commonly down-regulated. A total of 180 genes are respectively up-regulated for Hep-G2 while being down-regulated for THP-1, 83 genes are respectively down-regulated for Hep-G2 while being up-regulated for THP-1 (Figure 4.1 (c)). The results of Cd(II) treatment show 39 up-regulated genes common to both cell lines whereas the commonly down-regulated are 172. 224 genes are respectively up-regulated for HepG2 and down-regulated for THP-1, whereas 162 genes are respectively down-regulated for HepG2 and up-regulated for THP-1 (Figure 4.1 (d)).

Table 4.1: Number of significantly regulated genes in HepG2 and THP-1 cells, in response to CdS QDs and Cd(II).

	Significative DEGs			
	HepG2		THP-1	
	CdS QDs	Cd (II)	CdS QDs	Cd (II)
Up	1037	1359	838	935
Down	910	3227	1728	1010
Fold change: $\geq 2 \mid \leq -2$; p-value <0.05				

In general, the results of the transcriptomic data for HepG2 exposed to CdS QDs, reveals that the number of genes that are significantly up- and down-regulated is more balanced than in HepG2 exposed to Cd(II), which show a much higher number of significantly down-regulated genes than up-regulated ones. Whereas, THP-1 shows that the number of significantly regulated gene is unbalanced in both treatments. Particularly, it would appear that CdS QDs induce down-regulated genes once more than up-regulated ones. However, common to both cells lines is the higher number of gene

down regulated after Cd(II) exposure which highlight the alteration at transcription level and the difference in the two treatments.

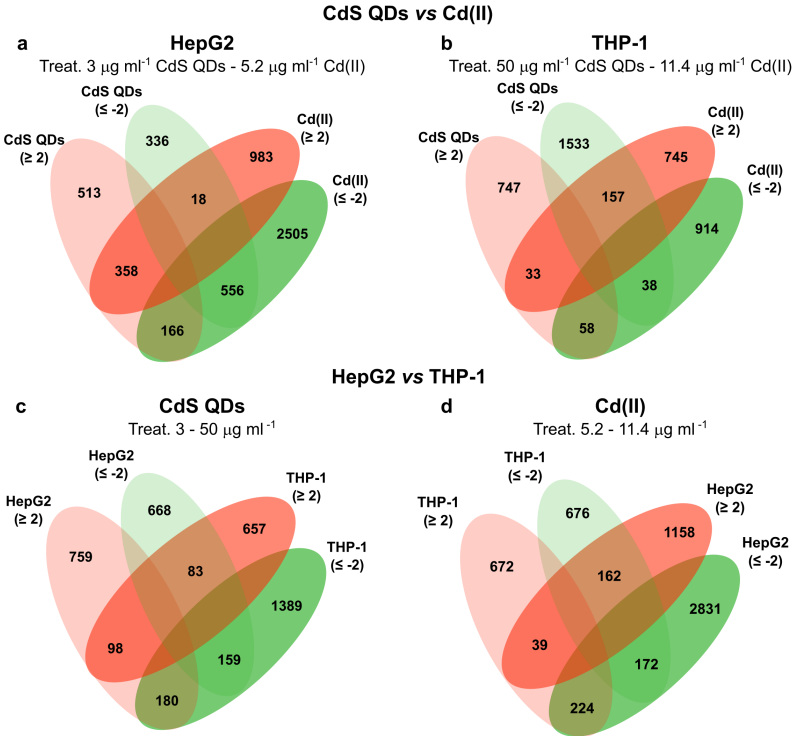

Figure 4.1: Venn diagrams representing the differences in response to the two treatments of the two different cell lines. In red = up-regulated genes, in green= down-regulated genes. Figure (a) shows the number of significantly up- and down-regulated genes per treatment and the number of those common between the two treatments, in HepG2 cells. Figure (b), same as figure (a) but in THP-1 cells. Figure (c) shows the comparison of significantly up- and down-regulated genes in HepG2 and THP-1 exposed to CDs QDs. Figure(d) like figure (c), but in response to Cd(II) exposure.

4.1.1 Gene Ontology Enrichment analysis

The transcriptomic data presented above were used to performed Gene Ontology (GO) enrichment analysis in order to observe which biological process these genes are involved in. We first looked at the total number of regulated genes, then went in depth and analyzed the up- and down-regulated

genes separately. The results of GO analysis show the involvement of all significantly regulated genes for HepG2, mainly in xenobiotic glucuronidation, calcium signaling pathway and inflammatory response (Figure 4.2 (a)). Analyzing them separately, we observed that positively regulated genes are mainly involved in cell detoxification, calcium regulation and activation of phospholipase C (Figure 4.3 (a)). While, negatively regulated genes are involved in positive protein oxidation, calcium regulation, inflammatory response and the extrinsic pathway of apoptosis (Figure 4.3 (b)). Turning to THP-1 exposed to CdS QDs, total regulated genes show involvement in Signal Transducer and Activator of Transcription (STAT) pathway activation and chemokine signaling, and acute inflammatory response (Figure 4.2 (b)). Again, we investigated the genes separately and the GO analysis for those up-regulated shows their involvement mainly in cell cycle progression, ion transport and Janus kinase (JAK)/STAT (Figure 4.3 (c)). Whereas those negatively regulated are implicated in metal ion response, inflammation and JAK/STAT cascade (Figure 4.3 (d)). Exposure to Cd(II), compared to that with CdS QDs, shows a different cellular responses for both cell lines; I have reported the figures of the GO analysis done separately for up- and down-regulated genes. The positively regulated HepG2 genes are mainly involved in cell cycle organization and DNA damage response, whereas the down regulated genes are mainly involved in general signal transduction, transmembrane ion transport and inflammatory response (Figure 4.4 (a),(b)). Concerning THP-1 exposed to Cd(II), up-regulated genes are generally implicated in cellular stress response, e.g. negative regulation of growth, in intrinsic apoptotic pathway and release of pro-inflammatory protein as IL-8. On the other hand, down regulated genes are involved in several different signaling pathways, such as production of cytokines, MAP kinase activity, and cell cycle (Figure 4.4 (c), (b)). In general, exposure to CdS QDs seems to be more related to the inflammatory response in both cell lines, whereas cadmium treatment seems to be mainly related to cell cycle regulation, DNA damage and apoptosis. It is an expected result, the toxicity of cadmium is well known and several studies that have been done, both *in vivo* and *in vitro*, demonstrate its negative effects even at low doses.

(a) Response of HepG2 cells exposed to CdS QDs.

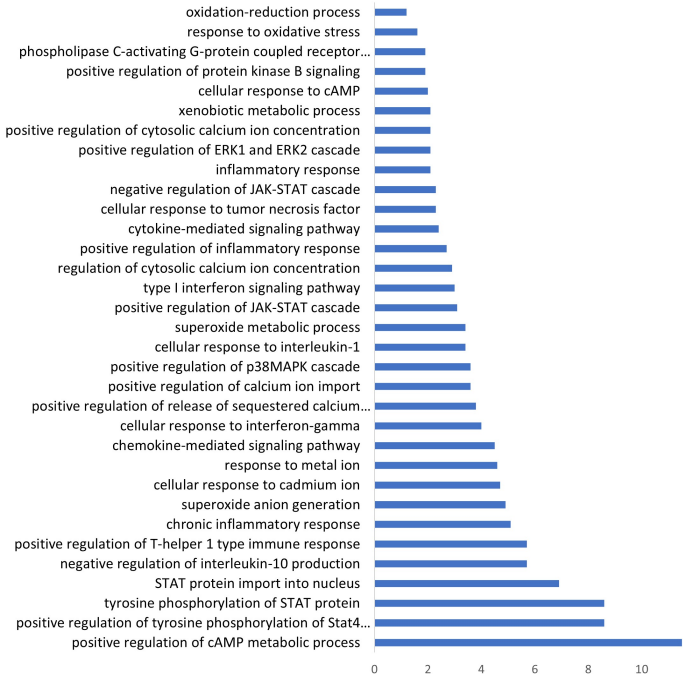

(b) Response of THP-1 exposed to CdS QDs.

Figure 4.2: Functional enrichment analysis of differentially expressed genes was performed and clustered by DAVID's Functional Annotation Chart (FDR <0.05).

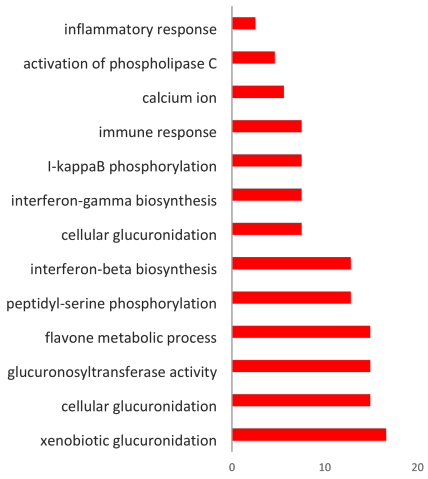

(a) HepG2- CdS QDs: up-reg. genes.

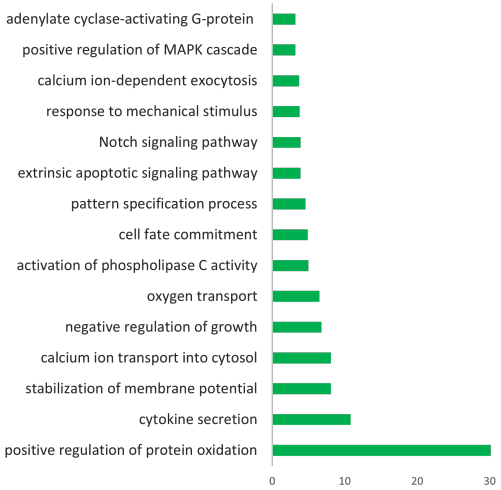

(b) HepG2- CdS QDs: down-reg. genes.

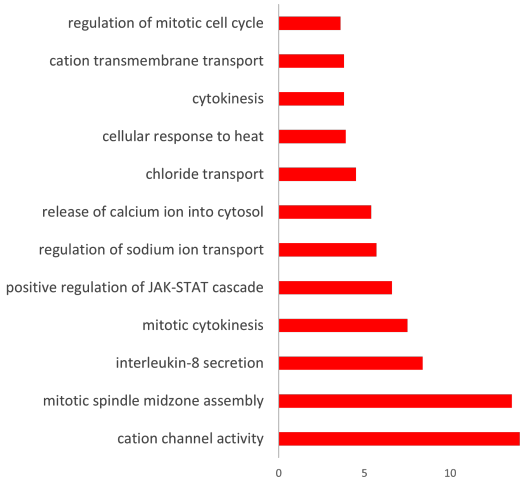

(c) THP-1- CdS QDs: up-reg. genes.

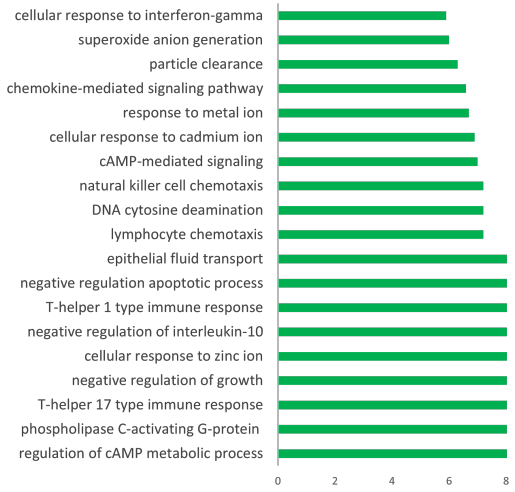

(d) THP-1- CdS QDs: down-reg. genes.

Figure 4.3: Divided GO enrichment analysis for HepG2 exposed to CdS QDs for up- (a) and down-regulated (b) genes. The results for THP-1 are shown in figure (c) the up-regulated and in figure (d) the down ones. Only classes with FDR <0.05 were selected.

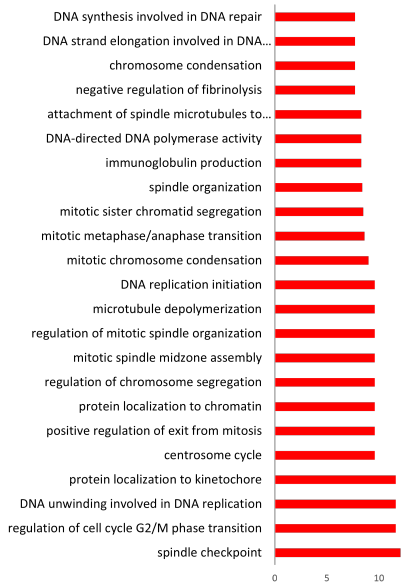

(a) HepG2- Cd(II): up-reg. genes.

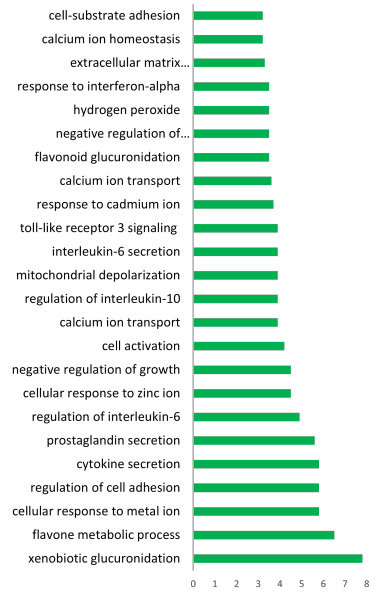

(b) HepG2- Cd(II): down-reg. genes.

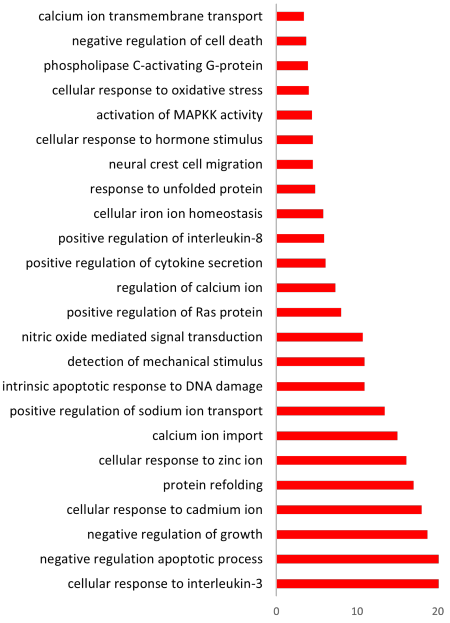

(c) THP-1- Cd(II): up-reg. genes.

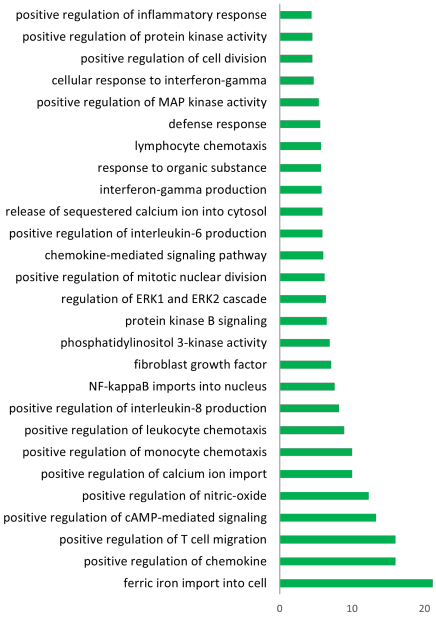

(d) THP-1- Cd(II): down-reg. genes.

Figure 4.4: Divided GO enrichment analysis for HepG2 exposed to Cd(II) for up- (a) and down-regulated (b) genes. The results for THP-1 are shown in figure (c) the up-regulated and in figure (d) the down one. Only classes with FDR <0.05 were selected.

GO enrichment analysis is a useful tool to interpreting at first step in which biological processes are involved the high throughput data generated. As a next step we will go deeper into the different signaling pathways and try to interpret the huge network of molecular interactions.

4.2 Mitochondria health and miRNome profiles

In this section I will report the mitochondria experiments' and miRNome profiles' results presented in [90], in which I participated during the laboratory experiments phase. Starting with the results of JC-1 assay, in HepG2 exposed to 3 µg mL^{-1} of CdS QDs, the membrane potential of the mitochondria did not appear to be particularly affected (Figure 4.5). THP-1 cells exposed to 50 µg mL^{-1} of CdS QDs, show a slight increase in JC-1 monomers and ENPs appear to be aggregated within the cells. The mitochondrial response to Cd(II) is different because the membrane potential looks to be affected since we observed an increase of the amount of JC-1 monomer (green fluorescence) suggesting alteration in mitochondrial functions (Figure 4.6).

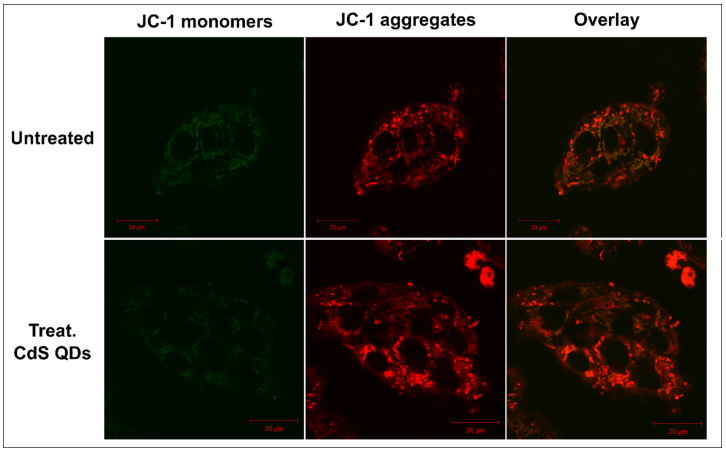

Figure 4.5: Confocal microscopy images show the mitochondria of HepG2 cells after 24 hours of exposure to CdS QDs. The JC-1 dye is mainly aggregated within the mitochondria (red light), which means that the membrane potential is not particularly altered.

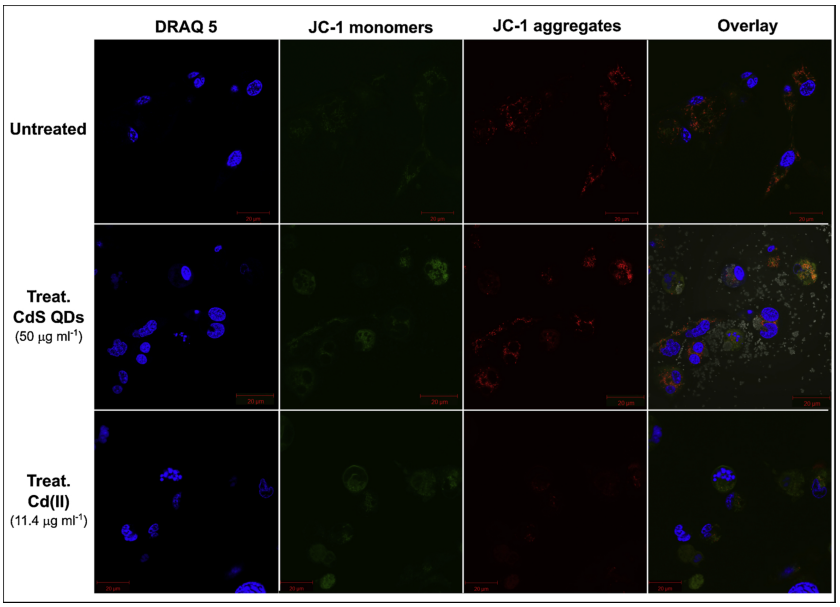

Figure 4.6: Confocal microscopy images show the mitochondria of THP-1 cells after 24 hours of exposure to CdS QDs and Cd(II). Here, DRAQ5 was used to label the nuclear morphology. The differences between the two treatments are visible: the red sign tends to disappear with exposure to Cd(II), which means that the JC-1 dye is in monomer form (green fluorescence) and the mitochondrial membrane potential is altered.

The results of the miRNome profiles are quite interesting: in THP-1 exposed to CdS QDs the majority of regulated miRNAs are down-regulated and mainly involved in autophagy, therefore Paesano and colleagues [90] have hypothesized its activation, which is also supported by the results of Western blot experiment. This, in HepG2 cells exposed to ENPs does not seem to be activated, the miRNome profile and previous studies [121] on specific genes linked to cellular stress, suggested a link with apoptosis despite the fact that the mitochondria appear to be not damaged.

4.3 Western blot analysis: Autophagy

The markers of autophagy analyzed are p62/SQSTM1 and LC3II. Sequestosome 1, SQSTM1, is a multi-functional protein, in autophagy is responsible for sequestering cargo proteins, such as damaged organelles and aggregates

proteins and, link them to autophagosomes which will degrade them [122]. p62 delivers cargo into autophagosomes through interaction with LC3II [123]. The synthesis and processing of LC3, a microtubule-associated 1A/1B-light chain 3 protein, increases during autophagy; LC3 conjugates to generate LC3II, which is recruited to autophagosomal membranes. As already stated, we treated THP-1 and HepG2 cells with different doses of CdS QDs and with the equivalent dose of Cd^{2+} as $CdSO_4$. The doses used to investigate the different response at protein level for THP-1 were: 6.4 µg mL^{-1} and 50 µg mL^{-1} CdS QDs, and 11.4 µg mL^{-1} of Cd (II); HepG2 were treated just with 3 µg mL^{-1} of CdS QDs in order to compare with THP-1 the ENPs response.

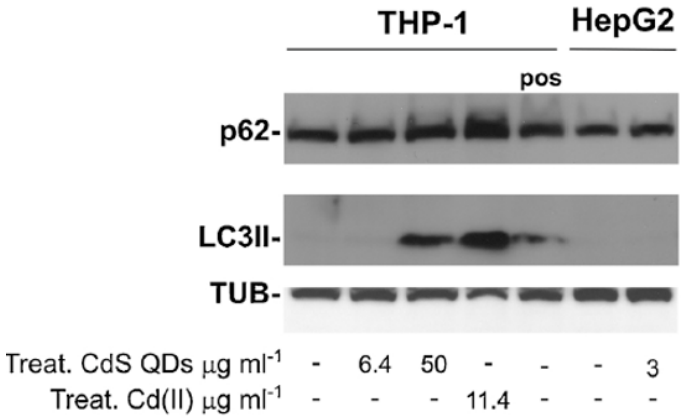

Figure 4.7: Visualization of western blot analysis results. p62 and LC3II proteins levels after 24h exposure to different doses of CdS QDs in THP-1 and HepG2 cells (further details in text). The higher intensity of the band indicates a higher concentration of proteins. Tubulin was used as loading control; pos indicates positive control of autophagy for THP-1 cells.

The miRNome profile results for THP-1 cells exposed to the highest dose of CdS QDs are confirmed by Western blot results due to the increased level of LC3II protein, however we also observed a high concentration of p62 protein suggesting a blockage of autophagy flux. In addition, the exposure to Cd(II) seems to show similar result. In contrast, in HepG2 cells exposed to ENPs, the levels of LC3II and p62 proteins are the same as in control cells (Figure 4.7).

4.4 Interaction analysis

In order to verify the results of the miRNome profile, the interaction analysis for HepG2 was performed by analyzing mainly the apoptosis signaling pathway while for THP-1 the autophagy one.
Preliminary analysis of miRNAs target genes expressed following different treatments were identified using the DIANATarbase v.7 database [109]. Furthermore, multiMiR [110] was used to get a complete picture of miRNAs–target interactions in order to deeply understand what is happening inside the two cell lines.

4.4.1 HepG2: Interactome analysis

HepG2 - CdS QDs

Based on the miRNome hypothesis, the apoptosis pathway was investigated. The first step was to investigate whether target genes were significantly regulated at transcriptome level; in Table 4.2, I have listed the main ones.

Table 4.2: Main miRNAs reported in [90] with corresponding mRNAs generated from RNAseq. Fold change: $\geq 2| \leq -2$; p-value ≤ 0.05; RQ ≥ 2; ≤ 0.5

Transcriptomic regulation in HepG2 cells exposed to 3 µg mL^{-1} of CdS QDs			
miRNAs involved in Apoptosis [90]	miRNAs regulation(RQ)	mRNAs target	mRNA regulation from RNAseq data (F.C.)
hsa-miR-34b	3.62 ↑	p53 response	no sign.
hsa-miR-149-3p	0.42 ↓	AKT1	no sign.
hsa-miR-32-5p	0.47 ↓	BIM	no sign.
hsa-miR-122	0,33 ↓	BCL2L2	no sign.
hsa-miR-193b-5p	5.18 ↑	MCL1	no sign.
hsa-miR-15a-3p	3,30 ↑	BCL-2	no sign.
hsa-miR-195-5p	0.23 ↓	BCL-2	no sign.
hsa-miR-92a-1-5p	2.98 ↑	FAF-1 (FAS)	no sign.

Table 4.3: Pathway analysis performed using DAVID Bioinformatics Resources 6.8 [124], based on the KEGG database. Adj.p-value*: method of Benjamini and Hochberg (1995).

KEGG pathway	Fold enrichment	p-value	Adj p-value*
Calcium signaling	3.0	$1.1 \times 10^{-}6$	$1.3 \times 10^{-}4$
RAS signaling	2.8	$5.6 \times 10^{-}3$	$5.9 \times 10^{-}3$
Drug metabolism	2.9	$2.6 \times 10^{-}3$	$5 \times 10^{-}2$
cAMP signaling	1.9	$4.6 \times 10^{-}3$	$5.7 \times 10^{-}2$
Metabolism xenobiotic	2.6	$5 \times 10^{-}3$	$5.7 \times 10^{-}2$

I went through the apoptotic pathway, evaluating each individual gene and found no significantly regulated genes. Therefore, based on the GO enrichment analysis I investigated the resulting pathways by delving into those around apoptosis.

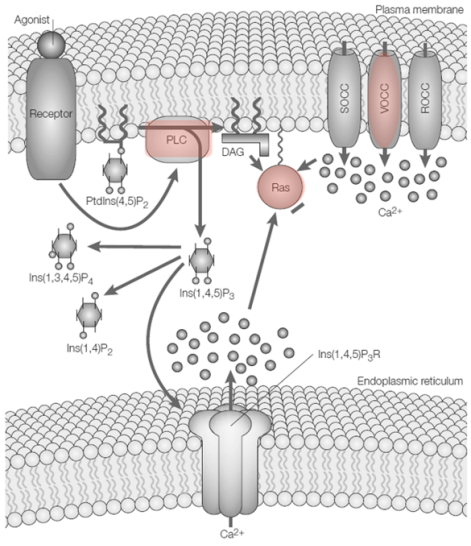

Figure 4.8: Cross-talk between RAS and Ca^{2+} signaling pathways. Re-adapted from [125].

The pathways reported in Table 4.3 were analyzed and we discerned the activation of RAS signaling pathway which is highly sensitive to intracellular Ca^{2+} variation [125]. This is supported by the up-regulation of RASGRP1, a proteins of the Ras guanyl nucleotide releasing proteins (RasGRPs) family which activate Ras through the exchange of bound GDP for GTP [126]. The Ras superfamily protein plays a critical roles in cellular survival, growth, cytosckeleton organization and others. Phospholipase C (PLC) isozymes (-β, -δ, -ζ, -ε, -γ, -υ) are regulated by RAS proteins [127, 128]. PLCE1 (-ε) gene, encodes for an enzyme, was found to be up-regulated. This enzyme catalyses the

phosphatidylinositol 4,5-bisphosphate (PI(4,5)P2) [129] to generate inositol 1,4,5-triphosphate (IP3) and diacylglycerol (DAG), which are involved in the control of calcium homeostasis. Specifically, IP3 diffuses into the cell and binds its receptor located in the endoplasmic reticulum, which induces the release of Ca^{2+} in the cytosol, (Figure 4.8). The activation of Calcium signaling is also supported by the miRNAs-mRNAs interaction analysis (Table 4.4). We observed two genes up-regulated, CACNA1C and CACNA1B, encoding for sub-units of voltage-dependent calcium channels and, by exploring the miRNAs that inhibit their translation, a large amount of them result down-regulated. Furthermore, RYR1 results up-regulated, which encode for a calcium channel located in the endoplasmic reticulum (ER) and lead to the release of Ca^{2+}; this is feedback mechanism as it is also activated by Ca^{2+}. RYR1 was found to be expressed in liver cells and to be involved in Ca^{2+} signaling by acting synergistic with inositol triphosphate, IP3. Basically, Ryanodine receptor (RyR) family are associated with muscles cells however reviewing in the literature, several studies reported their expression also in other tissues, especially in [130]. Continuing to follow the Ca^{2+} pathway, increasing intracellular level induce the formation of Ca^{2+} /calmodulin (CaM) complex which activates protein kinase dependent on Ca^{2+} /CaM (CaMK). CAMK1D encodes for a protein that is part of CaMK enzymes and it is up-regulated. It operates in the calcium signaling cascade and coordinates multiple phosphorylation events during gene expression, thus having control over a wide range of biological function [131]. We did not observe any expressed miRNAs that could inhibit its translation. The link between the increase in calcium and the consequences for the mitochondrion is well established and the mechanisms have been researched in several studies [132–134]. Prolonged increase in Ca^{2+} concentration in mitochondria alters ATP production which would lead to cytochrome C release and as a final step the activation of intrinsic apoptosis process [135]. Endoplasmic reticulum and mitochondria are interconnected in the maintenance of Ca^{2+} homeostasis. Our result suggested us the release of Ca^{2+} ions from the endoplasmic reticulum but, on the other hand, the membrane potential of mitochondria does not appear altered. Thus, we deduce that HepG2 cells exposed to subtoxic

doses of CdS QDs exhibit altered calcium homeostasis due to the release of Ca^{2+} ions from the endoplasmic reticulum, which may then be under stress. At the time of our experiment, the mitochondria appear to be unaffected, but if the cell fails to re-establish the intracellular balance of Ca^{2+} this could lead to more serious consequences such as apoptosis.

Table 4.4: HepG2-CdS QDs: Table displaying interactions between key regulated mRNAs and corresponding miRNAs. Validated miRNAs were selected from the database generated with MultiMiR.

From mRNA (RNAseq data) to miRNAs			
mRNA	Regulation (F.C.)	miRNAs	Regulation ($2^{-\Delta\Delta Ct}$)
RASGRP1	↑	hsa-mir-335-5p	↓
		hsa-mir-155-5p	↓
		hsa-mir-34b-3p	↑
		hsa-mir-155-5p	↓
RYR1	↑	-	-
PLCE1	↑	hsa-mir-335-5p	↓
		hsa-mir-149-3p	↓
		hsa-mir-34b-3p	↑
		hsa-mir-155-5p	↓
CAMK1D	↑	hsa-miR-323a-3p	↓
		hsa-miR-195-5p	↓
CAMK2A	↑	hsa-miR-149-3p	↓
		hsa-miR-126-5p	↓
CACNA1B	↑	hsa-miR-335-5p	↓
		hsa-miR-17-3p	↓
CACNA1C	↑	hsa-miR-218-5p	↓
		hsa-miR-133a-3p	↑
ATP2A3	↓	hsa-miR-149-3p	↓
		hsa-miR-155-5p	↓
		hsa-miR-17-3p	↓
		hsa-miR-340-3p	↑
CALML6	↓	hsa-miR-30a-5p	↑
PDE1A	↑	hsa-miR-218-5p	↓
		hsa-miR-155-5p	↓

HepG2 - Cd(II)

We analyzed the apoptotic response of the HepG2 cells exposed to cadmium in ionic form, as 5.2 µg mL^{-1} of Cd(II). Comparing this results with the CdS QDs treatment, we observed strong differences. Related to Cd(II) treatment, indeed the result show a general response to stress and specifically, several genes involved in apoptosis mediated by p53 signaling pathway are significantly regulated and the specific miRNAs as well. TP53 encodes for the tumour protein that decides cell fate through transcriptional regulation. We did not find significantly level of p53 mRNA in HepG2, however we observed the regulations of several genes that are activated by it. p21 (CDKN1A) encodes for a protein that can induce arrest of the G1 phase of the cell cycle through inhibition of cyclin-dependent CDKs kinase complexes. We found p21 down-regulated, whereas mRNAs encoding for cyclin proteins were up-regulated (Table 4.5).

Furthermore, by analyzing the miRNome profiles of HepG2 exposed to Cd(II) we discovered the up-regulation of several miRNAs (resulting validate in MultiMiR database) that inhibit p21 translation.
In particular, hsa-miR-372-3p is over-expressed (RQ equal to 24.75; threshold $\geq$2) in our cells; besides, this result is in agreement with other studies already present in the literature, such as [136]. We investigated the regulation of pro- and anti-apoptotic genes induced by p53. We found that most of the pro-apoptotic mRNAs are down-regulated such as PUMA (BBC3) and NOXA (PMAIP1); in contrast, the BCL2 protein is up-regulated, thus blocking apoptotic cell death (Figure 4.9). As a result of the miRNAs-mRNAs interaction analysis, we hypothesized that we did not observe regulation of TP53 at transcriptomic level because it has already been translated into protein, and translocated into the nucleus, activating as a consequence the regulation of the genes mentioned above. Furthermore, the blockade of cell cycle arrest (and possible apoptotic process) could be induced by the interaction between p21 and miR-372. This is supported by the down-regulation of pro-apoptotic genes and especially by the over-expression of BCL2. What remains in doubt is whether the cells have succeeded in resolving the damage caused by Cadmium, or whether they are in the process of carcinogenesis.

Table 4.5: HepG2-Cd(II): Interactions between miRNA-mRNA. From MultiMiR database. Fold change: $\geq 2| \leq -2$; p-value ≤ 0.05; RQ$\geq$2; ≤ 0.5

TP53 signaling - mRNAs regulated			
mRNA	Regulation (F.C.)	miRNAs	Regulation-RQ
BCL2	2.1	hsa-miR-34a-5p	0.44
		hsa-mir-15b-5p	0.11
		hsa-mir-17-5p	0.23
CDK1	3.4	hsa-mir-30b-5p	0.33
		hsa-mir-126-5p	0.01
		hsa-miR-99b-5p	0.43
		hsa-miR-30b-5p	0.33
CCNB1	2.6	hsa-mir-455-3p	0.13
		hsa-mir-766-3p	0.04
		hsa-mir-103a-3p	0.25
CCNB2	3.1	hsa-miR-92a-3p	0.45
		hsa-miR-21-3p	0.22
		hsa-miR-34a-5p	0.44
CHEK2	2.5	hsa-miR-26b-5p	0.39
		hsa-miR-130b-3p	0.36
		hsa-miR-19b-3p	0.37
CCNE2	2.1	hsa-miR-26a-5p	0.31
		hsa-miR-34a-5p	0.44
CDKN2A	-3.2	-	-
		hsa-miR-133a-3p	10.41
CDKN1A	-2.3	hsa-miR-372-3p	24.76
		hsa-miR-132-3p	2.26
		hsa-miR-589-3p	17.79
		hsa-miR-100-5p	14.12
CCND2	-3.4	hsa-miR-196b-5p	11.28
		hsa-miR-376c-3p	11.7
		hsa-miR-548b-3p	3.9
GADD45G	-6.9	-	-
GADD45B	-4.7	hsa-miR-128-3p	2.75
PMAIP1	-2.8	hsa-miR-202-3p	12.43
		hsa-miR-212-3p	2.6
		hsa-miR-133a-3p	10.41
BBC3	-1.8	hsa-miR-222-3p	2.1
		hsa-miR-31-5p	30.1

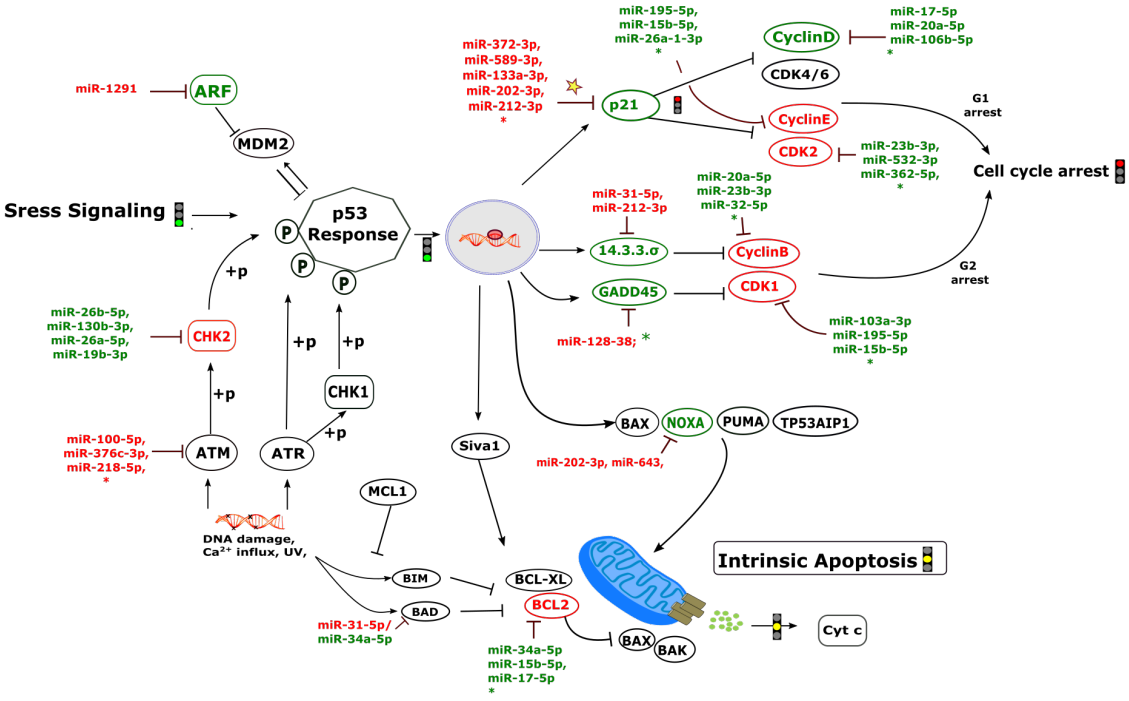

Figure 4.9: HepG2-Cd(II): p53 response pathway; up- and down-regulated miRNAs-mRNAs are represented in red and green respectively.

4.4.2 Cellular response considerations for HepG2

In HepG2 cells, the two treatments induced a different cellular response. From miRNAs-mRNAs interaction analysis, exposure to CdS QDs seems to cause an increase in intracellular calcium possible due to endoplasmic reticulum stress. On the other hand, the mitochondrial potential membrane does not appear to be altered and therefore, does not suggest any major alteration. From these results we can deduce that the apoptotic process has not yet been activated, but if calcium homeostasis is not restored, activation could indeed occur. In contrast, direct exposure to Cd(II) appears to induce DNA damage and a general regulation of genes involved in the intrinsic pathway of apoptosis; however miRNAs-mRNas interaction analysis did not show the apoptotic process to be active.

4.4.3 THP-1: Interactome analysis

THP-1 - CdS QDs

The miRNome profile analysis has directed us to investigate the regulation of genes involved in the pathway of Autophagy. The RNAseq results show no mRNAs significantly regulated involved in this pathway (Table 4.6).

Table 4.6: Main miRNAs reported in [90] with corresponding mRNAs generated from RNAseq.

Transcriptomic regulation in THP-1 cells exposed to 50 µg mL^{-1} of CdS QDs				
Autophagy	miRNAs involved in Autophagy [90]	miRNAs regulation (RQ)	mRNAs target	mRNA regulation from RNAseq data(F.C.)
Induction	hsa-miR-101-3p	0.02 ↓	mTOR	no sign.
	hsa-miR-100-5p	0.03 ↓	RPTOR	no sign.
	hsa-miR-27a-3p	0.05 ↓	DEPTOR	no sign.
Vescicle nucleation	hsa-miR-101-3p	0.02 ↓	RAB5A	no sign.
	hsa-miR-374-5p	0.22 ↓	UVRAG	no sign.
	hsa-miR-30a-5p	0.04 ↓	BECN1	no sign.
Vescicle elongation	hsa-miR-181a-5p	0.23 ↓	ATG5	no sign.
	hsa-miR-335-5p	0.46 ↓	MAP1LC3(A-B)	no sign.
	hsa-miR-1-3p	0.04 ↓	GABARAP(L1-L2)	no sign.
	hsa-miR-101-3p	0.02 ↓	ATG4D	no sign.
Fold change: $\geq 2 \mid \leq -2$; p-value <0.05 - $2^{-\Delta\Delta Ct} = 0.05 \mid 2$				

On the other hand, the results of Western blot assay (Figure 4.7) reveal rising levels of autophagy marker proteins, which are p62/SQSTM1, involved in the sequestration of cargo material and LC3II required for the autophagosomes membrane. The final step in the autophagic process consists in the fusion between autophagosomes and lysosomes in order to degrade the cargo material; in this process p62 is also degraded, so low levels of this protein are associated with an active autophagic process, conversely high levels are associated with impaired autophagy, which is what our Western bolt results suggested. Therefore, to better understand

what is happening inside THP-1 cells, we investigated in depth the pathways in which regulated genes are implicated.
We observed that most of the genes involved in the resulting pathways analysis shown in Table 4.7, were down-regulated and encode for several cytokines, Janus kinase (JAK), STAT proteins and Caspase 1. The activation of the JAK kinase induce the formation of STAT3 dimers, which can move into the cell nucleus and induce transcription of genes that inhibit or stimulate autophagy. In addition we observed genes involved in Calcium signaling and NF-Kβ signaling, which is the main player in response to inflammation. Everything points to an inflammatory response of the cells. So we looked at the regulation of miRNAs involved in these pathways, and they were almost all down-regulated (Table 4.8).

Table 4.7: Pathway analysis performed in [124] based on KEGG database. Adj.p-value*: method of Benjamini and Hochberg (1995).

KEGG pathway	Fold enrichment	p-value	Adj p-value*
Cytokine-cytokine receptor interaction	4.0	1.5×10^{-11}	3.3×10^{-9}
Chemokine signaling	3.7	2.0×10^{-7}	2.2×10^{-5}
Toll-like receptor signaling	3.7	2.0×10^{-4}	1.1×10^{-2}
MAPK signaling	2.0	1×10^{-2}	2.5×10^{-1}
Calcium signaling	2.0	3.7×10^{-3}	5.9×10^{-1}
NF-kappa B signaling	2.4	7.0×10^{-2}	7×10^{-1}

Inflammatory and autophagic processes are connected [80,137–139]. Autophagy, with the degradation of cargo in autolysosomes as the final step, seeks to maintain cellular homeostasis. Thus, in a stressful condition leading to an inflammatory response, autophagy attempts to restore the balance by removing inflammatory components such as inflammosomes, DAMPs etc., thereby inhibiting the inflammatory process. Putting together the results obtained we discerned that CdS QDs enter in THP-1 cells through endocytosis; here, ENPs could impaire various organelles and induce the generation of ROS which is supported by the up-regulation of NOXO1 and DUOX1, which are second messengers in redox-sensitive path-

ways [140]. Then, the damaged organelles are sequestered by autophagosomes to maintain recycling, confirmed by the high levels of LC3II protein. The process can continue in two ways, the first, in which the cargo material is degraded and there are no negative consequences for the cells; the second is the blockage of the autophagic process due to the accumulation of in-cell autophagosomes (Figure 4.10). This can occur as a consequence of prolonged exposure to CdS QDs, which can cause an accumulation of NPs in lysosomes resulting in alkalinisation and damage to lysosomes, which is also supported by the accumulation p62 in the cells. This, can lead to an increased inflammatory state, and in the worst case to necroptosis.

In our case of study, we observed up-regulation of genes involved in the cell cycle such as PLK1 and CDC25C encoding for two proteins that trigger entry into mitosis, hence we did not deduce activation of necroptosis/apoptosis. The down-regulation at transcriptomic level can be explained by the fact that inflammation is a time-dependent process, so after 24h of exposure everything may already have been translated into proteins.

Table 4.8: THP-1-CdS QDs: Table displaying interactions between key regulated mRNAs and corresponding miRNAs. Validated miRNAs were selected from the database generated with MultiMiR.

From mRNA (RNAseq data) to miRNAs			
mRNA	Regulation (F.C.)	miRNAs	Regulation ($2^{-\Delta\Delta Ct}$)
JAK3	↓	hsa-mir-29b-1-5p	↑
		hsa-mir-222-3p	↓
		hsa-mir-335-5p	↓
		hsa-mir-223-5p	↓
STAT	↓	hsa-mir-155-5p	↓
		hsa-mir-501-5p	↓
		hsa-mir-24-3p	↓
CXCL9	↓	hsa-mir-335-5p	↓
		hsa-mir-26b-5p	↓
CXCL10	↓	hsa-miR-550a-3p	↓
		hsa-miR-15a-5p	↓
CXCL11	↓	hsa-miR-30d/c/b-5p	↓
IL6	↓	hsa-miR-98-5p	↓
		hsa-let-7b-5p	↓
ILFNB1	↓	hsa-miR-26a-5p	↓
		hsa-miR-145-5p	↑
CASP1	↓	hsa-miR-17-5p	↓
		hsa-miR-133a-3p	↓
NOXO1	↑	hsa-miR-192-5p	↑
		hsa-miR-215-5p	↓
CACNA1D	↑	hsa-miR-101-3p	↓
		hsa-miR-46a-5p	↓
Fold change: ≥ 2 | $\leq$-2; p-value <0.05 - $2^{-\Delta\Delta Ct}$= 0.05 | 2			

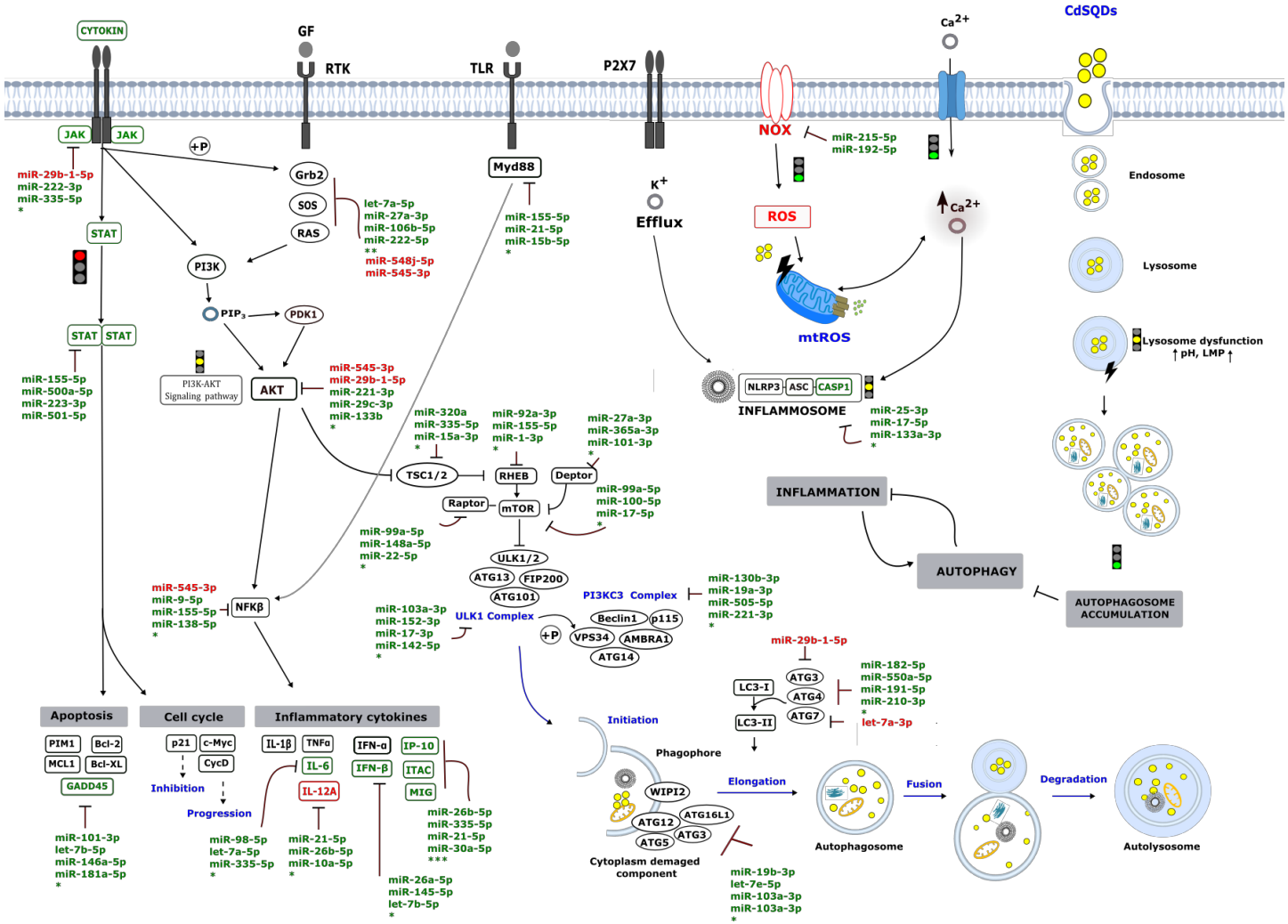

Figure 4.10: Response of THP-1 cells exposed to CdS QDs; up- and down-regulated miRNAs-mRNAs are represented in red and green respectively. The figure depicts a general down-regulation of genes involved in the inflammatory response and shows the accumulation of autophagosomes that could lead to the blockage of the autophagy process (further details are provided in the text).

THP-1 - Cd (II)

THP-1 cells exposed to 11.4 µg mL^{-1} of Cd(II) the response is completely different compared to CdS QDs at trancriptomic level, here the cells appear to be preparing for apoptosis. The Western blot results are comparable to those of THP-1 exposed to CdS QDs; p62 is not only involved in the autophagy pathway, but is also a regulator of the NF-kβ pathway which could explain its high concentration at the protein level. In addition, the stress induced at cellular level by Cd(II) due to the increasing in ROS leve may have generated a type of selective autophagy because of the damaged peroxisomes, organelles that are responsible for detoxifying reactive oxygen species [141, 142]. In order to eliminate damaged peroxisomes and maintain the balance, Pexophagy may have been activated, which would also explain the increase in LC3II; however, we did not investigate this process further as we did not observe any regulation at the transcriptomic level and, moreover, because the apoptotic response seems to be already activated. We began from the pathway analysis, the results are reported in Table 4.9 which shows the result for all significantly regulated genes.

Table 4.9: Pathway analysis for total genes regulated performed in [124] based on KEGG database. Adj.p-value*: method of Benjamini and Hochberg (1995).

KEGG pathway	Fold enrichment	p-value	Adj p-value*
Cytokine-cytokine receptor interaction	2.0	$2.6\times10^{-}6$	$9.9\times10^{-}4$
Cell cycle	2.4	$2.2\times10^{-}4$	$1.5\times10^{-}2$
MAPK signaling	1.8	$1.3\times10^{-}3$	$5.8\times10^{-}2$
TNF signaling	2.3	$1.5\times10^{-}3$	$6.0\times10^{-}2$
p53 signaling	2.5	$5.4\times10^{-}3$	$1.3\times10^{-}2$
Calcium signaling	1.7	$1.2\times10^{-}3$	$2.6\times10^{-}1$
NF-kβ signaling	2	$1.7\times10^{-}2$	$3\times10^{-}1$

We observed that most of the up-regulated genes are involved in Calcium signaling and MAPK pathway. Conversely, the down-regulated ones are mainly involved in cell cycle regulation, TNF signaling, NF-Kβ pathway and p53. Examining in depth the p53 signaling pathway, we observed that TP53 gene, encode

for p53 protein, is down-regulated. We found up-regulated miR-361-3p targeting TP53, but we also found two down-regulated oncosopressors miR-1285 and miR-125b [143]. By navigating the p53 signaling pathway, we identified GADD45B and GADD45G (growth arrest and inducible beta and gamma DNA damage respectively) both up-regulated, encoding for two proteins whose levels increase in response to cellular stress and are implicated in the regulation of growth and apoptosis. Furthermore, cyclin proteins such as CCNB1, CCNE1, CCNE2 and CCND2 result down-regulated,suggesting cell cycle arrest. BBC3 (PUMA) is up-regulated, this gene, as mentioned above, encodes for a protein that can bind to the anti-apoptotic Bcl-2 and induce mitochondrial dysfunction, resulting in caspase activation (Table 4.10). This could be confirmed by what we observed using the JC-1 dye, that is a depolarization of mitochondrial membrane. Furthermore, DDIT3 (DNA damage inducible transcript) is up-regulated; it responds to endoplasmic reticulum stress and promotes apoptosis through inhibition of anti-apoptotic Bcl-2 proteins, as PUMA does. The corresponding miRNAs were analyzed, and given the general down-regulation of them, the corresponding ones are all down-regulated. Everything points to the activation of the intrinsic pathway of apoptosis, similar to that seen for HepG2 but in a more intense form (Figure 4.11).

Table 4.10: THP-1-Cd(II): Table displaying interactions between key regulated mRNAs and corresponding miRNAs. Validated miRNAs were selected from the database generated with MultiMiR.

From mRNA (RNAseq data) to miRNAs			
mRNA	Regulation (F.C.)	miRNAs	Regulation ($2^{-\Delta\Delta Ct}$)
BBC3	4.1 ↑	hsa-miR-221-3p	↓
		hsa-mir-222-3p	↓
		hsa-mir-29b-3p	↓
DDIT3	1.8 ↑	hsa-miR-211-5p	↓
		hsa-miR-335-5p	↓
GADD45B	5.2 ↑	hsa-miR-155-5p	↓
		hsa-miR-1-3p	↓
GADD45G	6.3 ↑	hsa-miR-16-5p	↓
		hsa-let-7b-5p	↓
CACNA1D	2.1 ↑	hsa-miR-101-3p	↓
CCND2	-2.8 ↓	hsa-miR-656-3p	↑
		hsa-miR-1255b-5p	↑
		hsa-miR-941	↑
CCNE1	-2.1 ↓	hsa-miR-181c-5p	↑
CCNE2	-2.5 ↓	hsa-miR-26a-1-3p	↑
		hsa-miR-548j-5p	↑
CCNB1	-1.7↓	hsa-miR-548j-5p	↑
		hsa-miR-181c-5p	↑
TP53	-1.9 ↓	hsa-miR-361-3p	↑
		hsa-miR-1225-3p	↑
		hsa-miR-26a-1-3p	↑
Fold change: ≥ 2 | $\leq$-2; p-value <0.05 - $2^{-\Delta\Delta Ct}$= 0.05 | 2			

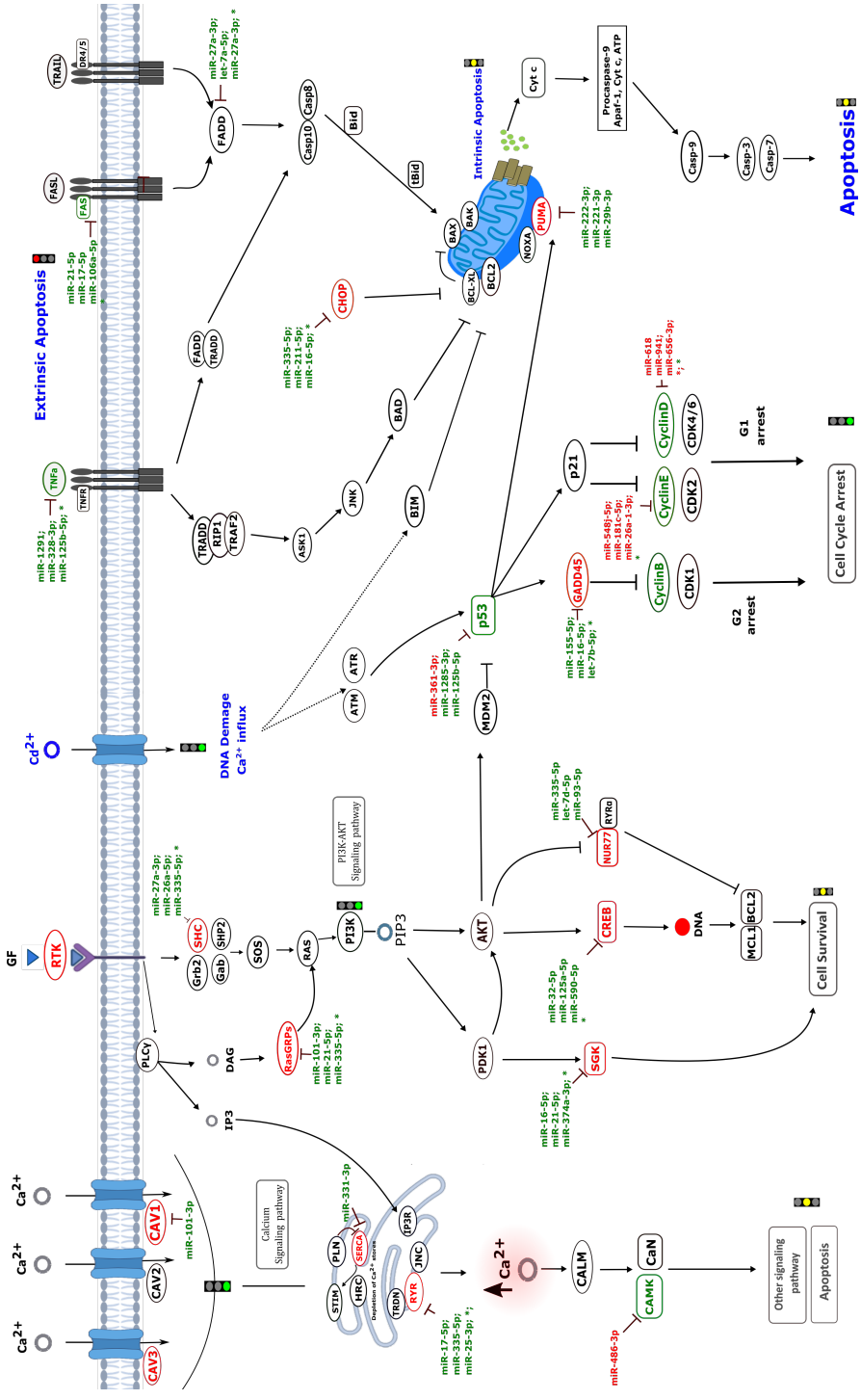

Figure 4.11: Response of THP-1 cells exposed to Cd(II); up- and down-regulated miRNAs-mRNAs are represented in red and green respectively. The figure shows the possible increase in intracellular Ca^{2+} and the activation of intrinsic apoptosis pathway.

4.4.4 Cellular response considerations for THP-1

The response of THP-1 cells to the two treatments is clearly different. Exposure to CdS QDs after 24 hours shows a general silencing of the inflammatory response at the transcriptomic level, which could be explained as a consequence of the autophagic process that has already taken place. In addition, a possible blockage of the autophagy process was observed due to the accumulation of autophagosomes within the cell as a result of ENP-induced lysosomal damage. ENPs appear to increase ROS levels within the cell, probably as a result of interaction with mitochondria. It is clear that after 24 hours of exposure ENPs induce a generalized stress response which, according to our results, does not appear to lead to cell death. In contrast, according to various experiments, THP-1 cells exposed to subtoxic doses of Cd(II) appear to induce intrinsic apoptosis.

Chapter 5

Conclusion I

The aim of this part of the work was to investigate the effects of UFPs on human cells using ENPs as surrogate particles. We used two different cell lines to study the human response conditional on different exposure routes. Once NPs enter the human body they can be recognized by macrophages, such as THP-1 cells, as a first line of defense of the immune system; we investigated the consequences of such interaction on THP-1 themselves. Given their size, NPs can also enter into the bloodstream, where they can reach and accumulate in the liver. HepG2 liver cells are deputed to the detoxification process, therefore we assessed the consequence of this interaction as well.

We conducted different experiments, focusing mainly on gene expression responses and how these can be modified through post-transcriptional epigenetic interactions: miRNAs-mRNAs. Understanding the effects of ENPs on mitochondria was another key aspect of our study, as well as the analysis of specific autophagy markers. To investigate whether the toxicity of CdS QDs could be induced by a possible release of cadmium, we treated the cells with an equivalent dose of Cd as $CdSO_4$, as a control. We conducted this control treatment, the same experiments and data analysis as with the CdS QDs, in order to make a meaningful and coherent comparison between the two treatments possible. Putting together the results from the different experiments and navigating through the pathways' KEGG maps, we came to the following conclusions regarding cells exposure to ENPs:

- in HepG2: the transcriptomic response did not confirm the involvement of apoptotic pathways as we had initially assumed due to the miRNome profile.

Based on the analysis of the miRNAs-mRNAs interactions we concluded that the activation of RAS and Ca^{2+} signaling pathways could happen. Consequently, this induces an increase in intracellular Ca^{2+} which could lead to apoptosis as the final step in a worst-case scenario. Moreover, the mitochondria experiment results hints this conclusion since they appear not affected after 24h exposure of 3 µg mL^{-1}.

- in THP-1: Here, as in HepG2, the transcriptomic response did not directly confirm the assumption of the miRNome profile, i.e. direct involvement in the autophagic process [90]. Nevertheless, miRNAs-mRNAs interaction analysis points at JAK/STAT signaling and inflammatory pathways, which are directly related to autophagy. In addition, the mitochondrial membrane potential was found to be affected by 50 µg mL^{-1} of CdS QDs, confirming impairment of these organelles by ENPs. LC3II protein levels increased in the treated compared to the control cells as well as p62 protein levels. Therefore, all considered, we inferred a block of autophagy flow due to the increased of autophagosomes as a consequence of damaged lysosomes in THP-1 cells after 24h exposure to ENPs.

In both cell lines the response to Cd(II) is different compared to the ones for CdS QDs treatments. The apoptotic pathway seems to be imminent after 24h exposure. However, in THP-1 cells it seems to be more intense than in HepG2.
In conclusion, this study highlighted the potential risk correlated with exposure to engineered nanoparticles at the molecular level, which might not be strictly related to cadmium content in CdS QDs alone, as it could be inferred from our case study (*manuscript in preparation*). Further validation studies on the significantly regulated genes resulted from RNAseq process are needed and will be part of the continuation of this research.

Part II

Long-term exposure to ambient air pollutants and blood biomarkers of inflammation and coagulation

Chapter 6

Background II

I began this doctoral thesis by introducing what air pollutants are and what are the main processes that generate them. Here, in this epidemiological study, I describe the effects of air pollutants on human health, particularly as a result of long-term exposure.

Air pollution is associated with oxidative stress and inflammation in human cells. Given the ability of inflammatory mediators and UFPs to travel within our bodies, the effects on human health are not only limited to the lungs but almost all organs can be negatively affected [144]. Increased levels of ROS and prolonged inflammatory status can lead to chronic diseases and cancer [145]. Indeed, in 2013, the International Agency for Research on Cancer (IARC) classified outdoor air pollution as carcinogenic to humans (IARC Group 1) [146]. Several epidemiological long-term studies reported positive associations with cardiovascular and pulmonary diseases such as lung cancer, coronary heart disease, hypercoagulability and thrombosis [147–149]. Other studies show that air pollutants are a significant factor in the pathogenesis of neurodevelopmental and neurodegenerative disorders such as changes in cognitive function and Alzheimer's [18, 150, 151] and even they contribute to depression and anxiety [151, 152]. In addition, positive associations with reproductive capacity have been reported, supporting the notion that air pollutants can cause defects during gametogenesis [153]. In general, studies can be divided into short- and long-term. Short-term studies examine the association between short-term changes in air pollution and health outcomes, for example

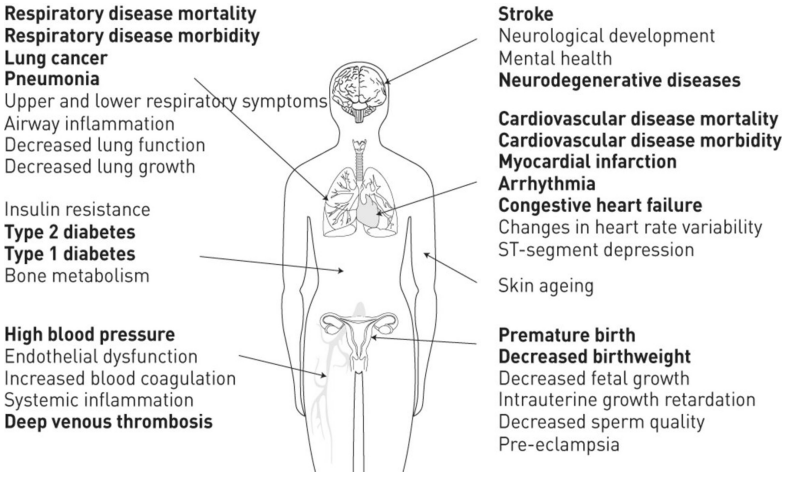

Figure 6.1: Organs that can be impacted by air pollution and disease related. From [154] - Updated based on [144].

the level of air pollutants and the number of daily deaths and hospital admissions. [155]. In contrast, studies on the long-term effects of air pollution compare mortality among populations that vary in their long-term exposure to air pollution (Figure 6.1). Long-term exposure increases the risk for cardiovascular (CV) mortality, specifically in [21] is reported that there is a causal relationship between $PM_{2.5}$ exposure and CV morbidity and mortality.

Here, I will focus mainly on the link between long-term exposure to air pollutants and blood biomarkers related to cardiovascular health.

6.1 Biomarkers and air pollution

The study by Peters and colleagues [156] was the first one to investigate ambient air pollution in association with blood markers. They observed that the increase of plasma viscosity might represent a part of the pathophysiological link between high ambient air pollution and increase of cardiovascular mortality and hospital admission. In subsequent years, several epidemiological studies [148, 149, 157] have reported associations between air pollutants and a changing level of specific biomarkers reflecting inflammation and coagulation, but most of them are related to short-term exposure. Evidence regarding long-term exposure is still limited.

In this cross-sectional study we analyzed the following biomarkers:

- Fibrinogen: a blood coagulation biomarker with pro-inflammatory effect [158]. It is an essential factor in blood clotting, is required when there is tissue damage to prevent bleeding. Fibrinogen is synthesized primarily in hepatocytes as a result of inflammatory stimuli. Increased fibrinogen levels are associated with an increased cardiovascular risk.

- C-Reactive protein (CRP): an acute-phase marker of inflammation and tissue damage [159]; it is synthesized by the liver in response to inflammatory stimuli. CRP has profound pro-inflammatory properties [160] and promotes the inflammatory component of atherosclerosis [161]. In this work we used high-sensitivity CRP (hs-CRP) which, being measured in a lower range of values (mg/L), is more indicative of low levels of inflammation and it is reported to be a predictor of increased risk of cardiovascular disease [162].

- Serum Amyloid A (SAA): a positive acute-phase reactant and a sensitive marker of an acute inflammation [163]. SAA proteins contribute to high density lipoproteins (HDL) and cholesterol transport, thus being associated with cardiovascular disease (CVD) and atherogenesis [164].

- Interleukin-6 (IL-6): a multifunctional pro-inflammatory cytokine, synthesized at the initial phase of inflammation. It enters the bloodstream and induces the synthesis of acute phase proteins such as CRP, serum amyloid A and Fbrinogen by the liver [165].

- Adiponectin: an adipokine, generally secreted by the adipose tissue [166]. It is an anti-inflammatory agent, reducing inflammation in various cell types

[167]. Several studies report that the plasma level of this protein decreases in obesity, type 2 diabetes and coronary heart disease [168].

The general mechanism by which these biomarkers are involved in the inflammatory response is shown in Figure 6.2. After inhalation of air pollutants, two main pathways related to the inflammatory response are activated: the first one refers mainly to a local inflammation, the second one to a systemic effect. Starting with the former, inhalation of air pollutants can cause respiratory tissue damage that can trigger local oxidative stress and inflammation. The propagation of inflammation triggers the activation of immune cells, with possible release of inflammatory mediators such as IL-6, Interleukin-1 (IL-1), Tumor necrosis factor alpha (TNFα), etc., decreasing level of anti-oxidants [21, 169]. The second mechanism relates mainly to UFPs, in particular to their translocation from the lungs into the circulation with direct effects on systemic inflammation and consequent release of pro-inflammatory agents here too. With regard to the biomarkers under study, the increasing level of IL-6 in the blood stream promotes the release of inflammatory markers from the liver such as Fibrinogen and CRP and the release of adipocytokines from adipocytes, such as Adiponectin.

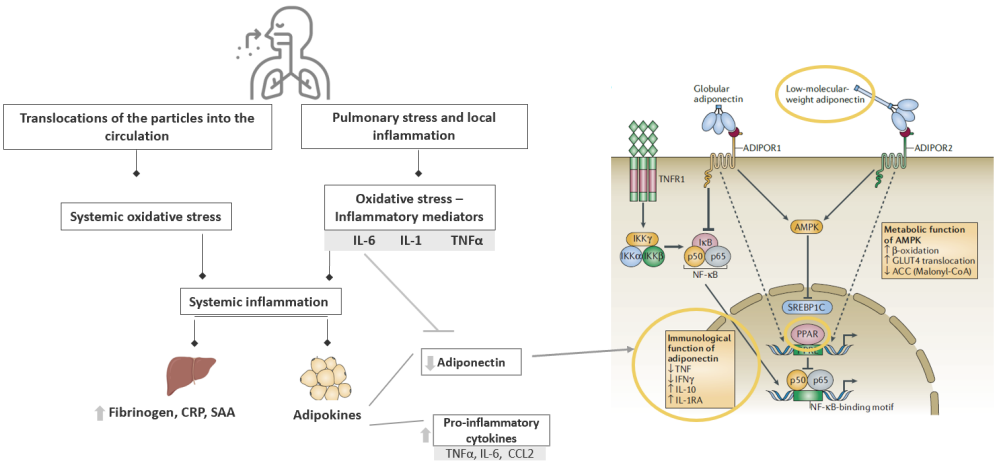

Figure 6.2: General scheme showing the involvement of the markers under study in the inflammatory process [21, 169–171]. The pathway representation shows the mechanisms by which Adiponectin exerts its anti-inflammatory action. Binding between adipose and its receptors mediates activation of the peroxisome proliferator-activated receptor alpha (PPAR), which induces expression of anti-inflammatory target genes such as Interleukin-10 (IL-10) and the inhibition of pro-inflammatory targets, such as Nf-Kβ [172].

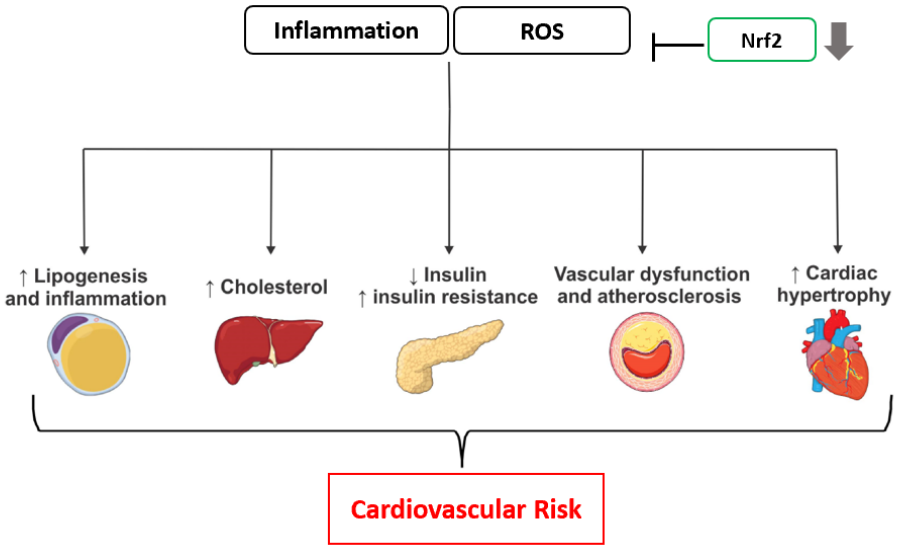

Figure 6.3: Reduction in Nfr2 function leads to an accumulation of ROS and an increased inflammatory state, which may lead to target-organ damage and metabolic disturbances, thus increasing cardiovascular risk. Re-adapted from [24].

Adiponectin is inversely related to inflammation because it can inhibit the NF-kβ pathway resulting in a decrease in pro-inflammatory markers (TNFα, INFγ) and an increase in anti-inflammatory markers (IL-10) [172] (Figure 6.2). The resulting systemic inflammation affects endothelial function, formation of thrombi, progression of atherosclerotic lesions and also epigenomic changes with impact on the cardiovascular health [24, 169] (Figure 6.3).

Particles may also lead to a change in autonomic control of the heart: directly, via reflex receptors in the lungs affecting the autonomic nervous system and/or indirectly via oxidative stress and/or lungs inflammation. This can contribute to the instability of a vascular plaque or cardiac arrhythmia [18]. Autonomic imbalance and activation of the hypothalamic pituitary adrenal (HPA) axis contribute to immune response and release of hormone such as cortisol that consequently can increase common risk factors for heart disease [173]. I reported the Figure 6.4 from [169], which clearly summaries the mechanisms of action of air pollution related to cardiovascular health.

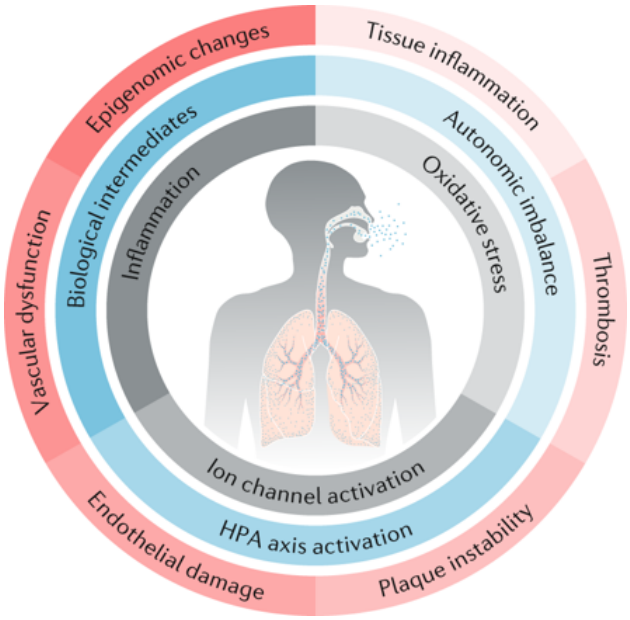

Figure 6.4: The mechanisms linking air pollution to cardiovascular diseases. From [169].

6.2 Hypothesis

The main objective of this work was to explore whether there is an association between long-term exposure to air pollutants and levels of blood markers reflecting inflammation and coagulation, thus linked to cardiovascular risk. The blood-biomarker under investigation are Fibrinogen, hs-CRP, SAA, IL-6 and Adiponectin. Whereas the air pollutants included in this analysis are: particle mass concentration (PM_{10}, PM_{coarse}, $PM_{2.5}$), particle number concentration of UFP (PNC), soot ($PM_{2.5}$ absorbance), Ozone (O_3), Nitrogen oxides (NO_2, NO_x). We hypothesized that increased exposure to ambient air pollution levels would lead to increased levels of Fibrinogen, hs-CRP, SAA and IL-6, whereas we expected a decrease in Adiponectn concentration with higher air pollution levels. We used the data from the KORA study (Cooperative Health Research in the region of Augsburg [174], Germany) to address such hypothesis. The exposure data where provided by the ULTRA III project (Environmental Nanoparticles and Health: Exposure, Modeling and Epidemiology of Nanoparticles and their composition). Details will be provided in the next chapter.

Chapter 7

Methods II

7.1 Study population

The Cooperative Health Research in the Region of Augsburg (KORA) is a research platform for population-based surveys in the fields of health related disciplines and epidemiology [175]. There are in total four baseline surveys S1-S4 which have been conducted in the region of Augsburg, began in 1984 and continued at regular five-year intervals. S1-S4 participants took part in interviews and follow-up examinations at regular intervals as shown in Figure 7.1 [174].

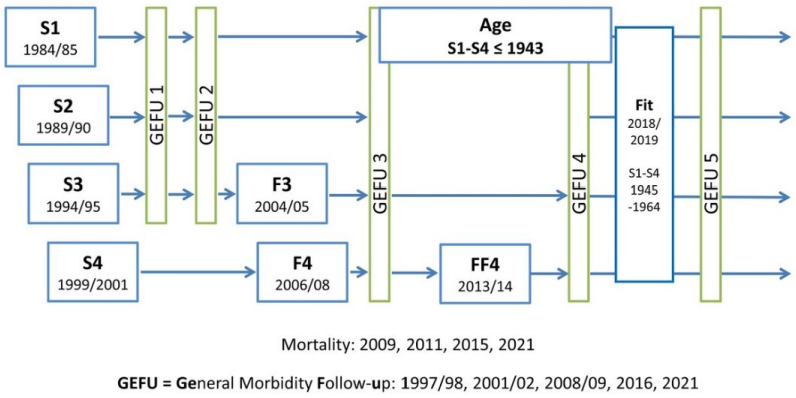

Figure 7.1: Overview of KORA cohort. From [174].

Our analysis is based on data of the population-based cohort study KORA-S4 in which 4261 participants aged 25 - 74 years took part in the time period

1999-2001. Demographic, socio-economic, lifestyle information, medical history and medication used were collected in a face-to-face interview, while clinical and anthropometric measures were collected during the medical examination.

All study participants provided written informed consent. The KORA study was approved by the ethics committee of the Bavarian Chamber of Physicians (Munich, Germany).

7.2 Outcome data

Blood samples were collected from the KORA S4 population and biomarkers concentration was measured. Plasma CRP (hs-CRP) (in mg/L) concentrations were assessed by using a high-sensitivity latex-enhanced nephelometric assay on a BN II System analyser (Dade Behring, Marburg, Germany) [176]. Plasma Fibrinogen (g/L) and SAA (mg/L) concentrations were analysed by immunonephelometry (Behring, Marburg, Germany) [177]. Serum levels of IL-6 (pg/mL) were measured by using sandwich ELISA [178], values below detection limit set to 0.001 pg/mL. Serum Adiponectin were determined using the human radioimmunoassay [179].

7.3 Exposure data

The exposure data used in this work were provided by ULTRA III project. The annual average exposure of air pollutants was calculated using the Land Use Regression (LUR) model for each study participant at their home address. LUR is a widely used method for modeling and explaining the spatial variability of long-term outdoor air pollutants using predictor variables derived from the Geographic Information System (GIS) [180]. Sampling campaign took place between March 2014 and April 2015 at 20 locations within the KORA study region. Specifically, to cover warm, cold and intermediate seasons, it was organized into three measurement campaigns of two weeks each during the year. PM_{10} and $PM_{2.5}$ were measured using a Harvard impactor, a filter-based gravimetric method. PM_{coarse} was calculate by the difference of the two fractions of PM. Soot was quantified by measuring the absorbance of $PM_{2.5}$.

PNC was sampled with four GRIMM ultrafine particle counters (model EDM 465 UFPC, GRIMM aerosol, Ainring, Germany) measuring total PNC with a cut-off at

7 nm and one NanoScan-SMPS Nanoparticle Sizer (model 3910, TSI, Shoreview, MN, USA) measuring NPs in the size range 13-420 nm; the latter was used until 18 July 2014 because it was then replaced by the fourth GRIMM due to a damage. Throughout the ULTRA sampling campaign one fixed urban background site carried out continuous measurements in order to adjust the measurements of the discontinuous sites. Here, PNC was sampled with a combination of custom-made Twin Differential mobility Particle Spectrometry (TDMPS, 3-800nm) [181] and aerodynamic particle sizer; the comparison of instruments was carried out every fortnight with appropriate adjustments. The LUR models for almost all pollutants indicate a good fit. The adjusted model-explained variance - R^2 - ranged from 68% for PM_{coarse} to the higher 94% for NO_2 and the corresponding adjusted leave-one-out cross-validation R^2 - LOOCV- were between 55% PM_{coarse} and 89% NO_2, still indicating a good fit [182].

7.4 Covariates

Potential confounding factors were considered by exploring demographic, socioeconomic, lifestyle, clinical and medical history covariates. Included in the cluster of socioeconomic covariates there are: education level reported as a cumulative number of total years of education; marital status (single/ married or living with partner/ divorced or separated/ marriedm, living apart); and occupational status (employed, self-employed or in training/ unemployed/ homemaker/ retired); the neighborhood socioeconomic status (SES) is reported as percentage of households with low income in $(1\ km)^2$ grid cell. Lifestyle covariates cover the following behaviors and physical characteristics. Cumulative exposure to smoking is reported as total pack- years; current smoking status at the examination time (smoker/ no smoker/ ex-smoker). Alcohol intake was reported as g/day, considering that 1 unit = 12 gr. Body mass index (BMI) and waist hip ratio were measured for each participant. Physical activity is reported as inactive/active. As clinical covariates we considered total cholesterol (mg/dL) and HDL-cholesterol (mg/dL). Participants reported in a double choice (yes/no) whether they were currently suffering from and/or under pharmacological control of hypertension and diabetes mellitus; they also stated whether or not they used non-steroidal anti-inflammatory drugs (NSAIDS). The history of cardiovascular events, specifically the occurrence of stroke or myocardial infarction, was assessed, also them as binary variables.

7.5 Statistical methods

Multiple linear regression adjusting for confounders was performed to assess the potential association between each biomarker and each pollutant. The distribution of the residuals for each outcome was checked. To better approximate the normal distribution all biomarkers were log-transformed. The selection of potential confounders was performed based on the protocol developed by Dr. S. Zhang and Dr. U. Kraus ("Environmental Risks" research group, Institute of Epidemiology, Helmholtz Zentrum, München) and proceeded as follows. The first step consisted of sorting the covariates by topic and the exclusion of variables with more than 10% of missing values. Furthermore, to avoid multicollinearity the correlation between variables was evaluated and subsequently, based on previous studies, we selected the variables best representing the relation with the outcomes. Then, the covariates selection was made using the following 3 methods:

- the first using the Bayesian information criterion, BIC, which is a model selection tool. We performed a stepwise analysis for each category and chose the model with the lowest BIC score.
- the second method is to use Spearman's correlation between the covariates and each outcome to measure the strength of the relationship. We have selected the variables with a coefficient correlation >0.1/0.2.
- in the third one, we performed multivariate analysis, then we selected only the significant variables with p-value < 0.1.

The variables that have been selected across the three methods and that are representative for all outcomes were selected as potential confounders and therefore included in the model building. Three models were constructed: the *crude* model consists only of age, sex and month of blood withdrawal; the *main* model was adjusted for crude model covariates plus year of education, occupational status, marital status, cumulative smoking exposure, smoking status, alcohol consumption and physical activity. The *extended* model consists of the main model plus BMI, waist-hip ratio, total and HDL cholesterol, current hypertension (or drug-controlled), Diabetes mellitus (or use of antidiabetic drugs) and regular use of NSAIDs. The same three models were built for each outcome. The linearity of the exposure-response function was checked using the generalized additive model (GAM), using a penalized spline of the air pollutant.

Effect modification analysis was performed in order to evaluate difference between some specific subgroups. The modifier included in the analysis are: age (<60; ≥60), sex (female vs. male), smoking status (smoker vs. ex-smoker or no-smoker), BMI (<25 vs. ≥25), physical activity (no vs. yes), hypertension (no vs. yes), diabetes (no vs. yes) and NSAIDs medication use (no vs. yes).

7.6 Sensitivity analyses

We performed a sensitivity analysis excluding outliers which we identified as values $> 75^{th}$ percentile + 3× interquartile range (IQR) and values $< 25^{th}$ percentile − 3× IQR. We assessed the impact of neighborhood SES by adding it in the main model as a confounding variable. Moreover, two-pollutant model were calculated by adding a second pollutant variable; we selected O_3 and $PM_{2.5}$ based on the Spearman's correlation coefficient at <0.70.
Finally, quantile regression was carried out in order to evaluate the association between each pollutant and each biomarker across quantiles.

All analyses were conducted with R version 3.4.1 using the "mgcv" and "quantreg" packages.

Chapter 8

Results II

8.1 Study population

The KORA S4 study population consists of 4261 participants, of which 4051 participants have information regarding the biomarkers under investigation in our research. All of the individuals in this dataset, with the exception of 17 of them, have information on Fibrinogen, hs-CRP and SAA levels, while 1404 individuals have complete information on IL-6 and Adiponectin. These participants are considered as a subset dataset, within the complete one, for the conduction of our statistical analysis.

To evaluate the statistically significant difference between the whole dataset and the subset dataset we used Mann-Whitney U test for continuous variables and Chi squared for categorical ones.

The average age for the entire study is 49 years while the subsample of older participants has an average age of 64 years. This difference is reflected in the other characteristics that are presented in Table 8.2. Specifically, the percentage of ex-smokers in the younger population is 21.8% compared to 38% in the older one, we also observed 26.3% of smoker in the whole dataset while only 14.1% in second one. The occupational status shows for the older subsample a percentage of retired of 61.8% compared to 24.4% of younger one. In addition, medical status and medication use show a significant difference the whole study and the subsample. Among the latter, the 7.5% answered to have diabetes or to be making use of antidiabetic medication and 56.5% confirmed to be affected by hypertension or to be controlling it with medication. This data can be compared to 3.9% and 37.2%

respective shares within the entire study. In general, the levels of all biomarkers do not exceed the mean normal reference levels for each. The arithmetic mean for all the participants is for Fibrinogen 3 (± 1) g/L, for hs-CRP is 3 (± 5) mg/L and for SAA is 6 (± 18) (mg/L). The mean for IL-6 and Adiponectin is 4 (± 12) (pg/mL) and 10 (± 5) (µg/mL) respectively. Spearman's correlation between biomarkers was assessed. The inflammatory markers show strong correlation among them, especially between hs-CRP and SAA. Adiponectin, as expected, shows an inverse correlation with inflammatory markers, especially with hs-CRP (Table 8.1).

Table 8.1: Descriptive statistics of blood biomarkers, cumulative of both datasets: mean ± standard deviation (SD) and Spearman's correlation coefficient among biomarkers.

Biomarker	Mean ± SD	Spearman's correlation coefficient			
		IL-6	Adiponectin	hs-CRP	Fibrinogen
IL-6 (pg/mL)	4±12				
Adiponectin (µg/mL)	10±5	-0.05			
hs-CRP (mg/L)	3±5	0.44	-0.11		
Fibrinogen (g/L)	3±1	0.27	0	0.49	
SAA (mg/L)	6±18	0.30	0.02	0.60	0.36

IL-6: Interleukin 6;
hs-CRP: high-sensitivity C-reactive protein;
SAA: Serum Amyloid A.

Table 8.2: Descriptive statistics of the study population: mean ± standard deviation (SD) or number in % , missing number of observations (in %) and statistically significant difference.

	KORA S4 N= 4051		Subsample N= 1404		
Variables	**Mean ± SD or N(%)**	**Miss. N(%)**	**Mean ± SD or N(%)**	**Miss. N(%)**	**p-value**
Personal characteristics					
Age	49 ± 14	-	64 ± 5	-	< 0.001
Sex (Female)	2064 (51)	-	675 (48.1)	-	0.07
Socio-economic covariates					
Education (years)	12 ± 3	-	11 ± 2	-	<0.001
Occupational status					< 0.001
Employed, self-employed or in training	2458 (60.7)		324 (23.1)		
Unemployed	142 (3.5)		56 (4)		
Homemaker	464 (11.5)		157 (11.2)		
Retired	987 (24.4)		867 (61.8)		
Marital status					< 0.001
Single	459 (11.3)		64 (4.6)		
Married or living with partner	2987 (73.7)		1035 (73.7)		
Divorced or separated	364 (9.0)		120 (8.5)		
Widowed	241 (5.9)		185 (13.2)		
Percentage of households with low income in (1 km)^2 grid cell (%)	27 ± 23	-	28 ± 23	-	0.18
Lifestyle covariates					
Cumulative smoking exposure (pack-years)	12 ± 20	-	15 ± 24		0.42
Smoking status					<0.001
Smoker	1066 (26.3)		197 (14.1)		
Ex-smoker	1289 (21.8)		533 (38)		
Non-smoker	1696 (41.9)		674 (48.1)		
Acohol consumption (g/day)	16 ± 22	-	16 ± 21	-	0.36
Body mass index (kg/m^2)	27 ± 5	32 (0.8)	29 ± 4	7 (0.5)	<0.001
Waist-hip ratio	1 ± 0	24 (0.6)	1 ± 0	2 (0.1)	<0.001
Physical active					<0.001
Inactive	2079 (51.3)		817 (58.2)		
Active	1972 (48.7)		587 (41.8)		
Clinical covariates					
Total cholesterol (mg/dL)	228 ± 44	2 (0.05)	243 ± 42	1 (0.1)	<0.001
HDL cholesterol (mg/ dL)	58 ± 17	8 (0.2)	58 ± 16	2 (0.1)	0.89
Medical history and medication					
Current hypertension or drug-controlled (yes)	1506 (37.2)	8 (0.2)	792 (56.5)	1 (0.1)	< 0.001
Diabetes mellitus or use of antidiabetic drugs only metformin (yes)	158 (3.9)	-	106 (7.5)	-	<0.001
Regular use of NSAIDs, anti-inflammatory (yes)	103 (2.5)	6 (0.1)	50 (3.6)	1 (0.1)	0.06

HDL-cholesterol: high-density lipoprotein (HDL); NSAIDs: non-steroidal anti-inflammatory drug.

8.2 Exposure data

The descriptive statistics of air pollutants is reported in Table 8.3. There is no statistically significant difference between the annual average of each pollutant calculated between the whole study population and the subsample. Spearman's correlation among pollutants was investigated, results are shown in Figure 8.2. Almost all pollutants are highly correlated with each other, with the exception of O_3 for which the correlation is either null or inverse, in particular with NO_x as expected, since it is a product of chemical reactions between nitrogen oxides (NOx) and volatile organic compounds (VOC) [183]. Also the correlation of O_3 with $PM_{2.5}$ is relevant and it has already been observed in other studies as in [184]. The maximum value of the correlation coefficient observed is between PNC and NO_x with a percentage share of 90%. According to the threshold of the European Directive, the pollutants did not exceed the annual limit values in the year 2014-2015.

Table 8.3: Descriptive statistics of air pollutants. The mean ± standard deviation (SD) and interquartile range (IQR) for each pollutant is reported.

	KORA S4 N= 4051		Subsample N= 1404	
Pollutants	Mean ± SD	IQR	Mean ± SD	IQR
PM_{10} µg/m^3	17 ± 2	2.12	17 ± 2	2.06
PM_{coarse} µg/m^3	5 ± 1	1.37	5 ± 1	1.29
$PM_{2.5}$ µg/m^3	12 ± 1	1.39	12 ± 1	1.32
$PM_{2.5abs}$ 10^{-5}/m^3	1 ± 0	0.27	1 ± 0	0.26
NO_x µg/m^3	22 ± 7	8.50	22 ± 7	8.03
NO_2 µg/m^3	14 ± 5	7.17	15 ± 4	7.05
O_3 µg/m^3	39 ± 2	3.59	39 ± 2	3.46
PNC 10^3/m^3	7.4 ± 1.8	1.94	7.4 ± 1.8	1.81

PM_{10}, PM_{coarse}, $PM_{2.5}$: particulate matter with aerodynamic diameter < 10 µm, 2.5–10 µm and < 2.5 µm, respectively; $PM_{2.5abs}$: absorbance of $PM_{2.5}$; PNC: particle number concentration; NO_2: nitrogen dioxide; NO_x: nitrogen oxides; O_3: ozone.

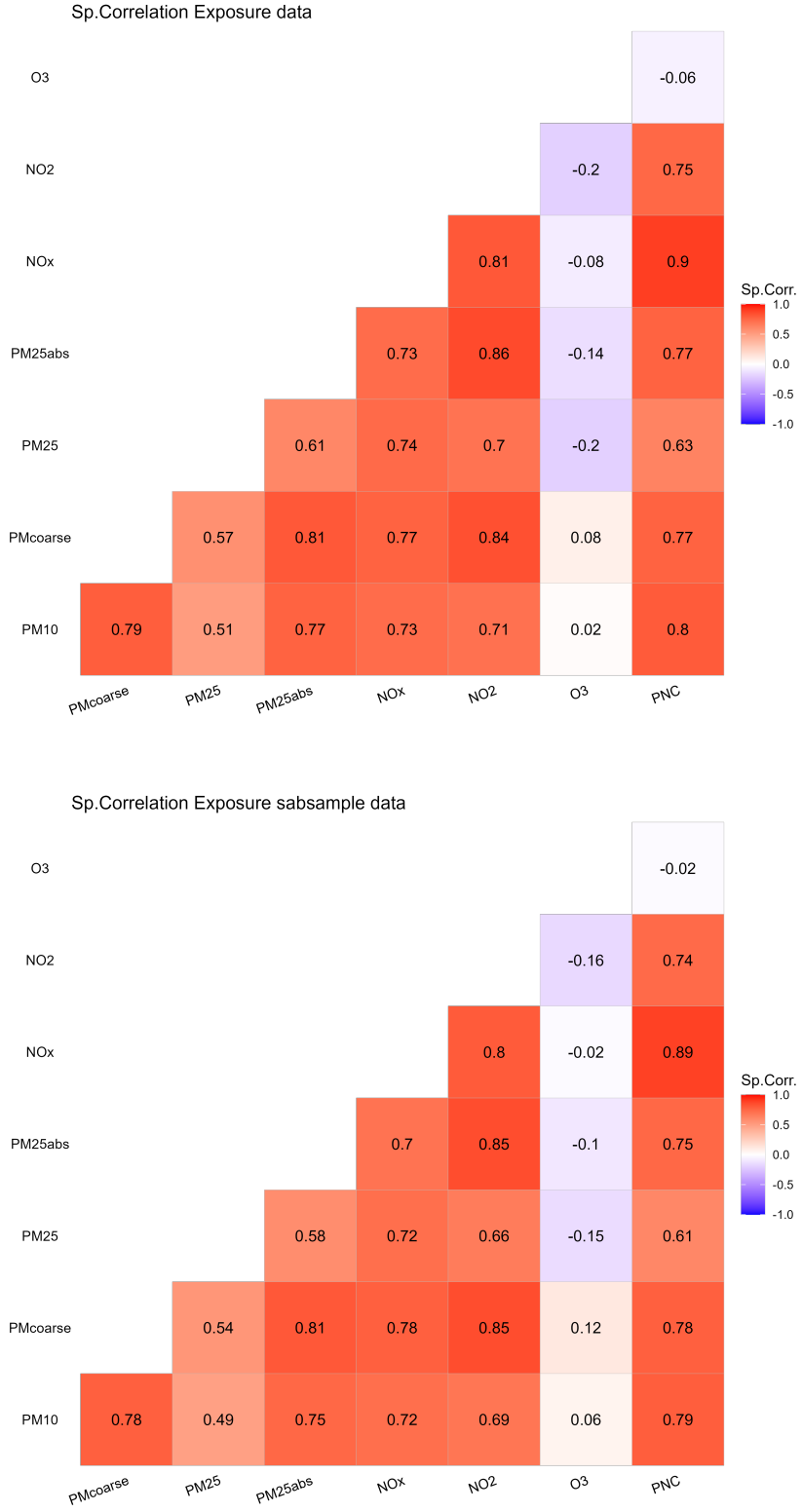

Figure 8.1: Spearman's correlation between pollutants. The positive correlation is shown in red and increases with increasing colour intensity. Conversely, colour in blue represents negative correlation and in white null.

8.3 Regression analysis

The regression analysis was performed for the three models taking into consideration different potential confounding factors. The crude model, considering age, sex and month (of blood collection); the main model, including also socio-economic and lifestyle covariates; finally the extended model, added of clinical and medical history variables. This approach was chosen to allow for a more complete assessment of the influence that different confounders have on the parameters. This assessment will be performed by comparing the independent variables' parameters and the confounding variables' ones in each model.
The associations between air pollutants and biomarkers results are expressed as the percentage change in the biomarker per interquartile range (IQR) increase of each pollutant. The results of the regression analysis are shown in Tables 8.4 to 8.8 and Figures 8.2 to 8.6; which depict the comparison among models. Statistically significant positive results, p-value <0.05, were observed for Fibrinogen with PNC in general in all three models (Table 8.4). Adjusting the model for age, sex and month of blood withdrawal, given an increase of IQR in NO_x (8.5 µg/m^3), Fibrinogen increases by 0.7 % (0; 1.5). The addition of covariates regarding lifestyle, medical history and clinical variables leads to smaller, not statistically significant association with NO_x. A positive trend is observable also with $PM_{2.5}$ and NO_2 both in the crude model. Similar to Fibrinogen, hs-CRP shows strong positive relation with PNC across the three models (Table 8.5); into the main model, an interquartile range (1941 particles/cm^3) increase was associated with a 3.1% (-0.5; 6.9) increase in hs-CRP. Positive associations with PM_{10} and NO_x are also observed but not statistically significant. SAA shows a positive association with PM_{10} and PNC which are not statistically significant (Table 8.6).
With regard to IL-6, in the main model it increases by 11.4% with $PM_{2.5}$ increase of 1.32 µg/m^3 (Table 8.7); the statically significant positive association persists in all adjusted models (main and extended). On the other hand Adiponectin shows a general inverse relation with almost all the pollutants. Statistical significance is observed in relation to O_3 which persists in all three models, specifically in the main model, Table 8.8 shows a decrease of -5.4% (-8.8; -1.9) of Adiponectin when O_3 increases by 3.5 µg/m^3.

Tables with the results for each biomarker are shown below; each table is followed by its respective graph in order to allow visualisation of the results.

Table 8.4: Fibrinogen: comparison of estimates across the three models: crude, main and extended in term of percent change of biomarkers per interquartile range (IQR) change of pollutants (N= 4034; 95% CI; ** = p-value <0.05; * = p-value <0.1)

	Fibrinogen			
Pollutant	**IQR-poll.**	**Crude[a]**	**Main[b]**	**Extended[c]**
PM_{10} µg/m^3	2.12	0.2 (-0.7; 1)	0.2 (-0.7; 1)	0.2 (-0.6; 1)
PM_{coarse} µg/m^3	1.37	0.1 (-0.8; 0.9)	0.1 (-0.8; 0.9)	0.2 (-0.6; 1)
$PM_{2.5}$ µg/m^3	1.39	0.6 (-0.2; 1.5)	0.4 (-0.5; 1.2)	0.3 (-0.5; 1.2)
$PM_{2.5abs}$ 10^{-5}/m^3	0.27	0.6 (-0.4; 1.5)	0.4 (-0.5; 1.4)	0.4 (-0.5; 1.3)
NO_x µg/m^3	8.50	0.7 (0; 1.5)**	0.5 (-0.2; 1.3)	0.5 (-0.2; 1.2)
NO_2 µg/m^3	7.17	0.7 (-0.3; 1.7)	0.5 (-0.5; 1.5)	0.4 (-0.6; 1.4)
O_3 µg/m^3	3.59	-0.7 (-1.6; 0.3)	-0.3 (-1.2; 0.6)	0 (-1; 0.9)
PNC 10^3/m^3	1.94	0.8 (0.1; 1.5)**	0.7 (0; 1.3)**	0.6 (0; 1.3)*

CI: confidence interval; PM_{10}, PM_{coarse}, $PM_{2.5}$: particulate matter with aerodynamic diameter < 10 µm, 2.5–10 µm and < 2.5 µm, respectively; $PM_{2.5abs}$: absorbance of $PM_{2.5}$; PNC: particle number concentration; NO_2: nitrogen dioxide; NO_x: nitrogen oxides; O_3: ozone.
[a]: Age, sex, month; [b]: crude model covariates + year of education, occupational status, marital status, cumulative smoking exposure, smoking status, alcohol consumption and physical activity; [c]: main model + body mass index (BMI), waist-hip ratio, total and high-density lipoprotein (HDL) cholesterol, current hypertension (or drug controlled), diabetes mellitus (or use of antidiabetic drugs) and regular use of non-steroidal anti-inflammatory drug (NSAIDs).

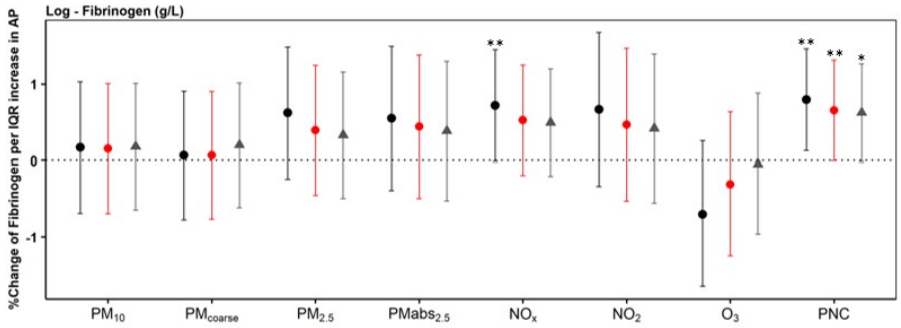

Figure 8.2: Percent change of Fibrinogen per IQR increase in air pollutant. Comparison across the three models; in black is represented the crude model, in red the main one, and in grey the extended one (95% CI; ** = p-value <0.05; * = p-value <0.1).

Table 8.5: high-sensitivity C-reactive protein (hs-CRP): comparison of estimates across the three models: crude, main and extended in term of percent change of biomarkers per interquartile range (IQR) of pollutants (N= 4034; 95% CI; ** = p-value <0.05; * = p-value <0.1)

		hs-CRP		
Pollutant	**IQR-poll.**	**Crude**	**Main**	**Extended**
PM_{10} µg/m^3	2.12	3.1 (-1.7; 8.1)	3 (-1.7; 7.9)	2.7 (-1.7; 7.3)
PM_{coarse} µg/m^3	1.37	-1 (-5.5; 3.7)	-0.7 (-5.2; 4)	0.4 (-3.8; 4.8)
$PM_{2.5}$ µg/m^3	1.39	1.8 (-2.9; 6.7)	0.8 (-3.8; 5.6)	0.8 (-3.6; 5.3)
$PM_{2.5abs}$ 10^{-5}/m^3	0.27	2.9 (-2.3; 8.3)	2.6 (-2.5; 8)	2.2 (-2.6; 7.2)
NO_x µg/m^3	8.50	3.2 (-0.8; 7.5)	2.4 (-1.6; 6.5)	2.2 (-1.5; 6.1)
NO_2 µg/m^3	7.17	2.1 (-3.3; 7.9)	1.4 (-4; 7.2)	1.3 (-3.8; 6.6)
O_3 µg/m^3	3.59	-4.4 (-9.3; 0.8)*	-2.1 (-7.1; 3.1)	-0.7 (-5.5; 4.2)
PNC 10^3/m^3	1.94	3.7 (0; 7.6) **	3.1 (-0.5; 6.9) *	2.9 (-0.5; 6.4)*

CI: confidence interval; PM_{10}, PM_{coarse}, $PM_{2.5}$: particulate matter with aerodynamic diameter < 10 µm, 2.5–10 µm and < 2.5 µm, respectively; $PM_{2.5abs}$: absorbance of $PM_{2.5}$; PNC: particle number concentration; NO_2: nitrogen dioxide; NO_x: nitrogen oxides; O_3: ozone.
[a]: Age, sex, month; [b]: crude model covariates + year of education, occupational status, marital status, cumulative smoking exposure, smoking status, alcohol consumption and physical activity; [c]: main model + body mass index (BMI), waist-hip ratio, total and high-density lipoprotein (HDL) cholesterol, current hypertension (or drug controlled), diabetes mellitus (or use of antidiabetic drugs) and regular use of non-steroidal anti-inflammatory drug (NSAIDs).

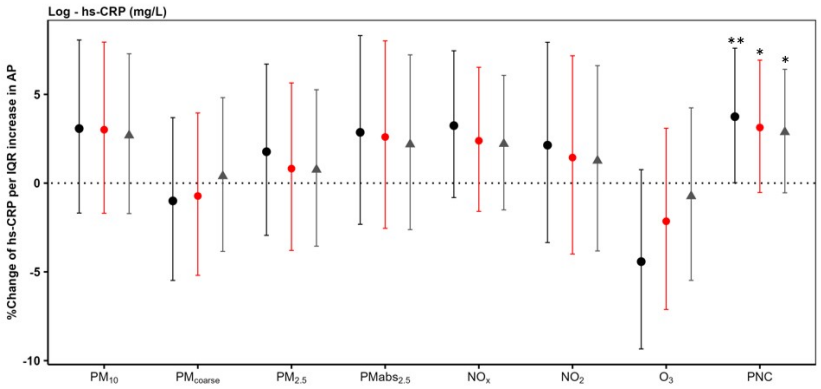

Figure 8.3: Percent change of hs-CRP per IQR increase in air pollutant. Comparison across the three models; in black is represented the crude model, in red the main one, and in grey the extended one (95% CI; ** = p-value <0.05; * = p-value <0.1).

Table 8.6: Serum amyloid A (SAA): comparison of estimates across the three models: crude, main and extended in term of percent change of biomarkers per interquartile range (IQR) change of pollutants (N= 4034; 95% CI; ** = p-value <0.05; * = p-value <0.1)

		SAA		
Pollutant	**IQR-poll.**	**Crude**	**Main**	**Extended**
PM_{10} µg/m^3	2.12	2.4 (-1; 6)	2.7 (-0.8; 6.3)	2.6 (-0.8; 6.1)
PM_{coarse} µg/m^3	1.37	-0.7 (-4; 2.7)	-0.2 (-3.6; 3.2)	0 (-3.3; 3.4)
$PM_{2.5}$ µg/m^3	1.39	0.2 (-3.2; 3.7)	0.1 (-3.3; 3.6)	0.1 (-3.2; 3.6)
$PM_{2.5abs}$ $10^{-5}/m^3$	0.27	1.7 (-2.1; 5.6)	2 (-1.8; 5.9)	2 (-1.8; 5.8)
NO_x µg/m^3	8.50	1.3 (-1.6; 4.3)	1.3 (-1.7; 4.3)	1.2 (-1.6; 4.2)
NO_2 µg/m^3	7.17	0.2 (-3.7; 4.3)	0.4 (-3.6; 4.6)	0.4 (-3.5; 4.5)
O_3 µg/m^3	3.59	0.1 (-3.7; 4)	0.7 (-3.1; 4.7)	0.5 (-3.2; 4.4)
PNC $10^3/m^3$	1.94	2 (-0.7; 4.7)	2 (-0.7; 4.8)	2 (-0.7; 4.7)

CI: confidence interval; PM_{10}, PM_{coarse}, $PM_{2.5}$: particulate matter with aerodynamic diameter < 10 µm, 2.5–10 µm and < 2.5 µm, respectively; $PM_{2.5abs}$: absorbance of $PM_{2.5}$; PNC: particle number concentration; NO_2: nitrogen dioxide; NO_x: nitrogen oxides; O_3: ozone.
[a]: Age, sex, month; [b]: crude model covariates + year of education, occupational status, marital status, cumulative smoking exposure, smoking status, alcohol consumption and physical activity; [c]: main model + body mass index (BMI), waist-hip ratio, total and high-density lipoprotein (HDL) cholesterol, current hypertension (or drug controlled), diabetes mellitus (or use of antidiabetic drugs) and regular use of non-steroidal anti-inflammatory drug (NSAIDs).

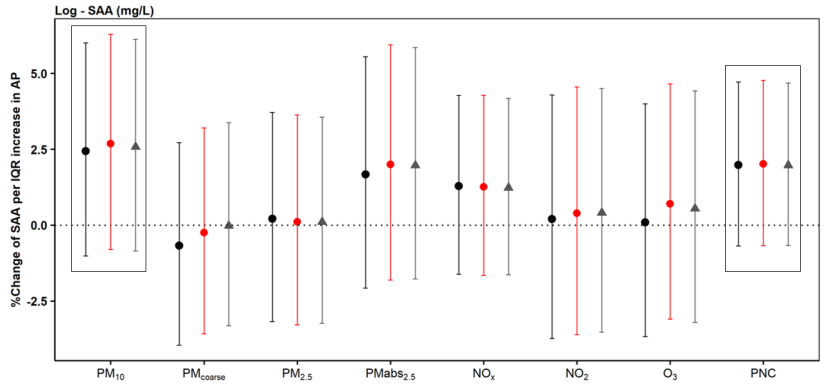

Figure 8.4: Percent change of SAA per IQR increase in air pollutant. Comparison across the three models; in black is represented the crude model, in red the main one, and in grey the extended one (95% CI; ** = p-value <0.05; * = p-value <0.1).

Table 8.7: Interleukin 6 (IL-6): comparison of estimates across the three models: crude, main and extended in term of percent change of biomarkers per interquartile range (IQR) change of pollutants (N= 1404; 95% CI; ** = p-value <0.05; * = p-value <0.1)

IL-6				
Pollutant	**IQR-poll.**	**Crude**	**Main**	**Extended**
PM_{10} µg/m^3	2.06	-3.8 (-15; 8.8)	-4.8 (-15.8; 7.8)	-5.4 (-16.4; 7)
PM_{coarse} µg/m^3	1.29	-3.1 (-13.8; 9)	-4.6 (-15.3; 7.5)	-4.8 (-15.5; 7.2)
$PM_{2.5}$ µg/m^3	1.32	12 (-1.1; 26.8)*	11.4 (-1.6; 26.1)*	11.2 (-1.8; 25.8)*
$PM_{2.5abs}$ $10^{-5}/m^3$	0.26	-3.9 (-15.7; 9.6)	-5.4 (-17.2; 8)	-6 (-17.6; 7.2)
NO_x µg/m^3	8.03	3.9 (-6.2; 15.1)	3.6 (-6.5; 14.8)	3.5 (-6.5; 14.6)
NO_2 µg/m^3	7.05	2.7 (-11.3; 18.9)	0.8 (-13.1; 16.8)	0.2 (-13.5; 16.1)
O_3 µg/m^3	3.46	-5.7 (-17.8; 8.1)	-4.8 (-17; 9.2)	-3.6 (-15.9; 10.5)
PNC $10^3/m^3$	1.81	1.7 (-7.2; 11.5)	1.1 (-7.8; 10.9)	0.9 (-8; 10.6)

CI: confidence interval; PM_{10}, PM_{coarse}, $PM_{2.5}$: particulate matter with aerodynamic diameter < 10 µm, 2.5–10 µm and < 2.5 µm, respectively; $PM_{2.5abs}$: absorbance of $PM_{2.5}$; PNC: particle number concentration; NO_2: nitrogen dioxide; NO_x: nitrogen oxides; O_3: ozone.
[a]: Age, sex, month; [b]: crude model covariates + year of education, occupational status, marital status, cumulative smoking exposure, smoking status, alcohol consumption and physical activity; [c]: main model + body mass index (BMI), waist-hip ratio, total and high-density lipoprotein (HDL) cholesterol, current hypertension (or drug controlled), diabetes mellitus (or use of antidiabetic drugs) and regular use of non-steroidal anti-inflammatory drug (NSAIDs).

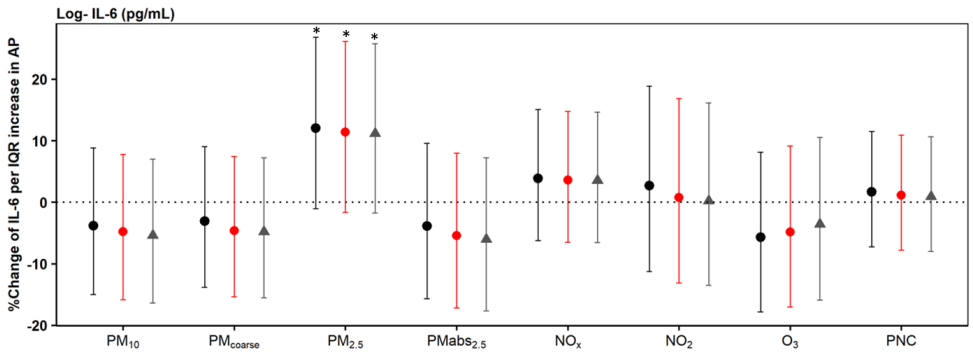

Figure 8.5: Dataset 2: Percent change of IL-6 per IQR increase in air pollutant. Comparison across the three models; in red is represented the main one(95% CI; ** = p-value <0.05; * = p-value <0.1)

Table 8.8: Adiponectin: comparison of estimates across the three models: crude, main and extended in term of percent change of biomarkers per interquartile range (IQR) change of pollutants (N= 1404; 95% CI; ** = p-value <0.05; * = p-value <0.1)

Adiponectin				
Pollutant	**IQR-poll.**	**Crude**	**Main**	**Extended**
PM_{10} µg/m^3	2.06	0 (-3.2; 3.3)	-0.5 (-3.7; 2.9)	0 (-3; 3.1)
PM_{coarse} µg/m^3	1.29	-1.5 (-4.6; 1.6)	-2.2 (-5.3; 0.9)	-2.3 (-5.2; 0.6)
$PM_{2.5}$ µg/m^3	1.32	-2 (-5.2; 1.3)	-1.8 (-5; 1.5)	-2 (-4.9; 1.1)
$PM_{2.5abs}$ 10^{-5}/m^3	0.26	-0.4 (-3.9; 3.1)	-0.8 (-4.3; 2.7)	-0.8 (-4; 2.5)
NO_x µg/m^3	8.03	-1.1 (-3.7; 1.6)	-1.3 (-4; 1.4)	-1 (-3.4; 1.6)
NO_2 µg/m^3	7.05	-0.7 (-4.4; 3.3)	-1.2 (-5; 2.8)	-1.2 (-4.8; 2.5)
O_3 µg/m^3	3.46	-5.5 (-8.8; -2)**	-5.4 (-8.8; -1.9) **	-6.1 (-9.2; -2.8)**
PNC 10^3/m^3	1.81	-1.1 (-3.5; 1.3)	-1.5 (-3.9; 1)	-1 (-3.3; 1.3)

CI: confidence interval; PM_{10}, PM_{coarse}, $PM_{2.5}$: particulate matter with aerodynamic diameter < 10 µm, 2.5–10 µm and < 2.5 µm, respectively; $PM_{2.5abs}$: absorbance of $PM_{2.5}$; PNC: particle number concentration; NO_2: nitrogen dioxide; NO_x: nitrogen oxides; O_3: ozone.
[a]: Age, sex, month; [b]: crude model covariates + year of education, occupational status, marital status, cumulative smoking exposure, smoking status, alcohol consumption and physical activity; [c]: main model + body mass index (BMI), waist-hip ratio, total and high-density lipoprotein (HDL) cholesterol, current hypertension (or drug controlled), diabetes mellitus (or use of antidiabetic drugs) and regular use of non-steroidal anti-inflammatory drug (NSAIDs).

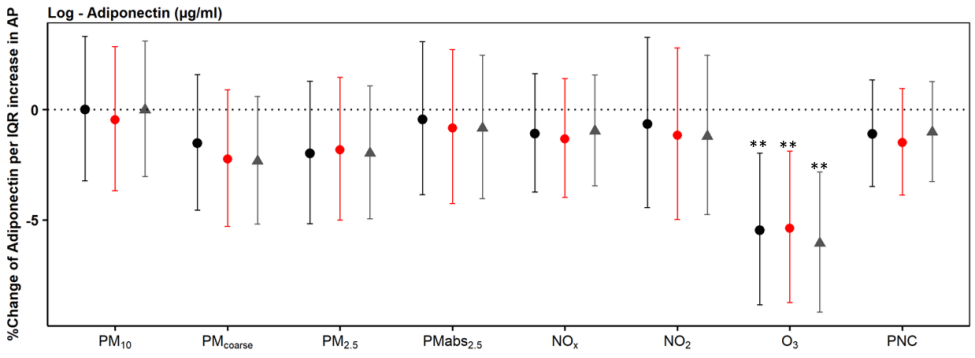

Figure 8.6: Percent change of Adiponectin per IQR increase in air pollutant. Comparison across the three models; in red is represented the main one(95% CI; ** = p-value <0.05; * = p-value <0.1)

8.4 Effect modification

Effect modification analysis was performed to investigate the difference between the subgroups. We found the major difference in the groups with and without intaking inflammatory medication (NSAIDs), in those who answered yes, the results show a strong positive association between IL-6 and $PM_{2.5abs}$, NO_x, NO_2 and UFPs. As well as for hs-CRP, which results significantly association with PM_{10} and O_3. This could be explained by the fact that people taking anti-inflammatory drugs start with a higher baseline level of inflammatory markers than those not taking these drugs, due to the underlying disease the drugs were prescribed for. Furthermore, the average age, for both databases, of people using NSAIDs is higher than those not using them. hs-CRP was found to be negative significantly associated with PM_{coarse} within those who practice physical activity [-6.74% (-12.92; -0.13), p-value < 0.05]. In the male subcategory, SAA exhibit significantly negative effect estimates per IQR increase with $PM_{2.5}$ [-4.48% (-9.08; 0.36), p-value < 0.05] and NO_x [-1.7% (-5.65; 2.41), p-value < 0.05]. It is an expected result, in [185] was found that males have statistically significantly lower level of SAA compared to females. Adiponectin shows positive association in people with diabetes (or under drug control). Adiponectin is generally negatively associated with diabetes; this positive association may be due to the intake of antidiabetic drugs since the release of Adiponectin from adipose tissue is stimulated by insulin [186]. In addition, it results statistically significant negative associated with $PM_{2.5}$ in the elderly population ($\geq$60) [-3.82% (-7.44; -0.06), p-value < 0.05].

No other clear and consistent modifier effects were observed.

8.5 Sensitivity analyses

We performed the sensitivity analyses in the main model, adjusted for age, sex, month of blood withdrawal, years of education, occupational status, marital status, cumulative smoking exposure, smoking status, alcohol consumption and physical activity. We first checked the strength of our results without including outlying biomarkers, this did not show statistically significant changes from the previous results (Figure 8.7).

We performed another sensitivity analysis investigating the impact of the neighborhood SES, defined as percentage of households with low income within (1 km)^2

grid cell, on the association between biomarkers of inflammation and air pollutants. Adding this variable to the main model significantly influences the outcomes, in particular regarding SAA, IL-6 and Adiponectin (Figure 8.8). SAA results to be statistically significantly associated with PM_{10} [3.4% (-0.5; 7.5), p-value < 0.1] and PNC [2.7% (-0.4; 5.8), p-value < 0.1]. The association of IL-6 with $PM_{2.5}$ is now stronger compared to when it was excluded from the model. Adiponectin is found to be statistically significantly negatively associated with $PM_{2.5}$ [-3.3% (-6.9; 0.5), p-value < 0.1] and PNC, which was not foreseeable from the previous results.

The analysis of the two-pollutant model was carried out by adjusting for O_3 the main model and the results tend to remain robust for almost all biomarkers (Figure 8.9). Whereas the adjustment with $PM_{2.5}$ reveals other results (Figure 8.10). SAA in the single-pollutant model shows no significant association with any pollutant, instead in two-pollutant model for $PM_{2.5}$ we observed a statistical significant positive association with PM_{10} [3.54% (-0.52; 7.78), p-value <0.1] and PNC [3.12% (-0.28; 6.65), p-value <0.1]. We noticed also in IL-6, two-pollutant model was negatively significant associated with PM_{10} [-12.6% (-24.15; 0.72), p-value <0.1], PM_{coarse}[-13.24% (-24.6; -0.17), p-value <0.05] and $PM_{2.5abs}$ [-16.96% (-29.43; -2.3), p-value <0.05], in contrast to the single-pollutant model.

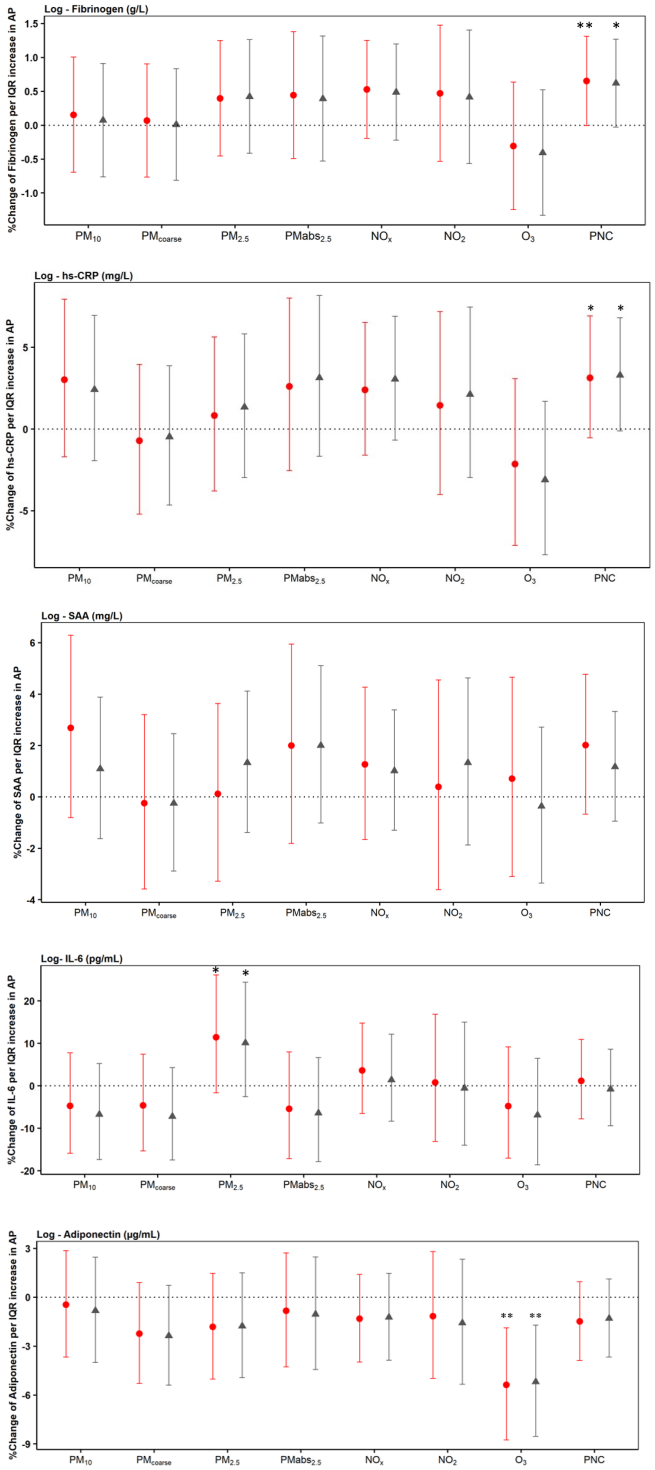

Figure 8.7: Comparison between the main model including outliers (red) and excluding outliers (grey). Represented as percent change of biomarker per IQR increase in air pollutant. (95% CI; ** = p-value <0.05; * = p-value <0.1)

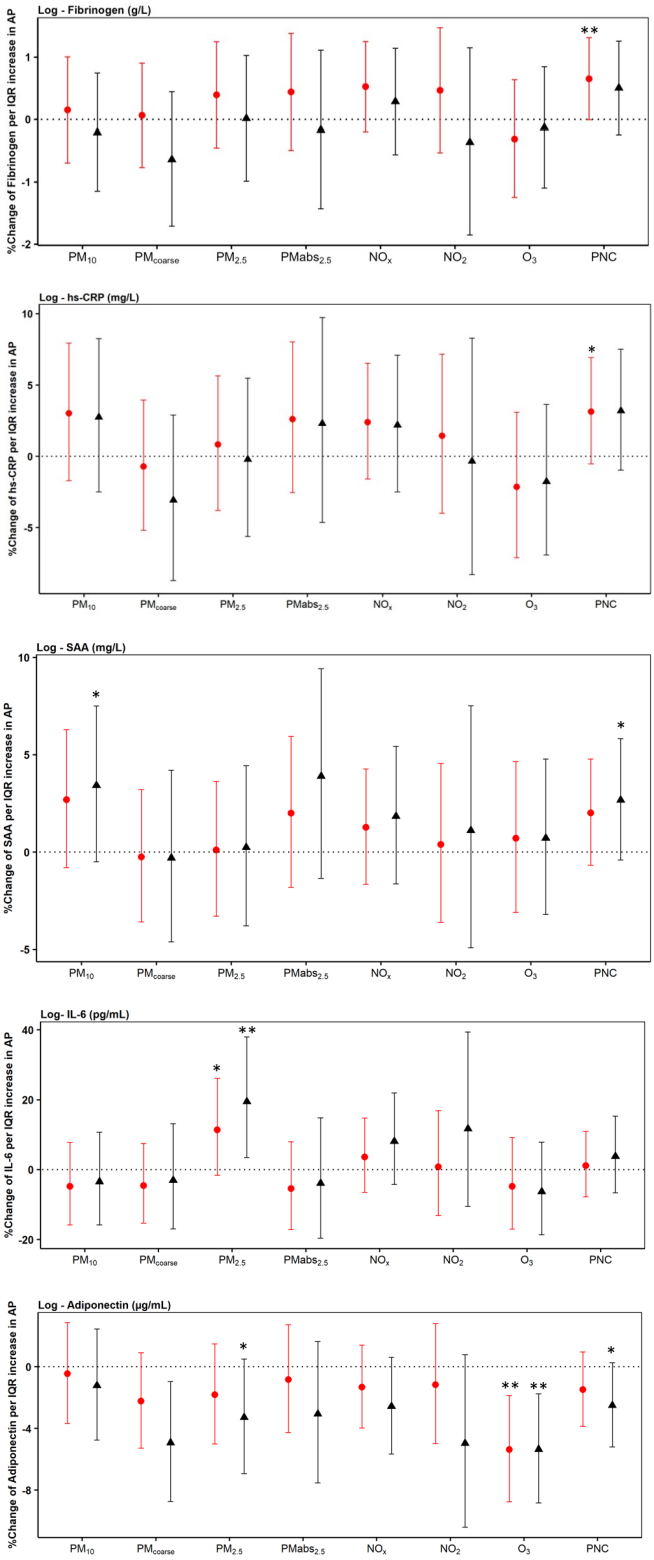

Figure 8.8: Percent change of biomarker per IQR increase in air pollutant in the main model (red) and in main model including the neighborhood SES variable (black), defined as percentage of households with low income in $(1\ \text{km})^2$ grid cell (95% CI; ** = p-value <0.05; * = p-value <0.1).

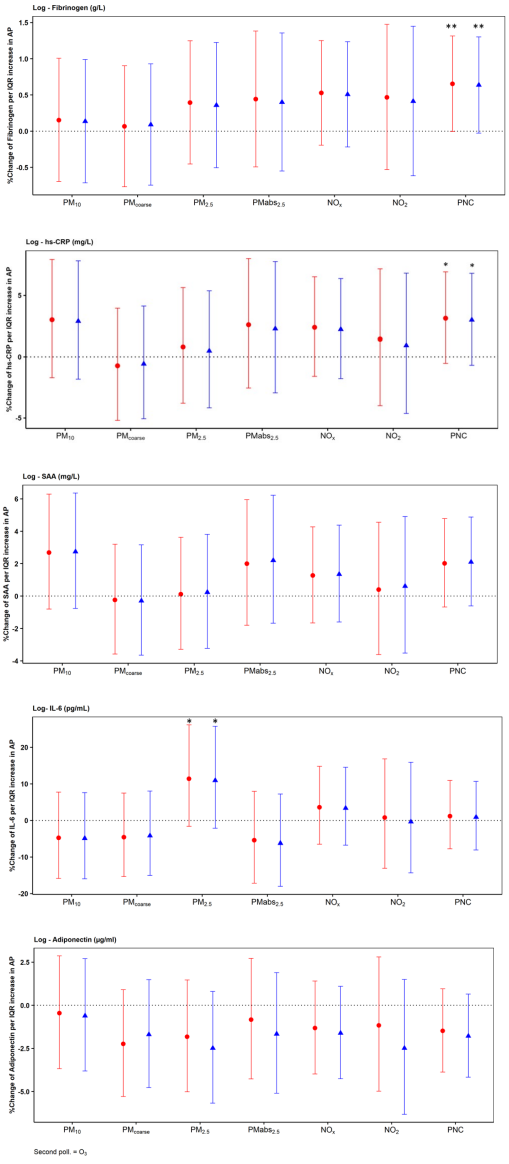

Figure 8.9: Second pollutant O_3: comparison between single (red) and two-pollutant (blue) models.

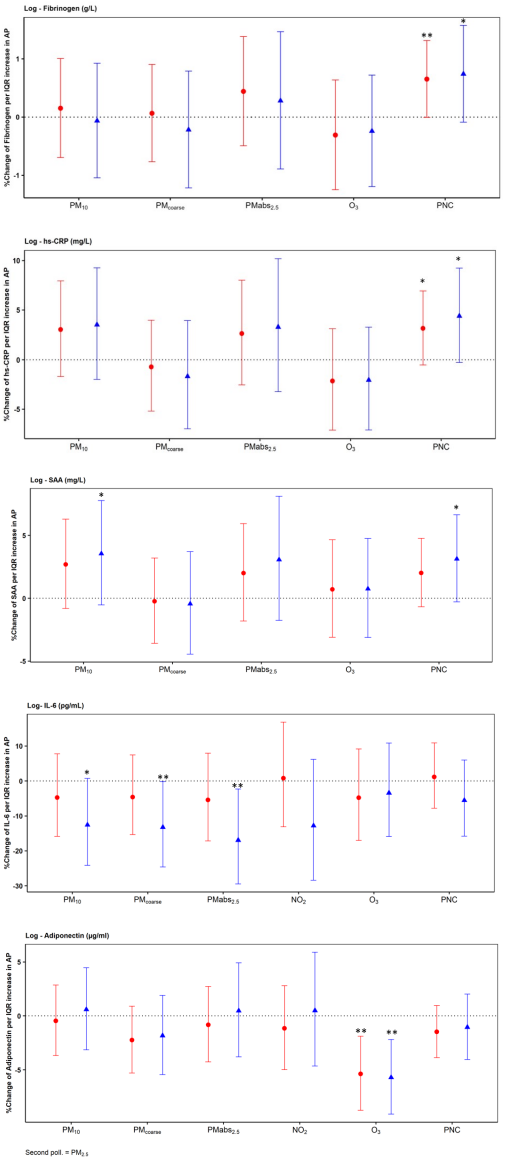

Figure 8.10: Second pollutant $PM_{2.5}$: comparison between single (red) and two-pollutant (blue) models.

Percent change of biomarker per IQR increase in air pollutant (95% CI; ** = p-value <0.05; * = p-value <0.1).

8.6 Quantile regression

Quantile regression analyses, adjusted for the covariates included in the main model, were conducted for all biomarkers. Some effects persisted across all quantiles while some effects occurred only at the lowest/highest quantiles. High percentiles identify high protein levels; conversely, lower percentiles identify lower levels. Thus, the relationship at lower percentiles highlights the impact of air pollutants on people with a healthy baseline level of inflammatory markers. In the next pages, I have reported the results for each biomarker; the y-axis represents the absolute change of the biomarker for the increase in the IQR of air pollutants, while the x-axis shows the biomarker of interest distributed along the quantiles.
For Fibrinogen, in the regression analysis for the main model we did not observe any associations except for PNC. However, in the quantile regression analysis we observed that $PM_{2.5}$, $PM_{2.5abs}$ and NO_x exhibit positive associations with Fibrinogen at the 90^{th} percentile; NO_x, also at 10^{th} percentile (Figure 8.11). hs-CRP shows similar results to those obtained with Fibrinogen; moreover, most pollutants are associated with hs-CRP at the 10^{th} percentile (Figure 8.12). Hs-CRP is an effective marker of low levels of inflammation, these results show how the impact of air pollutants can be statistically significant even at these levels. SAA in the regression analysis was not significantly associated with any pollutant. Exploring across quantiles we observed a positive association with PM_{10} at the low percentiles and with PNC at the central ones (Figure 8.13).
IL-6 shows negative associations at the 10^{th} percentile with $PM_{10,\ coarse,\ 2.5abs}$ and NO_2. With $PM_{2.5}$ there is strong association around central percentiles (Figure 8.14). For Adiponectin PM_{coarse} turns out to be negatively associated at almost all percentiles. NO_x, $PM_{2.5}$ and PNC exhibit positive association at lower percentiles (Figure 8.15).

In summary, these results show that also low levels of inflammatory markers are associated with increasing levels of different air pollutants.

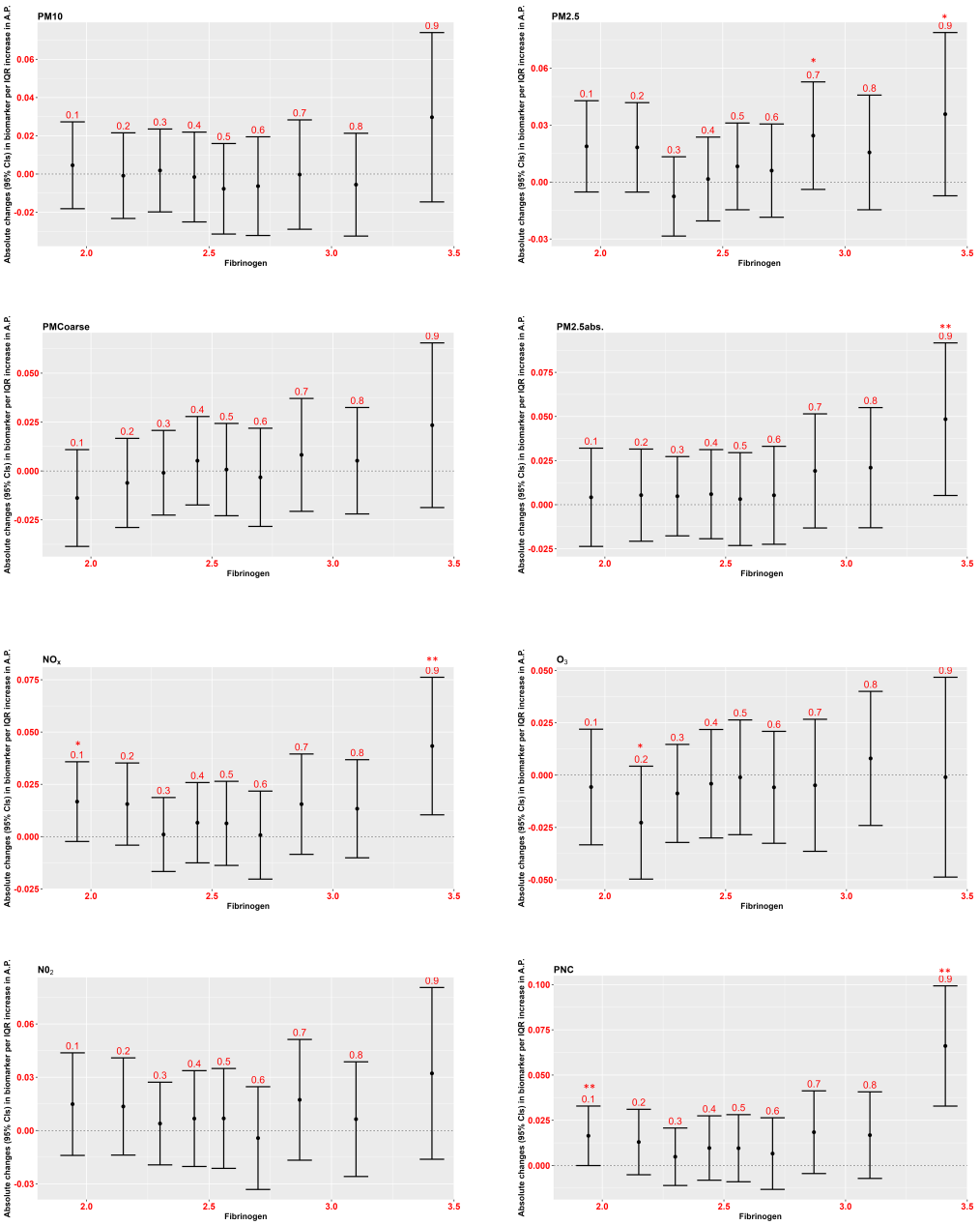

Figure 8.11: Fibrinogen quantile regression: in each graph the absolute change in Fibrinogen per IQR increase in individual air pollutant is shown, as well as its distribution across the quantile (Fibrinogen (g/L); 95% CI; ** = p-value <0.05; * = p-value <0.1).

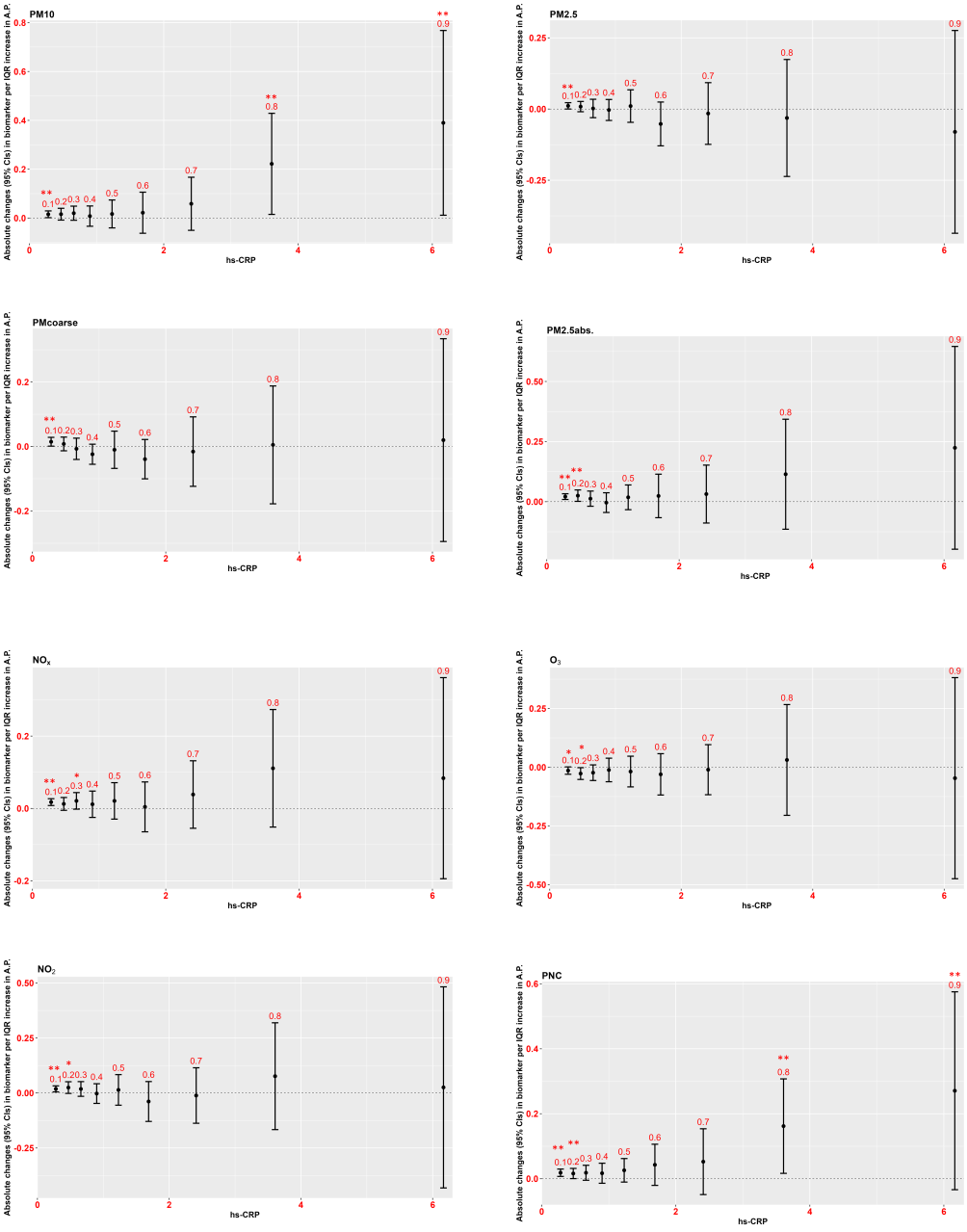

Figure 8.12: hs-CRP quantile regression: in each graph the absolute change in hs-CRP per IQR increase in individual air pollutant is shown, as well as its distribution across the quantile (hs-CRP (mg/L); 95% CI; ** = p-value <0.05; * = p-value <0.1).

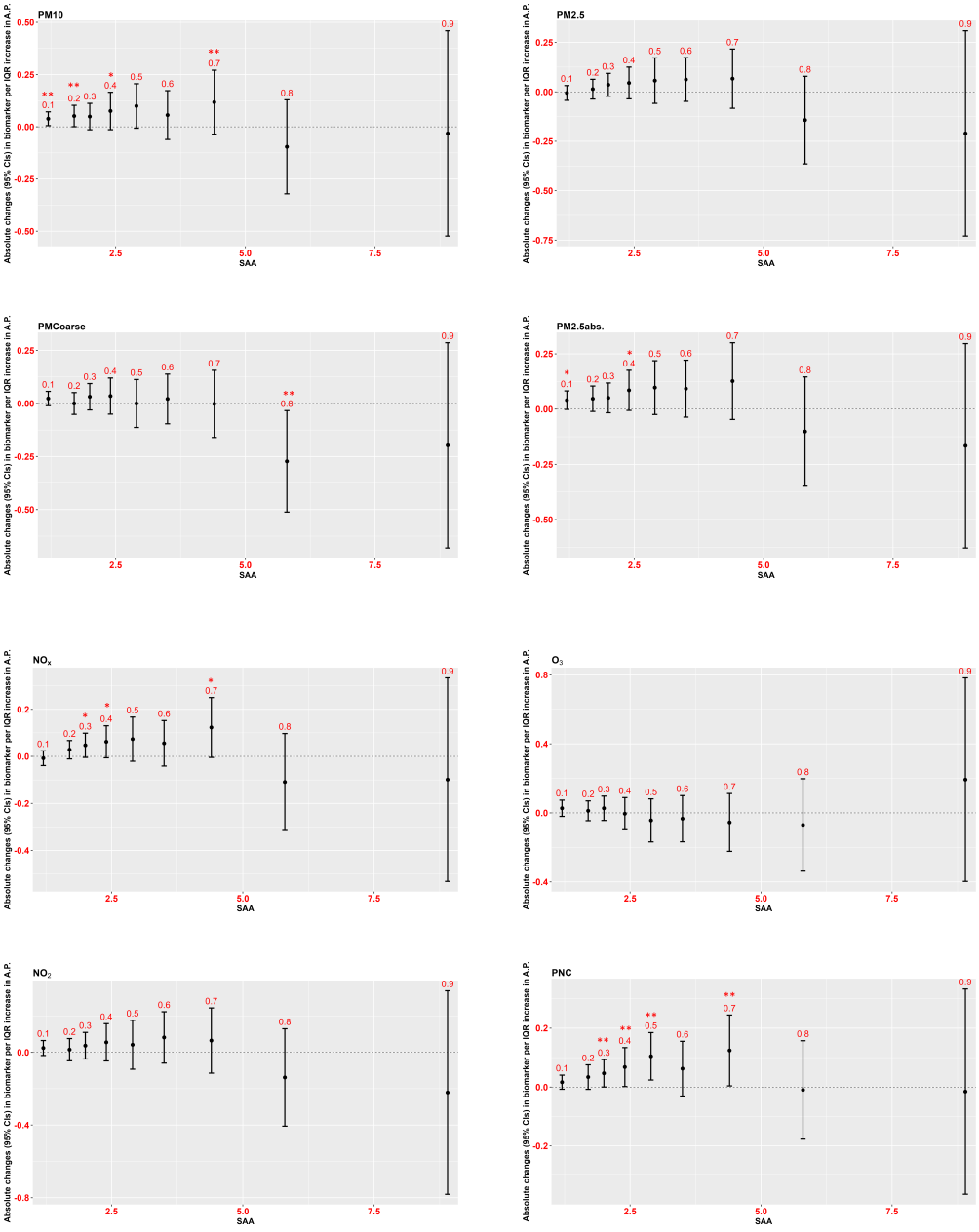

Figure 8.13: SAA quantile regression: in each graph the absolute change in SAA per IQR increase in individual air pollutant is shown, as well as its distribution across the quantile (SAA (mg/L); 95% CI; ** = p-value <0.05; * = p-value <0.1).

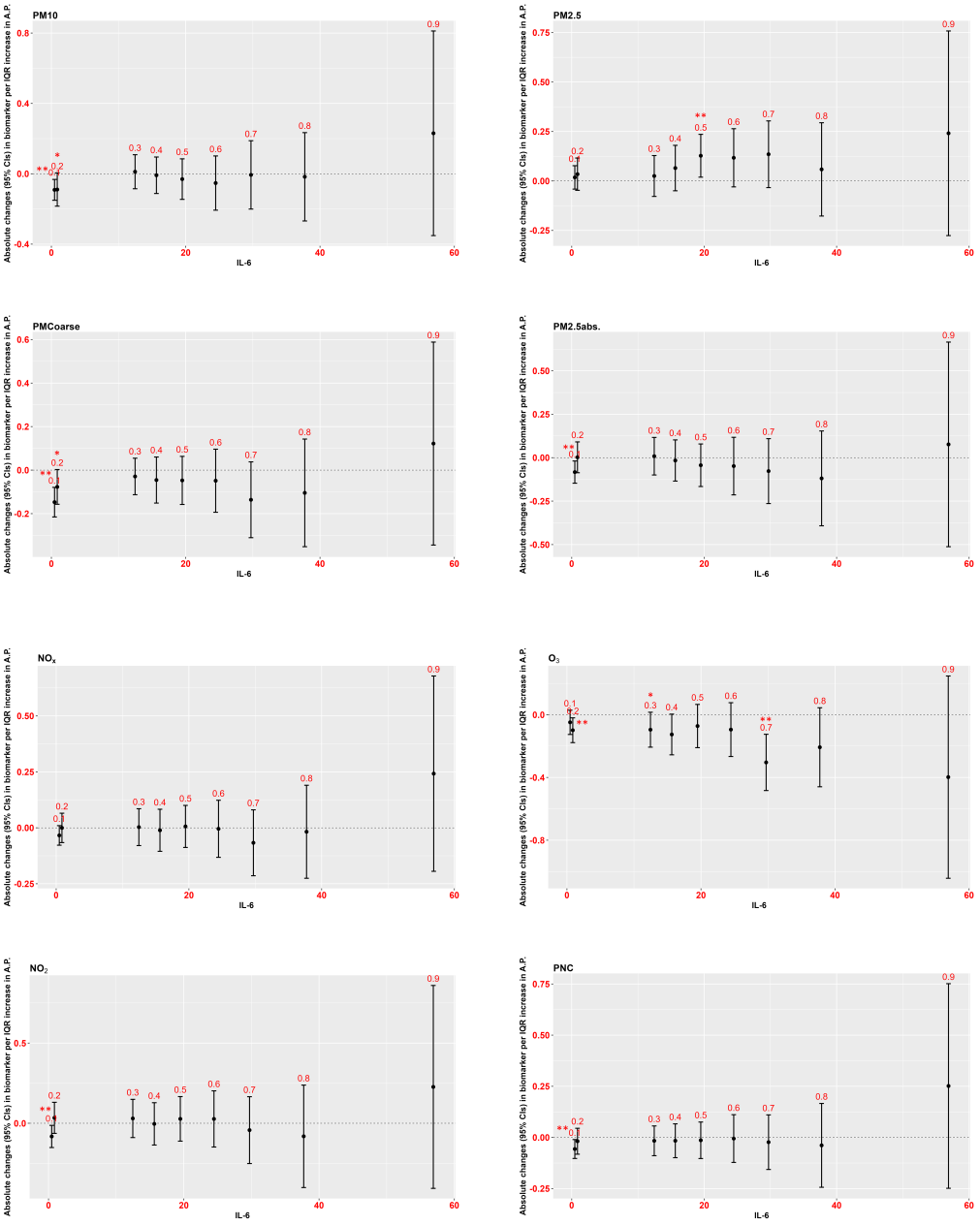

Figure 8.14: IL-6 quantile regression: in each graph the absolute change in IL-6 per IQR increase in individual air pollutant is shown, as well as its distribution across the quantile (IL-6 (pg/mL); 95% CI; ** = p-value <0.05; * = p-value <0.1).

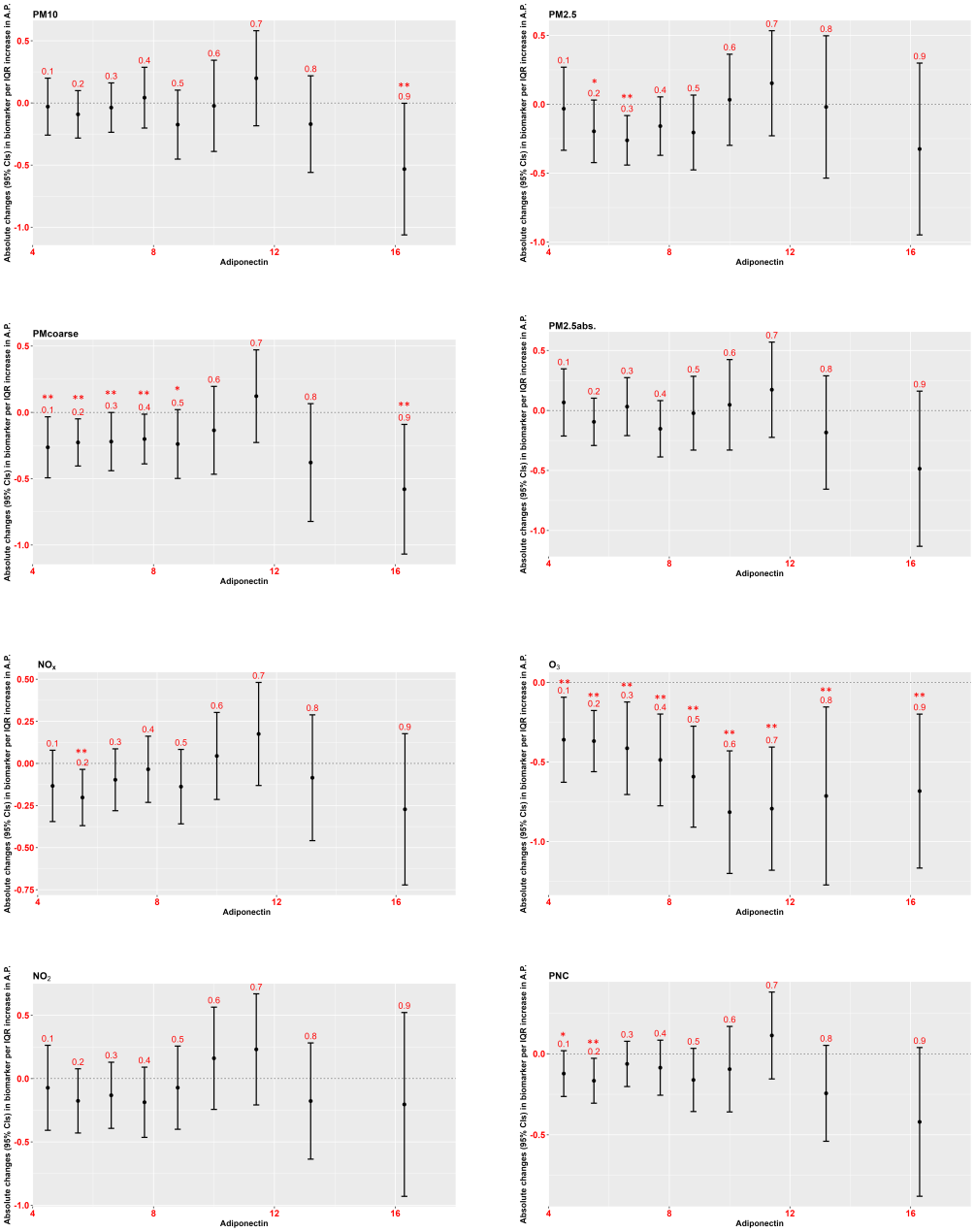

Figure 8.15: Adiponectin quantile regression: in each graph the absolute change in Adiponectin per IQR increase in individual air pollutant is shown, as well as its distribution across the quantile (Adiponectin (µg/mL); 95% CI; ** = p-value <0.05; * = p-value <0.1).

Chapter 9

Discussion and conclusion II

In this cross-sectional study we investigated the relation between long-term exposure to ambient air pollutants and blood biomarkers of inflammation and coagulation reflecting cardiovascular health. The blood biomarkers studied in this work are all involved in the local and systemic inflammatory response. We hypothesized that long-term inhalation of gaseous air pollutants and particulate matter can directly or indirectly generate oxidative stress. Consequently, we hypothesized that increased exposure to ambient air pollution levels would lead to increased levels of Fibrinogen, hs-CRP, SAA and IL-6, whereas we expected a decrease in Adiponectin concentration with higher air pollution levels.

The analysis for Fibrinogen, hs-CRP and SAA was carried out for 4034 participants, while for IL-6 and Adiponectin we only have data of 1404 participants. Regarding Fibrinogen and hs-CRP were found to be positively associated with UFPs (measured as PNC); SAA also shows a positive correlation with PNC but not statistically significant, as well as with PM_{10}. IL-6 is positively associated with $PM_{2.5}$, while Adiponectin is negatively associated with O_3. In comparison to the literature linking short-term exposure to air pollution with changes in the levels of blood markers reflecting inflammatory and coagulatory processes, the evidence regarding long-term exposure is still limited, especially for UFP, in term of PNC. Most of these studies have been conducted mainly on Fibrinogen, hs-CRP and IL-6 [148, 187, 188]. To the best of our knowledge, so far, no epidemiological studies were carried out considering the association between long-term exposure to air pollutants and SAA levels, while few studies assessed Adiponectin, but results are still limited [157, 189, 190]. In Lee and colleagues [187] work, Fibrinogen was

found to be positive associated with 1-year exposure to $PM_{2.5}$, NO_2 and O_3; in contrast, hs-CRP did not show significant associations with any pollutant. These results differ from our findings, in which there were no significant associations for Fibrinogen with the aforementioned pullutants in regression analyses. Instead, in quantile regression we found positive association with $PM_{2.5}$ at the 70^{th} and 90^{th} percentiles. One of the studies conducted investigating the association with PNC, was carried out by Lane and colleagues [188]. They found positive non-significant associations for IL-6 and CRP with annual exposure to PNC, whereas Fibrinogen did not shows association. These results also differ from our findings since we observed significant association for Fibrinogen and hs-CRP and not for IL-6. However, the methods used in Lane's work differ from ours since they conducted mobile monitoring of particle number concentration (PNC) and applied a spatial-temporal model to determine individual time-activity [188]. Studies that have investigated changes in IL-6 with $PM_{2.5}$ levels are rare. However, our positive results for IL-6 are consistent with A.Hajat and colleagues [148], they found a positive association between IL-6 and $PM_{2.5}$. Adiponectin shows strong association in non-obese participants with air pollutants, in the work conducted by Lucht and colleagues [157]. In our main results we observed strong association just with O_3. Furthermore, when adjusting the main model with the neighborhood SES variable we also noticed negative association with $PM_{2.5}$ and PNC. This result is agreement with their work [157]; however, we did not notice any differences between obese and non-obese participants.

The impact of air pollution exposure on the inflammatory response may vary among population subgroups, especially in those most susceptible. We investigated the effect modifications and we observed more consistent results in people who regularly intake anti-inflammatory medications. This subgroup was found to be more sensitive to air pollutants exposure, especially with regard to hs-CRP and IL-6 levels. For inviduals intaking anti-inflammatory medications, Hs-CRP is more influenced by PM_{10} and UFPs than for the subgroup not intaking such drugs. IL-6 is more affected by most pollutants, both gaseous and PM, in people regularly intaking anti-inflammatory medications. This may be due to the fact that people who regularly use anti-inflammatory drugs already start with a higher level of pro-inflammatory proteins. Examining our data, we observed that in the whole dataset the subgroup that regularly uses anti-inflammatory drugs is older, 57 ± 13 years, compared to the subgroup that does not intake the medications,

49±14 years. Consequently, this is reflected in the blood concentration of hs-CRP, which is higher in people taking anti-inflammatory drugs, 4±7 (mg/mL), than in those not intaking them, 3±5 (mg/mL). The subsample dataset does not shows this difference in the average age between the two subgroups, but the mean of IL-6 concentration is higher in those who intake anti-inflammatory medications, 5±10 (pg/mL) compared to 4±13 (pg/mL) for those who do not intake such drugs. This result shows an increased sensitivity to air pollution in people belonging to more vulnerable groups.

The results of the sensitivity analyses performed confirmed the statistically significant relationships observed in the regression analysis results, and also revealed other associations. First, we excluded outliers from the main model and this did not lead to changes in the main results. Then, we conducted a sensitivity analysis including the neighbourhood SES variable in the main model. Several studies have reported that neighbourhoods with a high proportion of low socio-economic status households are more exposed to air pollution, and therefore may have a higher risk of developing cardiovascular diseases [191–193]. Furthermore, low income is correlated with greater psychological stress and it is also reflected on diet, smoking and physical activity, all of which are directly linked to inflammation. A recent publication from H.S. Iyer and colleagues [194] examines in detail the impact of neighbourhood SES with blood biomarkers of inflammation. They found that higher neighbourhood socioeconomic status was associated with lower inflammation, both in woman and men. In particular, they found that an IQR increase in neighborhood SES was inversely associated with CRP and IL-6 and positive associated with Adiponectin. In our analysis, after adjusting the main model with neighbourhood SES, SAA protein is significantly positively associated with PM_{10} and PNC. IL-6 shows a stronger association with $PM_{2.5}$; whereas Adiponectin shows a further negative relationship with $PM_{2.5}$ and PNC. Our results highlight the contribution of low neighbourhood SES on inflammation status, specifically linked to air pollution exposure, which are in agreement with the work of H.S. Iyer and colleagues.

Quantile regression analysis produced interesting results. Regarding hs-CRP, using the linear regression model we observed a statistically significant association only with PNC, however, in the quantile regression analysis, most pollutants were associated with hs-CRP at the 10^{th} percentile. This effect on hs-CRP is rather interesting in the sense that people with a healthy hs-CRP level seem to react

to increasing levels of air pollutants, thus highlighting the potential inflammatory effect induced by most air pollutants. The SAA protein was found to be associated with PM_{10} at the 10^{th} and 20^{th} percentile, which explain the positive trend observed in the main results using linear regression. Quantile regression analysis point out also negative associations, both at low and high percentiles, between Adiponectin with PNC and PM_{coarse}. High level of Adiponectin promotes the inhibition of inflammatory markers and induces the production of anti-inflammatory ones, in a linked mechanism of feedbacks [195]. Low Adiponectin level are associated with obesity and insulin resistance, type 2 diabetes, and cardiovascular disease [196, 197]. Our results suggest that people with already low concentration of Adiponectin are more sensitive to increased levels of UFPs and PM_{coarse}, whose exposure could negative affect pre-existing health issues. As well as the association at the highest percentiles suggests the negative effects of exposure to air pollutants on people with healthy levels of Adiponectin.

These analyses confirmed our initial hypothesis, observing that exposure to higher levels of ambient air pollution leads to increased levels of Fibrinogen, hs-CRP, SAA and IL-6 and decreased concentrations of Adiponectn with higher levels of air pollution.

9.1 Conclusion

In conclusion, our study suggests that long-term exposure (365-days) to air pollutants is positively associated with increasing level of pro-inflammatory markers and lower levels of anti-inflammation markers. The major finding seems to be related to UFPs, as PNC, associated with both pro- and anti- inflammatory markers.

Chapter 10

Summary and conclusion

Although the awareness on the topic has increased sharply, air pollution is still a major problem of our time. It affects health conditions of humans around the world, reducing the quality and expectancy of life. In his book Dr Gary Fuller's [198], calls it the "invisible killer", since we cannot see it, but it is always around, and we are constantly affected by it as we cannot stop breathing. Recently, particular attention in research has been given to the nanoscale fraction of particulate matter, namely ultrafine particles (UFPs), because their size affects the impact they have on human health. UFPs are defined as incidental anthropogenic NPs [28, 47] in an aerodynamic diameter between 1 and 100 nm. Moreover, the absence of shared specific regulation regarding UFPs generates a potentially dangerous void from which negative direct and indirect impacts could arise.
The problem of exposure to UFPs is not exclusive to the outdoor environment, but it can concern indoor conditions as well. Specifically, exposure can be problematic in work environments in which a higher concentration of NPs is more probable. Examples of these environments are workplaces in sectors that produce or deal with ENPs specifically. These intentional anthropogenic NPs [28,50] have different artificial designs, depending on their intended application. So, as inferable from their definitions, a first difference between ENPs and UFPs lays in the intentionality of their generation. Also, the chemical and physical characteristics of UFPs depend mainly on the environmental conditions where they are generated and cannot be controlled. However, both categories share intrinsic characteristics such as size, exposure routes and metal content [23, 33, 54, 199]. These shared features trigger similar biological responses as a consequence of exposure, such as ROS generation

and inflammation at cellular level which can yield to several pathologies.

My PhD project aims at generating relevant knowledge for a deeper understanding of the effects that UFPs can have on human health. It will do so by applying two different investigative approaches. In the first section we researched how human cell lines are impacted by the interaction with specific ENPs, used as a proxy to investigate the molecular mechanisms induced by UFPs. HepG2 and THP-1 cells were exposed for 24h to subtoxic doses of ENPs, and to the equivalent dose of Cadmium in ionic form. The interactome analyses for both cell lines exposed to ENPs revealed alterations in cellular homeostasis, highlighting their ability to induce a potential alteration of the oxidative state and an inflammatory response. Furthermore, the adverse effects of exposure to ENPs appear not to be strictly related to cadmium release, since treatment with an equivalent dose clearly induces stronger effects.
In the second section an epidemiological approach was used. We conducted a population-based long-term study to assess the link between air pollutants (including UFPs) with inflammation and coagulation blood-biomarkers reflecting cardiovascular health. The results exhibit a strong association between biomarkers of inflammation and coagulation with almost all pollutants. UFPs show the most consistent association with CRP, Fibrinogen, SAA and Adiponectin (the latter was negatively associated, in accordance with our initial hypothesis it is inversely related to inflammation).

We were also interested in potential common points between the two approaches. In the first part, we investigated gene regulation after a 24h treatment with ENPs, to see if it led to the gene transcription of the same proteins assessed in the second phase of the project. We observed a down regulation of the IL-6 gene in the THP-1 cell line and interpreted this as general silencing of inflammatory genes as a consequence of the autophagic process that had already taken place. IL-6 is a cytokine released in response to environmental stressors, as a result of biological infections and tissue damage (i.e. Damage-associated molecular patterns, DAMPs) [200]. Generally, it is expressed by immune-mediated cells in the early stages of the inflammatory response, as a results of the activation of NF-kB pathway. IL-6 enters the bloodstream and moves towards the liver inducing the release of Fibrinogen, CRP and SAA, as well as other inflammatory markers, and leading to a systemic inflammation. Different studies [201–206] have reported high expression of this protein after ENPs exposure; the few epidemiological studies which

have investigated the association between IL-6 and UFP (PNC) [188,207] found a positive association.
Our results show no association between IL-6 and UFPs but strong positive association with $PM_{2.5}$, which is not surprising given the high inflammatory potential of this fraction. It is evident that the biological mechanisms induced by particulate matter (PM) may overlap because of their similar chemical composition, and because the larger PM fractions also include the smaller particle sizes [34, 39]. Previous studies have shown that these two particulate fractions are significantly correlated with the occurrence of adverse cellular effects, cardiovascular and respiratory diseases [208].
The health effects caused by UFPs mainly depend to their size and chemical composition. With regard to the size aspect, we highlight the size-dependent cellular effects of ENPs. Their use in *in vitro* studies provides an excellent support, which allows researcher to conceptually extrapolate molecular information and apply them to the environmental UFPs. Furthermore, the use of ENPs as proxies for UFPs has the advantage of facilitating the sampling related procedure, specifically in relation to the large amount of UFPs particle mass necessary to perform *in vitro* studies. Indeed, recent publications on toxicological studies of UFPs [39, 209, 210] have raised concerns about the lack of a unified toxicological method which best mimics a real-exposure, without having to resort to *in vivo* studies; to date, the air-liquid interface (ALI) in co-culture seems to be the most promising. The results presented here highlight that the exposure to ENPs, or unintentional anthropogenic nanoparticles, is indeed linked with an inflammatory response at both transcriptomic and systemic levels. This link might be subject to future research to further understand the dynamics that regulate such processes in more detail at molecular level.

A limitation of using this approach is that the chemical composition of UFPs is a fundamental variable in human toxicity studies. To date, it is still not entirely clear which component of UFPs has the most harmful effects on our health [209]. It might be interesting to use nanoparticles by trying to manipulate them to 'mimic' micro-environmental conditions, depending on the source. Related studies have been growing in number, especially in recent years. This is because the damage to health is evident, thanks in part to the rich literature on the effects of ENPs, which this has made it possible to understand them at the molecular level. Today, it is necessary to arrive at regulations that limit their emissions of NPs, reducing the

possible damage to human health. This concerns not only ambient air pollution but also the use of nanomaterials in working environments.

The two different parts of my research allowed me to understand the importance of approaching scientific topics from different points of view in order to obtain a better understanding of the complex problem, considering both the micro- and the macro-scale. This work indicates that toxicological studies on ENPs and UFPs are not so far apart and should go in the same direction, with the common goal of expanding the knowledge on them. It is also of paramount importance to achieve a unified method in the toxicological study of nanoparticles, creating more defined protocols common to all researchers, especially for the environmental ones. Last but not least, these studies study highlighted the association of inflammatory and coagulatory response after exposure to PM and gaseous air pollutants, linking it directly with the increased risk of cardiovascular disease, the main cause of premature death worldwide.

Acknowledgments

First, I would like to thank Prof. Dr. Nelson Marmiroli and Prof. Dr. Elena Maestri of the University of Parma, for giving me the opportunity to begin this academic journey. They allowed me to get to know new scientific perspectives within a dynamic and challenging working environment, in Parma and abroad, certainly making a better researcher of me.

I would like to thank Prof. Dr. Annette Peters, Director of the Institute of Epidemiology at the Helmholtz Zentrum München, who welcomed me into the research group that she manages, and provided me with all the necessary support for the development of my project there.

I would also like to thank Dr. Laura Paesano, who supported and encouraged me in my PhD journey. She provided me with valuable guidance for the realization of my PhD research, I could not have accomplished this thesis without her continuous support. Special thanks go to Prof. Roberta Ruotolo, who was always available to answer any questions I had during my journey. Thanks also to all my PhD colleagues from University of Parma, for the good times spent together.

I would like to express my great appreciation to Dr. Regina Pickford and Dr. Siqi Zhang, who taught and supported me a lot during my period at Helmholtz Zentrum. I could not have accomplished this part of the work without their scientific support. Final thanks go to all the colleagues in the Research Group "Environmental Risks", who have welcomed me and always helped me.

This work has benefited from the equipment and organizational framework of the COMP-HUB Initiative, funded by the "Departments of Excellence" program of the Italian Ministry for Education, University and Research (MIUR, 2018-2022).

Bibliography

[1] Robert B Hamanaka and Gökhan M Mutlu. Particulate matter air pollution: effects on the cardiovascular system. *Frontiers in endocrinology*, 9:680, 2018.

[2] Nadine Unger, Tami C Bond, James S Wang, Dorothy M Koch, Surabi Menon, Drew T Shindell, and Susanne Bauer. Attribution of climate forcing to economic sectors. *Proceedings of the National Academy of Sciences*, 107(8):3382–3387, 2010.

[3] Environmental Protection Agency. Particle pollution exposure, 2021.

[4] European Commission. Eur-lex - directive 2008/50/ec of the european parliament and of the council of 21 may 2008, 2021.

[5] 2018e; Eurostat 2018a. EEA, 2018c. Eea report no 10/2019, 2019.

[6] European Commission. Eur-lex - "the second clean air outlook", 2021.

[7] WHO European Centre for Environment and Health. Air quality guidelines, 2021.

[8] Zorana Jovanovic Andersen, Ulrike Gehring, Sara De Matteis, Erik Melen, Ana Maria Vicedo-Cabrera, Klea Katsouyanni, Arzu Yorgancioglu, Charlotte Suppli Ulrik, Sylvia Medina, Kjeld Hansen, et al. Clean air for healthy lungs–an urgent call to action: European respiratory society position on the launch of the who 2021 air quality guidelines, 2021.

[9] Marian Fierro. Particulate matter. *Air Info Now*, pages 1–11, 2000.

[10] Roy M Harrison. Airborne particulate matter. *Philosophical Transactions of the Royal Society A*, 378(2183):20190319, 2020.

[11] De-Ling Liu. Particle deposition onto enclosure surfaces. In *Developments in Surface Contamination and Cleaning*, pages 1–56. Elsevier, 2010.

[12] Regina Rückerl, Alexandra Schneider, Regina Hampel, Susanne Breitner, Josef Cyrys, Ute Kraus, Jianwei Gu, Jens Soentgen, Wolfgang Koenig, and Annette Peters. Association of novel metrics of particulate matter with vascular markers of inflammation and coagulation in susceptible populations–results from a panel study. *Environmental research*, 150:337–347, 2016.

[13] Hyouk-Soo Kwon, Min Hyung Ryu, and Christopher Carlsten. Ultrafine particles: unique physicochemical properties relevant to health and disease. *Experimental & molecular medicine*, 52(3):318–328, 2020.

[14] Scott D Lowther, Kevin C Jones, Xinming Wang, J Duncan Whyatt, Oliver Wild, and Douglas Booker. Particulate matter measurement indoors: A review of metrics, sensors, needs, and applications. *Environmental science & technology*, 53(20):11644–11656, 2019.

[15] Andreas Petzold, John A Ogren, Markus Fiebig, Pablo Laj, S-M Li, Urs Baltensperger, Thomas Holzer-Popp, Stefan Kinne, Gelsomina Pappalardo, Nobuo Sugimoto, et al. Recommendations for reporting" black carbon" measurements. *Atmospheric Chemistry and Physics*, 13(16):8365–8379, 2013.

[16] Stephen E Schwartz and Ernie R Lewis. Interactive comment on "are black carbon and soot the same?" by pr buseck et al.: Disagreement on proposed nomenclature. *Atmos. Chem. Phys. Discuss*, 12:C9099–C9109, 2012.

[17] Daniele Contini, Roberta Vecchi, and Mar Viana. Carbonaceous aerosols in the atmosphere, 2018.

[18] Regina Rückerl, Alexandra Schneider, Susanne Breitner, Josef Cyrys, and Annette Peters. Health effects of particulate air pollution: a review of epidemiological evidence. *Inhalation toxicology*, 23(10):555–592, 2011.

[19] Frank Kelly, H Ross Anderson, Ben Armstrong, Richard Atkinson, Benjamin Barratt, Sean Beevers, Dick Derwent, David Green, Ian Mudway, Paul Wilkinson, et al. The impact of the congestion charging scheme on air quality in london. part 2. analysis of the oxidative potential of particulate matter. *Research Report (Health Effects Institute)*, (155):73–144, 2011.

[20] Ning Li, Constantinos Sioutas, Arthur Cho, Debra Schmitz, Chandan Misra, Joan Sempf, Meiying Wang, Terry Oberley, John Froines, and Andre Nel. Ultrafine particulate pollutants induce oxidative stress and mitochondrial damage. *Environmental health perspectives*, 111(4):455–460, 2003.

[21] Robert D Brook, Sanjay Rajagopalan, C Arden Pope III, Jeffrey R Brook, Aruni Bhatnagar, Ana V Diez-Roux, Fernando Holguin, Yuling Hong, Russell V Luepker, Murray A Mittleman, et al. Particulate matter air pollution and cardiovascular disease: an update to the scientific statement from the american heart association. *Circulation*, 121(21):2331–2378, 2010.

[22] Anisha A Gupte, Christopher J Lyon, and Willa A Hsueh. Nuclear factor (erythroid-derived 2)-like-2 factor (nrf2), a key regulator of the antioxidant response to protect against atherosclerosis and nonalcoholic steatohepatitis. *Current diabetes reports*, 13(3):362–371, 2013.

[23] Ning Li, Steve Georas, Neil Alexis, Patricia Fritz, Tian Xia, Marc A Williams, Elliott Horner, and Andre Nel. A work group report on ultrafine particles (american academy of allergy, asthma & immunology): Why ambient ultrafine and engineered nanoparticles should receive special attention for possible adverse health outcomes in human subjects. *Journal of Allergy and Clinical Immunology*, 138(2):386–396, 2016.

[24] Rafael M da Costa, Daniel Rodrigues, Camila A Pereira, Josiane F Silva, Juliano V Alves, Núbia S Lobato, and Rita C Tostes. Nrf2 as a potential mediator of cardiovascular risk in metabolic diseases. *Frontiers in Pharmacology*, 10:382, 2019.

[25] Annette Peters, Tim S Nawrot, and Andrea A Baccarelli. Hallmarks of environmental insults. *Cell*, 184(6):1455–1468, 2021.

[26] Carlos I Falcon-Rodriguez, Alvaro R Osornio-Vargas, Isabel Sada-Ovalle, and Patricia Segura-Medina. Aeroparticles, composition, and lung diseases. *Frontiers in immunology*, 7:3, 2016.

[27] Feifei Wang, Jifang Liu, and Hongbo Zeng. Interactions of particulate matter and pulmonary surfactant: Implications for human health. *Advances in colloid and interface science*, page 102244, 2020.

[28] Michael F Hochella, David W Mogk, James Ranville, Irving C Allen, George W Luther, Linsey C Marr, B Peter McGrail, Mitsu Murayama, Nikolla P Qafoku, Kevin M Rosso, et al. Natural, incidental, and engineered nanomaterials and their impacts on the earth system. *Science*, 363(6434), 2019.

[29] Song Guo, Min Hu, Jianfei Peng, Zhijun Wu, Misti L Zamora, Dongjie Shang, Zhuofei Du, Jing Zheng, Xin Fang, Rongzhi Tang, et al. Remarkable nucleation and growth of ultrafine particles from vehicular exhaust. *Proceedings of the National Academy of Sciences*, 117(7):3427–3432, 2020.

[30] Markku Kulmala, Hanna Vehkamäki, Tuukka Petäjä, Miikka Dal Maso, Antti Lauri, V-M Kerminen, W Birmili, and PH McMurry. Formation and growth rates of ultrafine atmospheric particles: a review of observations. *Journal of Aerosol Science*, 35(2):143–176, 2004.

[31] Rui Chen, Bin Hu, Ying Liu, Jianxun Xu, Guosheng Yang, Diandou Xu, and Chunying Chen. Beyond pm2. 5: The role of ultrafine particles on adverse health effects of air pollution. *Biochimica et Biophysica Acta (BBA)-General Subjects*, 1860(12):2844–2855, 2016.

[32] AMEC Environment, Infrastructure UK Limited in partnership with the Institute for Occupational Medicine (IOM), and AetherEuropean Commission. European commission - industrial emissions of nano- and ultrafine particles - final report, 2021.

[33] Günter Oberdörster and Mark J Utell. Ultrafine particles in the urban air: to the respiratory tract–and beyond? *Environmental health perspectives*, 110(8):A440–A441, 2002.

[34] Dean E Schraufnagel. The health effects of ultrafine particles. *Experimental & molecular medicine*, 52(3):311–317, 2020.

[35] Yaobo Ding, Thomas AJ Kuhlbusch, Martie Van Tongeren, Araceli Sánchez Jiménez, Ilse Tuinman, Rui Chen, Iñigo Larraza Alvarez, Urszula Mikolajczyk, Carmen Nickel, Jessica Meyer, et al. Airborne engineered nanomaterials in the workplace—a review of release and worker exposure during nanomaterial production and handling processes. *Journal of hazardous materials*, 322:17–28, 2017.

[36] Colin AJ Dick, David M Brown, Ken Donaldson, and Vicki Stone. The role of free radicals in the toxic and inflammatory effects of four different ultrafine particle types. *Inhalation toxicology*, 15(1):39–52, 2003.

[37] Annette Peters, H Erich Wichmann, Thomas Tuch, Joachim Heinrich, and Joachim Heyder. Respiratory effects are associated with the number of ultrafine particles. *American journal of respiratory and critical care medicine*, 155(4):1376–1383, 1997.

[38] Maurizio Gualtieri, Maria Giuseppa Grollino, Claudia Consales, Francesca Costabile, Maurizio Manigrasso, Pasquale Avino, Michaela Aufderheide, Eugenia Cordelli, Luca Di Liberto, Ettore Petralia, et al. Is it the time to study air pollution effects under environmental conditions? a case study to support the shift of in vitro toxicology from the bench to the field. *Chemosphere*, 207:552–564, 2018.

[39] Eleonora Marta Longhin, Paride Mantecca, and Maurizio Gualtieri. Fifteen years of airborne particulates in vitro toxicology in milano: lessons and perspectives learned. *International Journal of Molecular Sciences*, 21(7):2489, 2020.

[40] Directorate-General for Environment. Additional tools nanomaterials, 2021.

[41] Cristina Buzea, Ivan I Pacheco, and Kevin Robbie. Nanomaterials and nanoparticles: sources and toxicity. *Biointerphases*, 2(4):MR17–MR71, 2007.

[42] VV Pokropivny and VV Skorokhod. Classification of nanostructures by dimensionality and concept of surface forms engineering in nanomaterial science. *Materials Science and Engineering: C*, 27(5-8):990–993, 2007.

[43] Sajid Bashir and JL Liu. Nanomaterials and their application. *Advanced Nanomaterials and Their Applications in Renewable Energy; Elsevier Inc.: Amsterdam, The Netherlands*, pages 1–50, 2015.

[44] Diana Sannino. Types and classification of nanomaterials. In *Nanotechnology*, pages 15–38. Springer, 2021.

[45] Hua Zhang. Ultrathin two-dimensional nanomaterials. *ACS nano*, 9(10):9451–9469, 2015.

[46] Tuang Yeow Poh, Nur A'tikah Binte Mohamed Ali, Micheál Mac Aogáin, Mustafa Hussain Kathawala, Magdiel Inggrid Setyawati, Kee Woei Ng, and Sanjay Haresh Chotirmall. Inhaled nanomaterials and the respiratory microbiome: clinical, immunological and toxicological perspectives. *Particle and fibre toxicology*, 15(1):1–16, 2018.

[47] Cristina Buzea and Ivan Pacheco. Nanomaterial and nanoparticle: origin and activity. In *Nanoscience and Plant–Soil Systems*, pages 71–112. Springer, 2017.

[48] Richard D Handy, Richard Owen, and Eugenia Valsami-Jones. The ecotoxicology of nanoparticles and nanomaterials: current status, knowledge gaps, challenges, and future needs. *Ecotoxicology*, 17(5):315–325, 2008.

[49] Günter Oberdörster, Eva Oberdörster, and Jan Oberdörster. Nanotoxicology: an emerging discipline evolving from studies of ultrafine particles. *Environmental health perspectives*, 113(7):823–839, 2005.

[50] Arindam Malakar, Sushil R Kanel, Chittaranjan Ray, Daniel D Snow, and Mallikarjuna N Nadagouda. Nanomaterials in the environment, human exposure pathway, and health effects: A review. *Science of the Total Environment*, page 143470, 2020.

[51] Sepehr Talebian, Tiago Rodrigues, José Das Neves, Bruno Sarmento, Robert Langer, and João Conde. Facts and figures on materials science and nanotechnology progress and investment. *ACS nano*, 15(10):15940–15952, 2021.

[52] Andre Nel, Tian Xia, Lutz Mädler, and Ning Li. Toxic potential of materials at the nanolevel. *science*, 311(5761):622–627, 2006.

[53] Ken Donaldson, Vicki Stone, CL Tran, Wolfgang Kreyling, and Paul JA Borm. Nanotoxicology, 2004.

[54] Vicki Stone, Mark R Miller, Martin JD Clift, Alison Elder, Nicholas L Mills, Peter Møller, Roel PF Schins, Ulla Vogel, Wolfgang G Kreyling, Keld Alstrup Jensen, et al. Nanomaterials versus ambient ultrafine particles: an opportunity to exchange toxicology knowledge. *Environmental health perspectives*, 125(10):106002, 2017.

[55] Tian Xia, Ning Li, and Andre E Nel. Potential health impact of nanoparticles. *Annual review of public health*, 30:137–150, 2009.

[56] Sohrab Nikazar, Vishnu Sankar Sivasankarapillai, Abbas Rahdar, Salim Gasmi, PS Anumol, and Muhammad Salman Shanavas. Revisiting the cytotoxicity of quantum dots: An in-depth overview. *Biophysical reviews*, 12(3):703–718, 2020.

[57] Angela M Wagner, Jennifer M Knipe, Gorka Orive, and Nicholas A Peppas. Quantum dots in biomedical applications. *Acta biomaterialia*, 94:44–63, 2019.

[58] Yanling Ma, Fei Yan, Li Liu, WuJie Wei, Zhenyu Zhao, and Jianhai Sun. The enhanced photo-thermal therapy of surface improved photoactive cadmium sulfide (cds) quantum dots entrenched graphene oxide nanoflakes in tumor treatment. *Journal of Photochemistry and Photobiology B: Biology*, 192:34–39, 2019.

[59] Marta Marmiroli, Francesca Mussi, Luca Pagano, Davide Imperiale, Giacomo Lencioni, Marco Villani, Andrea Zappettini, Jason C White, and Nelson Marmiroli. Cadmium sulfide quantum dots impact arabidopsis thaliana physiology and morphology. *Chemosphere*, 240:124856, 2020.

[60] Frank S Bierkandt, Lars Leibrock, Sandra Wagener, Peter Laux, and Andreas Luch. The impact of nanomaterial characteristics on inhalation toxicity. *Toxicology research*, 7(3):321–346, 2018.

[61] Günter Oberdörster, Andrew Maynard, Ken Donaldson, Vincent Castranova, Julie Fitzpatrick, Kevin Ausman, Janet Carter, Barbara Karn, Wolfgang Kreyling, David Lai, et al. Principles for characterizing the potential human health effects from exposure to nanomaterials: elements of a screening strategy. *Particle and fibre toxicology*, 2(1):1–35, 2005.

[62] Shahriar Sharifi, Shahed Behzadi, Sophie Laurent, M Laird Forrest, Pieter Stroeve, and Morteza Mahmoudi. Toxicity of nanomaterials. *Chemical Society Reviews*, 41(6):2323–2343, 2012.

[63] Manzoor Ahmad Gatoo, Sufia Naseem, Mir Yasir Arfat, Ayaz Mahmood Dar, Khusro Qasim, and Swaleha Zubair. Physicochemical properties

of nanomaterials: implication in associated toxic manifestations. *BioMed research international*, 2014, 2014.

[64] Alyona Sukhanova, Svetlana Bozrova, Pavel Sokolov, Mikhail Berestovoy, Alexander Karaulov, and Igor Nabiev. Dependence of nanoparticle toxicity on their physical and chemical properties. *Nanoscale research letters*, 13(1):1–21, 2018.

[65] Ayush Verma and Francesco Stellacci. Effect of surface properties on nanoparticle–cell interactions. *small*, 6(1):12–21, 2010.

[66] Eleonore Fröhlich. The role of surface charge in cellular uptake and cytotoxicity of medical nanoparticles. *International journal of nanomedicine*, 7:5577, 2012.

[67] Ilse Gosens, Jan Andries Post, Liset JJ de la Fonteyne, Eugene HJM Jansen, John W Geus, Flemming R Cassee, and Wim H de Jong. Impact of agglomeration state of nano-and submicron sized gold particles on pulmonary inflammation. *Particle and fibre toxicology*, 7(1):1–11, 2010.

[68] Saad Mohammad Ahsan, Chintalagiri Mohan Rao, and Md Faiz Ahmad. Nanoparticle-protein interaction: the significance and role of protein corona. *Cellular and Molecular Toxicology of Nanoparticles*, pages 175–198, 2018.

[69] Shruti R Saptarshi, Albert Duschl, and Andreas L Lopata. Interaction of nanoparticles with proteins: relation to bio-reactivity of the nanoparticle. *Journal of nanobiotechnology*, 11(1):1–12, 2013.

[70] Roberta Ruotolo, Giuseppe De Giorgio, Ilaria Minato, Massimiliano G Bianchi, Ovidio Bussolati, and Nelson Marmiroli. Cerium oxide nanoparticles rescue α-synuclein-induced toxicity in a yeast model of parkinson's disease. *Nanomaterials*, 10(2):235, 2020.

[71] Toren Finkel. Signal transduction by reactive oxygen species. *Journal of Cell Biology*, 194(1):7–15, 2011.

[72] Nationale Human Genome Research Institute. Glossary of genetic terms: Apoptosis, 2021.

[73] Abdelouahid El-Khattouti, Denis Selimovic, Youssef Haikel, and Mohamed Hassan. Crosstalk between apoptosis and autophagy: molecular mechanisms and therapeutic strategies in cancer. *Journal of cell death*, 6:JCD–S11034, 2013.

[74] Simone Fulda and Klaus-Michael Debatin. Extrinsic versus intrinsic apoptosis pathways in anticancer chemotherapy. *Oncogene*, 25(34):4798–4811, 2006.

[75] Susan Elmore. Apoptosis: a review of programmed cell death. *Toxicologic pathology*, 35(4):495–516, 2007.

[76] Hussain Mubarak Al-Aamri, Helen R Irving, Christopher Bradley, and Terri Meehan-Andrews. Intrinsic and extrinsic apoptosis responses in leukaemia cells following daunorubicin treatment. *BMC cancer*, 21(1):1–10, 2021.

[77] Liang Chen, Liu-Yun Wu, and Wan-Xi Yang. Nanoparticles induce apoptosis via mediating diverse cellular pathways. *Nanomedicine*, 13(22):2939–2955, 2018.

[78] Salik Hussain, Stavros Garantziotis, Fernando Rodrigues-Lima, Jean-Marie Dupret, Armelle Baeza-Squiban, and Sonja Boland. Intracellular signal modulation by nanomaterials. *Nanomaterial*, pages 111–134, 2014.

[79] Mark S D'Arcy. Cell death: a review of the major forms of apoptosis, necrosis and autophagy. *Cell biology international*, 43(6):582–592, 2019.

[80] Stephan T Stern, Pavan P Adiseshaiah, and Rachael M Crist. Autophagy and lysosomal dysfunction as emerging mechanisms of nanomaterial toxicity. *Particle and fibre toxicology*, 9(1):1–17, 2012.

[81] Lingling Guo, Nongyue He, Yongxiang Zhao, Tonghua Liu, and Yan Deng. Autophagy modulated by inorganic nanomaterials. *Theranostics*, 10(7):3206, 2020.

[82] Yan Wang and Meng Tang. Dysfunction of various organelles provokes multiple cell death after quantum dot exposure. *International journal of nanomedicine*, 13:2729, 2018.

[83] Houjun Xia, Douglas R Green, and Weiping Zou. Autophagy in tumour immunity and therapy. *Nature Reviews Cancer*, 21(5):281–297, 2021.

[84] Kanehisa Laboratories. Autophagy - animal - homo sapiens (human), 2021.

[85] Ivan Dikic and Zvulun Elazar. Mechanism and medical implications of mammalian autophagy. *Nature reviews Molecular cell biology*, 19(6):349–364, 2018.

[86] Willa Wen-You Yim and Noboru Mizushima. Lysosome biology in autophagy. *Cell discovery*, 6(1):1–12, 2020.

[87] Joshua J Rennick, Angus PR Johnston, and Robert G Parton. Key principles and methods for studying the endocytosis of biological and nanoparticle therapeutics. *Nature Nanotechnology*, 16(3):266–276, 2021.

[88] Daming Wu, Ying Ma, Yuna Cao, and Ting Zhang. Mitochondrial toxicity of nanomaterials. *Science of The Total Environment*, 702:134994, 2020.

[89] Yueh-Hsia Luo, Shi-Bei Wu, Yau-Huei Wei, Yu-Ching Chen, Ming-Hsien Tsai, Chia-Chi Ho, Shu-Yi Lin, Chung-Shi Yang, and Pinpin Lin. Cadmium-based quantum dot induced autophagy formation for cell survival via oxidative stress. *Chemical research in toxicology*, 26(5):662–673, 2013.

[90] Laura Paesano, Marta Marmiroli, Massimiliano G Bianchi, Jason C White, Ovidio Bussolati, Andrea Zappettini, Marco Villani, and Nelson Marmiroli. Differences in toxicity, mitochondrial function and mirnome in human cells exposed in vitro to cd as cds quantum dots or ionic cd. *Journal of hazardous materials*, 393:122430, 2020.

[91] Fujing Wei and Yixiang Duan. Crosstalk between autophagy and nanomaterials: internalization, activation, termination. *Advanced Biosystems*, 3(1):1800259, 2019.

[92] ME Blazka and ZA Shaikh. Differences in cadmium and mercury uptakes by hepatocytes: role of calcium channels. *Toxicology and applied pharmacology*, 110(2):355–363, 1991.

[93] Teresa Ostaszewska, Jerzy Śliwiński, Maciej Kamaszewski, Paweł Sysa, and Maciej Chojnacki. Cytotoxicity of silver and copper nanoparticles on rain-

bow trout (oncorhynchus mykiss) hepatocytes. *Environmental Science and Pollution Research*, 25(1):908–915, 2018.

[94] Francis Crick. Central dogma of molecular biology. *Nature*, 227(5258):561–563, 1970.

[95] Jacob O'Brien, Heyam Hayder, Yara Zayed, and Chun Peng. Overview of microrna biogenesis, mechanisms of actions, and circulation. *Frontiers in endocrinology*, 9:402, 2018.

[96] Robert F Place, Long-Cheng Li, Deepa Pookot, Emily J Noonan, and Rajvir Dahiya. Microrna-373 induces expression of genes with complementary promoter sequences. *Proceedings of the National Academy of Sciences*, 105(5):1608–1613, 2008.

[97] Thomas X Lu and Marc E Rothenberg. Microrna. *Journal of Allergy and Clinical Immunology*, 141(4):1202–1207, 2018.

[98] Julian Krauskopf, Marcha Verheijen, Jos C Kleinjans, Theo M de Kok, and Florian Caiment. Development and regulatory application of microrna biomarkers. *Biomarkers in medicine*, 9(11):1137–1151, 2015.

[99] Leigh-Ann MacFarlane and Paul R Murphy. Microrna: biogenesis, function and role in cancer. *Current genomics*, 11(7):537–561, 2010.

[100] Ahmet M Denli, Bastiaan BJ Tops, Ronald HA Plasterk, René F Ketting, and Gregory J Hannon. Processing of primary micrornas by the microprocessor complex. *Nature*, 432(7014):231–235, 2004.

[101] Scott M Hammond, Sabrina Boettcher, Amy A Caudy, Ryuji Kobayashi, and Gregory J Hannon. Argonaute2, a link between genetic and biochemical analyses of rnai. *Science*, 293(5532):1146–1150, 2001.

[102] Tingting Du and Phillip D Zamore. microprimer: the biogenesis and function of microrna. 2005.

[103] S Masala, V Bizzarro, M Re, G Nenna, F Villani, C Minarini, and T Di Luccio. Photoluminescence quenching and conductivity enhancement of pvk induced by cds quantum dots. *Physica E: Low-dimensional Systems and Nanostructures*, 44(7-8):1272–1277, 2012.

[104] Luca Pagano, Francesco Pasquali, Sanghamitra Majumdar, Roberto De la Torre-Roche, Nubia Zuverza-Mena, Marco Villani, Andrea Zappettini, Robert E Marra, Susan M Isch, Marta Marmiroli, et al. Exposure of cucurbita pepo to binary combinations of engineered nanomaterials: physiological and molecular response. *Environmental Science: Nano*, 4(7):1579–1590, 2017.

[105] Kenneth J Livak and Thomas D Schmittgen. Analysis of relative gene expression data using real-time quantitative pcr and the 2- $\delta\delta$ct method. *methods*, 25(4):402–408, 2001.

[106] R Foundation. R-project, 2021.

[107] Da Wei Huang, Brad T Sherman, and Richard A Lempicki. Systematic and integrative analysis of large gene lists using david bioinformatics resources. *Nature protocols*, 4(1):44–57, 2009.

[108] Da Wei Huang, Brad T Sherman, and Richard A Lempicki. Bioinformatics enrichment tools: paths toward the comprehensive functional analysis of large gene lists. *Nucleic acids research*, 37(1):1–13, 2009.

[109] Ioannis S Vlachos, Maria D Paraskevopoulou, Dimitra Karagkouni, Georgios Georgakilas, Thanasis Vergoulis, Ilias Kanellos, Ioannis-Laertis Anastasopoulos, Sofia Maniou, Konstantina Karathanou, Despina Kalfakakou, et al. Diana-tarbase v7. 0: indexing more than half a million experimentally supported mirna: mrna interactions. *Nucleic acids research*, 43(D1):D153–D159, 2015.

[110] Yuanbin Ru, Katerina J Kechris, Boris Tabakoff, Paula Hoffman, Richard A Radcliffe, Russell Bowler, Spencer Mahaffey, Simona Rossi, George A Calin, Lynne Bemis, et al. The multimir r package and database: integration of microrna–target interactions along with their disease and drug associations. *Nucleic acids research*, 42(17):e133–e133, 2014.

[111] Feifei Xiao, Zhixiang Zuo, Guoshuai Cai, Shuli Kang, Xiaolian Gao, and Tongbin Li. mirecords: an integrated resource for microrna–target interactions. *Nucleic acids research*, 37(suppl_1):D105–D110, 2009.

[112] Sheng-Da Hsu, Feng-Mao Lin, Wei-Yun Wu, Chao Liang, Wei-Chih Huang, Wen-Ling Chan, Wen-Ting Tsai, Goun-Zhou Chen, Chia-Jung Lee, Chih-Min Chiu, et al. mirtarbase: a database curates experimentally validated microrna–target interactions. *Nucleic acids research*, 39(suppl_1):D163–D169, 2011.

[113] Thanasis Vergoulis, Ioannis S Vlachos, Panagiotis Alexiou, George Georgakilas, Manolis Maragkakis, Martin Reczko, Stefanos Gerangelos, Nectarios Koziris, Theodore Dalamagas, and Artemis G Hatzigeorgiou. Tarbase 6.0: capturing the exponential growth of mirna targets with experimental support. *Nucleic acids research*, 40(D1):D222–D229, 2012.

[114] Manolis Maragkakis, Thanasis Vergoulis, Panagiotis Alexiou, Martin Reczko, Kyriaki Plomaritou, Mixail Gousis, Kornilios Kourtis, Nectarios Koziris, Theodore Dalamagas, and Artemis G Hatzigeorgiou. Diana-microt web server upgrade supports fly and worm mirna target prediction and bibliographic mirna to disease association. *Nucleic acids research*, 39(suppl_2):W145–W148, 2011.

[115] Sam Griffiths-Jones, Harpreet Kaur Saini, Stijn Van Dongen, and Anton J Enright. mirbase: tools for microrna genomics. *Nucleic acids research*, 36(suppl_1):D154–D158, 2007.

[116] Doron Betel, Manda Wilson, Aaron Gabow, Debora S Marks, and Chris Sander. The microrna. org resource: targets and expression. *Nucleic acids research*, 36(suppl_1):D149–D153, 2008.

[117] Xiaowei Wang. mirdb: a microrna target prediction and functional annotation database with a wiki interface. *Rna*, 14(6):1012–1017, 2008.

[118] Gerd Anders, Sebastian D Mackowiak, Marvin Jens, Jonas Maaskola, Andreas Kuntzagk, Nikolaus Rajewsky, Markus Landthaler, and Christoph Dieterich. dorina: a database of rna interactions in post-transcriptional regulation. *Nucleic acids research*, 40(D1):D180–D186, 2012.

[119] Michael Kertesz, Nicola Iovino, Ulrich Unnerstall, Ulrike Gaul, and Eran Segal. The role of site accessibility in microrna target recognition. *Nature genetics*, 39(10):1278–1284, 2007.

[120] Andrew Grimson, Kyle Kai-How Farh, Wendy K Johnston, Philip Garrett-Engele, Lee P Lim, and David P Bartel. Microrna targeting specificity in mammals: determinants beyond seed pairing. *Molecular cell*, 27(1):91–105, 2007.

[121] Laura Paesano, Alessio Perotti, Annamaria Buschini, Cecilia Carubbi, Marta Marmiroli, Elena Maestri, Salvatore Iannotta, and Nelson Marmiroli. Markers for toxicity to hepg2 exposed to cadmium sulphide quantum dots; damage to mitochondria. *Toxicology*, 374:18–28, 2016.

[122] Yoshinori Katsuragi, Yoshinobu Ichimura, and Masaaki Komatsu. p62/sqstm 1 functions as a signaling hub and an autophagy adaptor. *The FEBS journal*, 282(24):4672–4678, 2015.

[123] Danielle Glick, Sandra Barth, and Kay F Macleod. Autophagy: cellular and molecular mechanisms. *The Journal of pathology*, 221(1):3–12, 2010.

[124] DAVID Contributors. David bioinformatics resources 6.8 laboratory of human retrovirology and immunoinformatics (lhri), 2021.

[125] Peter J Cullen and Peter J Lockyer. Integration of calcium and ras signalling. *Nature reviews Molecular cell biology*, 3(5):339–348, 2002.

[126] James C Stone. Regulation and function of the rasgrp family of ras activators in blood cells. *Genes & cancer*, 2(3):320–334, 2011.

[127] T Kendall Harden, Stephanie N Hicks, and John Sondek. Phospholipase c isozymes as effectors of ras superfamily gtpases. *Journal of lipid research*, 50:S243–S248, 2009.

[128] Daria Illenberger, Frieder Schwald, Dominik Pimmer, Wolfhard Binder, Gernot Maier, Alexander Dietrich, and Peter Gierschik. Stimulation of phospholipase c-β2 by the rho gtpases cdc42hs and rac1. *The EMBO journal*, 17(21):6241–6249, 1998.

[129] Tom D Bunney and Matilda Katan. Phospholipase c epsilon: linking second messengers and small gtpases. *Trends in cell biology*, 16(12):640–648, 2006.

[130] Nicola Pierobon, Dominique C Renard-Rooney, Lawrence D Gaspers, and Andrew P Thomas. Ryanodine receptors in liver. *Journal of Biological Chemistry*, 281(45):34086–34095, 2006.

[131] Nobuaki Tamura, Yuji Tai, Katsuyoshi Sugimoto, Ryoji Kobayashi, Ryoji Konishi, Mikio Nishioka, Tsutomu Masaki, Shunichiro Nagahata, and Masaaki Tokuda. Enhanced expression and activation of ca2+/calmodulin-dependent protein kinase iv in hepatocellular carcinoma. *Cancer: Interdisciplinary International Journal of the American Cancer Society*, 89(9):1910–1916, 2000.

[132] Ernesto Carafoli. The interplay of mitochondria with calcium: an historical appraisal. *Cell calcium*, 52(1):1–8, 2012.

[133] Toren Finkel, Sara Menazza, Kira M Holmström, Randi J Parks, Julia Liu, Junhui Sun, Jie Liu, Xin Pan, and Elizabeth Murphy. The ins and outs of mitochondrial calcium. *Circulation research*, 116(11):1810–1819, 2015.

[134] Laura Contreras, Ilaria Drago, Enrico Zampese, and Tullio Pozzan. Mitochondria: the calcium connection. *Biochimica et Biophysica Acta (BBA)-Bioenergetics*, 1797(6-7):607–618, 2010.

[135] Jaime Santo-Domingo and Nicolas Demaurex. Calcium uptake mechanisms of mitochondria. *Biochimica et Biophysica Acta (BBA)-Bioenergetics*, 1797(6-7):907–912, 2010.

[136] C Urani, P Melchioretto, M Fabbri, G Bowe, E Maserati, and L Gribaldo. Cadmium impairs p53 activity in hepg2 cells. *International Scholarly Research Notices*, 2014, 2014.

[137] Qian Sun, Jie Fan, Timothy R Billiar, and Melanie J Scott. Inflammasome and autophagy regulation: a two-way street. *Molecular Medicine*, 23(1):188–195, 2017.

[138] Beth Levine, Noboru Mizushima, and Herbert W Virgin. Autophagy in immunity and inflammation. *Nature*, 469(7330):323–335, 2011.

[139] Romana T Netea-Maier, Theo S Plantinga, Frank L van de Veerdonk, Johannes W Smit, and Mihai G Netea. Modulation of inflammation by autophagy: consequences for human disease. *Autophagy*, 12(2):245–260, 2016.

[140] Andreas Petry, Michael Weitnauer, and Agnes Goerlach. Receptor activation of nadph oxidases. *Antioxidants & redox signaling*, 13(4):467–487, 2010.

[141] Jiangwei Zhang, Durga Nand Tripathi, Ji Jing, Angela Alexander, Jinhee Kim, Reid T Powell, Ruhee Dere, Jacqueline Tait-Mulder, Ji-Hoon Lee, Tanya T Paull, et al. Atm functions at the peroxisome to induce pexophagy in response to ros. *Nature cell biology*, 17(10):1259–1269, 2015.

[142] Dong-Hyung Cho, Yi Sak Kim, Doo Sin Jo, Seong-Kyu Choe, and Eun-Kyeong Jo. Pexophagy: molecular mechanisms and implications for health and diseases. *Molecules and cells*, 41(1):55, 2018.

[143] Heiko Hermeking. Micrornas in the p53 network: micromanagement of tumour suppression. *Nature reviews cancer*, 12(9):613–626, 2012.

[144] Annette Peters, Regina Rückerl, and Josef Cyrys. Lessons from air pollution epidemiology for studies of engineered nanomaterials. *Journal of Occupational and Environmental Medicine*, 53:S8–S13, 2011.

[145] Simone Reuter, Subash C Gupta, Madan M Chaturvedi, and Bharat B Aggarwal. Oxidative stress, inflammation, and cancer: how are they linked? *Free radical biology and medicine*, 49(11):1603–1616, 2010.

[146] IARC Working Group on the Evaluation of Carcinogenic Risks to Humans et al. Outdoor air pollution: Iarc monographs on the evaluation of carcinogenic risks to humans. 2016.

[147] Ioannis Manisalidis, Elisavet Stavropoulou, Agathangelos Stavropoulos, and Eugenia Bezirtzoglou. Environmental and health impacts of air pollution: a review. *Frontiers in public health*, page 14, 2020.

[148] Anjum Hajat, Matthew Allison, Ana V Diez-Roux, Nancy Swords Jenny, Neal W Jorgensen, Adam A Szpiro, Sverre Vedal, and Joel D Kaufman. Long-term exposure to air pollution and markers of inflammation, coagulation, and endothelial activation: a repeat-measures analysis in the multi-ethnic study of atherosclerosis (mesa). *Epidemiology (Cambridge, Mass.)*, 26(3):310, 2015.

[149] Anja Viehmann, Sabine Hertel, Kateryna Fuks, Lewin Eisele, Susanne Moebus, Stefan Möhlenkamp, Michael Nonnemacher, Hermann Jakobs, Raimund Erbel, Karl-Heinz Jöckel, et al. Long-term residential exposure to urban air pollution, and repeated measures of systemic blood markers of inflammation

and coagulation. *Occupational and environmental medicine*, 72(9):656–663, 2015.

[150] Richard L Jayaraj, Eric A Rodriguez, Yi Wang, and Michelle L Block. Outdoor ambient air pollution and neurodegenerative diseases: the neuroinflammation hypothesis. *Current environmental health reports*, 4(2):166–179, 2017.

[151] Cristina Vert, Gonzalo Sánchez-Benavides, David Martínez, Xavier Gotsens, Nina Gramunt, Marta Cirach, José Luis Molinuevo, Jordi Sunyer, Mark J Nieuwenhuijsen, Marta Crous-Bou, et al. Effect of long-term exposure to air pollution on anxiety and depression in adults: A cross-sectional study. *International journal of hygiene and environmental health*, 220(6):1074–1080, 2017.

[152] Vivian C Pun, Justin Manjourides, and Helen Suh. Association of ambient air pollution with depressive and anxiety symptoms in older adults: results from the nshap study. *Environmental health perspectives*, 125(3):342–348, 2017.

[153] Julie Carré, Nicolas Gatimel, Jessika Moreau, Jean Parinaud, and Roger Léandri. Does air pollution play a role in infertility?: a systematic review. *Environmental Health*, 16(1):1–16, 2017.

[154] George D Thurston, Howard Kipen, Isabella Annesi-Maesano, John Balmes, Robert D Brook, Kevin Cromar, Sara De Matteis, Francesco Forastiere, Bertil Forsberg, Mark W Frampton, et al. A joint ers/ats policy statement: what constitutes an adverse health effect of air pollution? an analytical framework. *European Respiratory Journal*, 49(1), 2017.

[155] Bert Brunekreef and Stephen T Holgate. Air pollution and health. *The lancet*, 360(9341):1233–1242, 2002.

[156] Annette Peters, Angela Döring, H-Erich Wichmann, and Wolfgang Koenig. Increased plasma viscosity during an air pollution episode: a link to mortality? *The Lancet*, 349(9065):1582–1587, 1997.

[157] Sarah Lucht, Frauke Hennig, Susanne Moebus, Dagmar Führer-Sakel, Christian Herder, Karl-Heinz Jöckel, Barbara Hoffmann, Heinz Nixdorf Recall

Study Investigative Group, et al. Air pollution and diabetes-related biomarkers in non-diabetic adults: A pathway to impaired glucose metabolism? *Environment international*, 124:370–392, 2019.

[158] Hong Tang, Zilu Cheng, Na Li, Shuyuan Mao, Runxue Ma, Haijun He, Zhiping Niu, Xiaolu Chen, and Hao Xiang. The short-and long-term associations of particulate matter with inflammation and blood coagulation markers: A meta-analysis. *Environmental Pollution*, page 115630, 2020.

[159] M Baltz Pepys and Marilyn L Baltz. Acute phase proteins with special reference to c-reactive protein and related proteins (pentaxins) and serum amyloid a protein. *Advances in immunology*, 34:141–212, 1983.

[160] Yanli Li, Kate Rittenhouse-Olson, William L Scheider, and Lina Mu. Effect of particulate matter air pollution on c-reactive protein: a review of epidemiologic studies. *Reviews on environmental health*, 27(2-3):133–149, 2012.

[161] Vincenzo Pasceri, James T Willerson, and Edward TH Yeh. Direct proinflammatory effect of c-reactive protein on human endothelial cells. *Circulation*, 102(18):2165–2168, 2000.

[162] Wolfgang Koenig, Hannelore Löwel, Jens Baumert, and Christa Meisinger. C-reactive protein modulates risk prediction based on the framingham score: implications for future risk assessment: results from a large cohort study in southern germany. *Circulation*, 109(11):1349–1353, 2004.

[163] R Baumann, M Gube, A Markert, S Davatgarbenam, V Kossack, B Gerhards, T Kraus, and P Brand. Systemic serum amyloid a as a biomarker for exposure to zinc and/or copper-containing metal fumes. *Journal of exposure science & environmental epidemiology*, 28(1):84–91, 2018.

[164] George H Sack. Serum amyloid a (saa) proteins. *Vertebrate and Invertebrate Respiratory Proteins, Lipoproteins and other Body Fluid Proteins*, pages 421–436, 2020.

[165] Toshio Hirano and TADAMITSU Kishimoto. Interleukin-6. In *Peptide growth factors and their receptors I*, pages 633–665. Springer, 1990.

[166] Mala Sharma, John Arthur McClung, and Nader G Abraham. Adiponectin: A mediator of obesity, insulin resistance, diabetes, and the metabolic syndrome. In *Translational Research in Coronary Artery Disease*, pages 33–42. Elsevier, 2016.

[167] MT Villarreal-Molina and B Antuna-Puente. Adiponectin: anti-inflammatory and cardioprotective effects. *Biochimie*, 94(10):2143–2149, 2012.

[168] Yoshio Takei, Hironori Ando, and Kazuyoshi Tsutsui. *Handbook of hormones: comparative endocrinology for basic and clinical research*. Academic Press, 2015.

[169] Sadeer G Al-Kindi, Robert D Brook, Shyam Biswal, and Sanjay Rajagopalan. Environmental determinants of cardiovascular disease: lessons learned from air pollution. *Nature Reviews Cardiology*, 17(10):656–672, 2020.

[170] Morihiro Matsuda and Iichiro Shimomura. Increased oxidative stress in obesity: implications for metabolic syndrome, diabetes, hypertension, dyslipidemia, atherosclerosis, and cancer. *Obesity research & clinical practice*, 7(5):e330–e341, 2013.

[171] Regina Ruckerl, Angela Ibald-Mulli, Wolfgang Koenig, Alexandra Schneider, Gabriele Woelke, Josef Cyrys, Joachim Heinrich, Victor Marder, Mark Frampton, H Erich Wichmann, et al. Air pollution and markers of inflammation and coagulation in patients with coronary heart disease. *American journal of respiratory and critical care medicine*, 173(4):432–441, 2006.

[172] Herbert Tilg and Alexander R Moschen. Adipocytokines: mediators linking adipose tissue, inflammation and immunity. *Nature Reviews Immunology*, 6(10):772–783, 2006.

[173] Anjum Hajat, Marnie F Hazlehurst, Sherita Hill Golden, Sharon Stein Merkin, Teresa Seeman, Adam A Szpiro, Joel D Kaufman, and Ana Diez Roux. The cross-sectional and longitudinal association between air pollution and salivary cortisol: evidence from the multi-ethnic study of atherosclerosis. *Environment international*, 131:105062, 2019.

[174] Helmholtz Munich. Overview kora cohort, 2021.

[175] Rolf Holle, Michael Happich, Hannelore Löwel, Heinz-Erich Wichmann, null for the MONICA/KORA Study Group, et al. Kora-a research platform for population based health research. *Das Gesundheitswesen*, 67(S 01):19–25, 2005.

[176] Birgit Klüppelholz, Barbara Thorand, Wolfgang Koenig, Tonia de las Heras Gala, Christa Meisinger, Cornelia Huth, Guido Giani, Paul W Franks, Michael Roden, Wolfgang Rathmann, et al. Association of subclinical inflammation with deterioration of glycaemia before the diagnosis of type 2 diabetes: the kora s4/f4 study. *Diabetologia*, 58(10):2269–2277, 2015.

[177] Albrecht Hoffmeister, Dietrich Rothenbacher, Ute Bäzner, Margit Fröhlich, Hermann Brenner, Vinzenz Hombach, and Wolfgang Koenig. Role of novel markers of inflammation in patients with stable coronary heart disease. *The American journal of cardiology*, 87(3):262–266, 2001.

[178] S Müller, S Martin, W Koenig, P Hanifi-Moghaddam, W Rathmann, B Haastert, G Giani, T Illig, B Thorand, and H Kolb. Impaired glucose tolerance is associated with increased serum concentrations of interleukin 6 and co-regulated acute-phase proteins but not tnf-α or its receptors. *Diabetologia*, 45(6):805–812, 2002.

[179] Christian Herder, Hans Hauner, Burkhard Haastert, Karin Röhrig, Wolfgang Koenig, Hubert Kolb, Sylvia Müller-Scholze, Barbara Thorand, Rolf Holle, and Wolfgang Rathmann. Hypoadiponectinemia and proinflammatory state: two sides of the same coin?: results from the cooperative health research in the region of augsburg survey 4 (kora s4). *Diabetes Care*, 29(7):1626–1631, 2006.

[180] Marloes Eeftens, Reto Meier, Christian Schindler, Inmaculada Aguilera, Harish Phuleria, Alex Ineichen, Mark Davey, Regina Ducret-Stich, Dirk Keidel, Nicole Probst-Hensch, et al. Development of land use regression models for nitrogen dioxide, ultrafine particles, lung deposited surface area, and four other markers of particulate matter pollution in the swiss sapaldia regions. *Environmental Health*, 15(1):1–14, 2016.

[181] N Ma and W Birmili. Estimating the contribution of photochemical particle formation to ultrafine particle number averages in an urban atmosphere. *Science of the Total Environment*, 512:154–166, 2015.

[182] Kathrin Wolf, Josef Cyrys, Tatiana Harciníková, Jianwei Gu, Thomas Kusch, Regina Hampel, Alexandra Schneider, and Annette Peters. Land use regression modeling of ultrafine particles, ozone, nitrogen oxides and markers of particulate matter pollution in augsburg, germany. *Science of the Total Environment*, 579:1531–1540, 2017.

[183] William PL Carter. Development of ozone reactivity scales for volatile organic compounds. *Air & waste*, 44(7):881–899, 1994.

[184] Maciej Strak, Gudrun Weinmayr, Sophia Rodopoulou, Jie Chen, Kees De Hoogh, Zorana J Andersen, Richard Atkinson, Mariska Bauwelinck, Terese Bekkevold, Tom Bellander, et al. Long term exposure to low level air pollution and mortality in eight european cohorts within the elapse project: pooled analysis. *bmj*, 374, 2021.

[185] Barbara Thorand, Jens Baumert, Angela Döring, Christian Herder, Hubert Kolb, Wolfgang Rathmann, Guido Giani, Wolfgang Koenig, KORA Group, et al. Sex differences in the relation of body composition to markers of inflammation. *Atherosclerosis*, 184(1):216–224, 2006.

[186] Linglin Xie, Cormac P O'Reilly, Stephen K Chapes, and Silvia Mora. Adiponectin and leptin are secreted through distinct trafficking pathways in adipocytes. *Biochimica et Biophysica Acta (BBA)-Molecular Basis of Disease*, 1782(2):99–108, 2008.

[187] Hyewon Lee, Woojae Myung, Byeong-Ho Jeong, Hong Choi, Byung Woo Jhun, and Ho Kim. Short-and long-term exposure to ambient air pollution and circulating biomarkers of inflammation in non-smokers: a hospital-based cohort study in south korea. *Environment international*, 119:264–273, 2018.

[188] Kevin J Lane, Jonathan I Levy, Madeleine K Scammell, Junenette L Peters, Allison P Patton, Ellin Reisner, Lydia Lowe, Wig Zamore, John L Durant, and Doug Brugge. Association of modeled long-term personal exposure to ultrafine particles with inflammatory and coagulation biomarkers. *Environment international*, 92:173–182, 2016.

[189] Wenyuan Li, Kirsten S Dorans, Elissa H Wilker, Mary B Rice, Itai Kloog, Joel D Schwartz, Petros Koutrakis, Brent A Coull, Diane R Gold, James B Meigs, et al. Ambient air pollution, adipokines, and glucose homeostasis: The framingham heart study. *Environment international*, 111:14–22, 2018.

[190] Sarah Lucht, Frauke Hennig, Susanne Moebus, Simone Ohlwein, Christian Herder, Bernd Kowall, Karl-Heinz Jöckel, and Barbara Hoffmann. All-source and source-specific air pollution and 10-year diabetes incidence: Total effect and mediation analyses in the heinz nixdorf recall study. *Environment international*, 136:105493, 2020.

[191] Sabrina Havard, Séverine Deguen, Denis Zmirou-Navier, Charles Schillinger, and Denis Bard. Traffic-related air pollution and socioeconomic status: a spatial autocorrelation study to assess environmental equity on a small-area scale. *Epidemiology*, pages 223–230, 2009.

[192] Gloria C Chi, Anjum Hajat, Chloe E Bird, Mark R Cullen, Beth Ann Griffin, Kristin A Miller, Regina A Shih, Marcia L Stefanick, Sverre Vedal, Eric A Whitsel, et al. Individual and neighborhood socioeconomic status and the association between air pollution and cardiovascular disease. *Environmental health perspectives*, 124(12):1840–1847, 2016.

[193] Anjum Hajat, Ana V Diez-Roux, Sara D Adar, Amy H Auchincloss, Gina S Lovasi, Marie S O'Neill, Lianne Sheppard, and Joel D Kaufman. Air pollution and individual and neighborhood socioeconomic status: evidence from the multi-ethnic study of atherosclerosis (mesa). *Environmental health perspectives*, 121(11-12):1325–1333, 2013.

[194] Hari S Iyer, Jaime E Hart, Peter James, Elise G Elliott, Nicole V DeVille, Michelle D Holmes, Immaculata De Vivo, Lorelei A Mucci, Francine Laden, and Timothy R Rebbeck. Impact of neighborhood socioeconomic status, income segregation, and greenness on blood biomarkers of inflammation. *Environment international*, 162:107164, 2022.

[195] Eric Lontchi-Yimagou, Eugene Sobngwi, Tandi E Matsha, and Andre Pascal Kengne. Diabetes mellitus and inflammation. *Current diabetes reports*, 13(3):435–444, 2013.

[196] Jordan Kawano and Rohit Arora. The role of adiponectin in obesity, diabetes, and cardiovascular disease. *Journal of the cardiometabolic syndrome*, 4(1):44–49, 2009.

[197] Hyung Muk Choi, Hari Madhuri Doss, and Kyoung Soo Kim. Multifaceted physiological roles of adiponectin in inflammation and diseases. *International journal of molecular sciences*, 21(4):1219, 2020.

[198] Gary Fuller. *The Invisible Killer: The Rising Global Threat of Air Pollution: and how We Can Fight Back*. Melville House Publishing, 2019.

[199] Günther Oberdörster, Zachary Sharp, Viorel Atudorei, Alison Elder, Robert Gelein, Wolfgang Kreyling, and Christopher Cox. Translocation of inhaled ultrafine particles to the brain. *Inhalation toxicology*, 16(6-7):437–445, 2004.

[200] Toshio Tanaka, Masashi Narazaki, and Tadamitsu Kishimoto. Il-6 in inflammation, immunity, and disease. *Cold Spring Harbor perspectives in biology*, 6(10):a016295, 2014.

[201] Tonje Skuland, Marit Låg, Arno C Gutleb, Bendik C Brinchmann, Tommaso Serchi, Johan Øvrevik, Jørn A Holme, and Magne Refsnes. Pro-inflammatory effects of crystalline-and nano-sized non-crystalline silica particles in a 3d alveolar model. *Particle and Fibre Toxicology*, 17(1):1–18, 2020.

[202] Saou-Hsing Liou, Tsui-Chun Tsou, Shu-Li Wang, Lih-Ann Li, Hung-Che Chiang, Wan-Fen Li, Pin-Pin Lin, Ching-Huang Lai, Hui-Ling Lee, Ming-Hsiu Lin, et al. Epidemiological study of health hazards among workers handling engineered nanomaterials. *Journal of Nanoparticle Research*, 14(8):1–15, 2012.

[203] Fan Zhang, Grace V Aquino, Amjad Dabi, and Erica D Bruce. Assessing the translocation of silver nanoparticles using an in vitro co-culture model of human airway barrier. *Toxicology in Vitro*, 56:1–9, 2019.

[204] Miruna-Silvia Stan, Cornelia Sima, Ludmila Otilia Cinteza, and Anca Dinischiotu. Silicon-based quantum dots induce inflammation in human lung cells and disrupt extracellular matrix homeostasis. *The FEBS Journal*, 282(15):2914–2929, 2015.

[205] Laura Capasso, Marina Camatini, and Maurizio Gualtieri. Nickel oxide nanoparticles induce inflammation and genotoxic effect in lung epithelial cells. *Toxicology letters*, 226(1):28–34, 2014.

[206] A Murphy, A Casey, G Byrne, G Chambers, and O Howe. Silver nanoparticles induce pro-inflammatory gene expression and inflammasome activation in human monocytes. *Journal of Applied Toxicology*, 36(10):1311–1320, 2016.

[207] Regina Rückerl, Sonja Greven, Petter Ljungman, Pasi Aalto, Charalambos Antoniades, Tom Bellander, Niklas Berglind, Christina Chrysohoou, Francesco Forastiere, Bénédicte Jacquemin, et al. Air pollution and inflammation (interleukin-6, c-reactive protein, fibrinogen) in myocardial infarction survivors. *Environmental health perspectives*, 115(7):1072–1080, 2007.

[208] Prashant Kumar, Gopinath Kalaiarasan, Alexandra E Porter, Alessandra Pinna, Michał M Kłosowski, Philip Demokritou, Kian Fan Chung, Christopher Pain, DK Arvind, Rossella Arcucci, et al. An overview of methods of fine and ultrafine particle collection for physicochemical characterisation and toxicity assessments. *Science of The Total Environment*, 756:143553, 2021.

[209] AT Juarez Facio, J Yon, C Corbière, T Rogez-Florent, C Castilla, H Lavanant, M Mignot, C Devouge-Boyer, C Logie, L Chevalier, et al. Toxicological impact of organic ultrafine particles (ufps) in human bronchial epithelial beas-2b cells at air-liquid interface. *Toxicology in Vitro*, 78:105258, 2022.

[210] Ana Teresa Juarez-Facio, Clément Castilla, Cécile Corbière, Hélène Lavanant, Carlos Afonso, Christophe Morin, Nadine Merlet-Machour, Laurence Chevalier, Jean-Marie Vaugeois, Jérôme Yon, et al. Development of a standardized in vitro approach to evaluate microphysical, chemical, and toxicological properties of combustion-derived fine and ultrafine particles. *Journal of Environmental Sciences*, 113:104–117, 2022.

Affidavit

LMU LUDWIG-MAXIMILIANS-UNIVERSITÄT MÜNCHEN

Promotionsbüro
Medizinische Fakultät

MMRS

Affidavit

Vogli Megi

Surname, first name

Via G.Mascherpa, 9

20841, Carate Brianza, Italy

Zip code, town, country

I hereby declare, that the submitted thesis entitled:

"Contribution of applied biology to mitigation of urban air pollution and prevention of its effects on health and environment" is my own work. I have only used the sources indicated and have not made unauthorised use of services of a third party. Where the work of others has been quoted or reproduced, the source is always given. I further declare that the submitted thesis or parts thereof have not been presented as part of an examination degree to any other university.

Muenchen, 20.09.2022

place, date

Signature doctoral candidate

MEGI VOGLI

PhD canditate

@ voglimegi@gmail.com - megi.vogli@unipr.it +39 3402905123 Carate Brianza (Italy)

EXPERIENCE

PhD period

Helmholtz Zentrum

03.21-09.21 Munich, Germany

- Epidemiological study focused on the effects of air pollution on human health centered on biomarkers of cardiovascular disease.

PhD

University of Parma

11.18-12.21 Parma, Italy

- Toxicological study with human cell lines to investigate the effects of nanomaterials at molecular level using omics technologies.

Internship

Sirti S.p.A

09.18-09.18 Milano, Italy

- Internship in the organizational structure of Compliance, Quality and Health Safety Environment (EHS). Certifications, internal audits.

Internship

Bayer HealthCare Manufacturing S.r.l

01.18-07.18 Garbagnate Milanese, Italy

- Internship in HSE Office. Activities concerning safety and health in the workplace, environment, and energy: definition of procedures, data collection, evaluation of analytical results, document management and participation in work groups.

INFORMATICS SKILLS

- O.S.: Windows; Linux / Microsoft office; Libre office.
- Software: LaTeX; ArcGis; Inkscape.
- IDE: PyCharm; Rstudio.
- Language programming: R – intermediate; Python – basic.
- Online Bioinformatic tools

OTHERS

I have also developed sense of responsibilities, soft and hard skills through diverse professional experiences that I have had since in early age.

MAIN

I am in the process of finishing my PhD, which is in co-tutorship between University of Parma and Ludwig Maximilian University of Munich. The project is focused on the relationship among human health and environment. Specifically, exposure to nanoparticles and other air pollutants and the relation of this last ones with cardiovascular diseases. I have a strong background in environmental science that taught me the importance of being versatile, to always investigate issues from different perspectives.

STRENGTHS

Hard-working | Data management | Curious learner | Teamwork | Innovative

LANGUAGES

Italian/Albanian

English

Spanish

German

EDUCATION

M.Sc., Science and Technologies for Environment and Landscape

University of Milano-Bicocca

Nov 2015 – Nov 2017 Milano

Thesis title: Ground Motion Prediction Equations for Probabilistic Seismic Assessment in Albania. In collaboration with the Polytechnic University of Tirana (Albania).
Finale score: 110/110 *cum laude*

B.Sc. in Environmental Science and Technologies

University of Milano-Bicocca

Oct 2011 – July 2015 Milano

Thesis title: Inflammatory effects induced by different particulate matter on *in vitro* system.
Finale score: 91/110